

Regulatory T Cell in Drug-Induced Severe Cutaneous Adverse Reactions (SCARs)  
During Acute and Recovery Phase



A Dissertation Submitted in Partial Fulfillment of the Requirements  
for the Degree of Doctor of Philosophy in Medical Sciences  
FACULTY OF MEDICINE  
Chulalongkorn University  
Academic Year 2022  
Copyright of Chulalongkorn University

Regulatory T Cell ในคนไข้ภาวะผื่นแพ้ยารุนแรง  
(Severe Cutaneous Adverse Reactions; SCARs) ในระยะเฉียบพลันและระยะกลับคืน



วิทยานิพนธ์นี้เป็นส่วนหนึ่งของการศึกษาตามหลักสูตรปริญญาวิทยาศาสตรดุษฎีบัณฑิต  
สาขาวิชาวิทยาศาสตร์การแพทย์ ไม่สังกัดภาควิชา/เทียบเท่า  
คณะแพทยศาสตร์ จุฬาลงกรณ์มหาวิทยาลัย  
ปีการศึกษา 2565  
ลิขสิทธิ์ของจุฬาลงกรณ์มหาวิทยาลัย



ศุภรดา คณารักษ์สมบัติ : Regulatory T Cell ในคนไข้ภาวะผื่นแพ้ยารุนแรง(Severe Cutaneous Adverse Reactions; SCARs) ในระยะเฉียบพลันและระยะกลับคืน. ( Regulatory T Cell in Drug-Induced Severe Cutaneous Adverse Reactions (SCARs) During Acute and Recovery Phase) อ.ที่ปรึกษาหลัก : ศ. นพ.เจตทชนง แก้วสงคราม, อ.ที่ปรึกษาร่วม : รศ. ดร. พญ.รังสิมา เจริญตระกูล

อาการผื่นแพ้ชนิด Drug reaction with eosinophilia and systemic symptoms (DRESS) เป็นกลุ่มอาการหนึ่งในผื่นแพ้ยาชนิดรุนแรง (SCARs) ซึ่งสามารถเกิดจากการกระตุ้นด้วยยาได้หลากหลายกลุ่ม โรคภูมิคุ้มกันทำลายเนื้อเยื่อตัวเองสามารถพบได้ประมาณร้อยละ 10 - 20 ของคนไข้แพ้ยาชนิด DRESS ในระหว่างการรักษาตัว ทั้งนี้เชื่อว่าการเปลี่ยนแปลงในปริมาณและความสามารถในการทำงานของเซลล์กลุ่ม regulatory T cells (Tregs) เป็นปัจจัยหลักในการดำเนินโรคภูมิคุ้มกันทำลายเนื้อเยื่อตัวเองให้คนไข้กลุ่มนี้ การศึกษานี้มีวัตถุประสงค์ในการศึกษาจำนวน และอิมมูโนฟีโนไทป์ รวมถึงความสามารถในการทำงานของเซลล์กลุ่ม  $CD4^+CD25^+CD127^+FoxP3^+$  Tregs โดยใช้เซลล์ PBMCs จากคนไข้ผื่นแพ้ยารุนแรงชนิด DRESS โดยใช้เทคนิค Flow cytometry และ suppression assay นอกจากนี้ เทคโนโลยี NanoString ถูกใช้เพื่อศึกษาการแสดงออกของ mRNA เพื่อสำรวจยีนที่เกี่ยวข้องกับ  $CD4^+CD25^+CD127^+FoxP3^+$  Tregs ในกลุ่มคนไข้แพ้ยารุนแรงชนิด DRESS ที่มีการเกิดโรคภูมิคุ้มกันทำลายเนื้อเยื่อตัวเองในภายหลัง ผลการศึกษาพบว่าในกลุ่มคนไข้แพ้ยารุนแรงชนิด DRESS ที่มีการเกิดโรคภูมิคุ้มกันทำลายเนื้อเยื่อตัวเองไม่มีความแตกต่างอย่างมีนัยสำคัญของจำนวน  $CD4^+CD25^+CD127^+FoxP3^+$  Tregs เมื่อเปรียบเทียบกับกลุ่มคนไข้แพ้ยารุนแรงชนิด SJS/TEN และกลุ่มคนสุขภาพดี แม้ว่า Tregs จะมีแนวโน้มลดลงก็ตาม การศึกษาอิมมูโนฟีโนไทป์แสดงให้เห็นว่าการแสดงออกของ CTLA-4, LAG-3, GITR และ IL-10 นั้นสูงขึ้นใน DRESS ที่มีการเกิดโรคภูมิคุ้มกันทำลายเนื้อเยื่อตัวเองในระยะเฉียบพลัน อย่างไรก็ตามพบว่าการทำงานของ Tregs ในการกดการแบ่งตัวของ effector T cells มีการลดลงในกลุ่มคนไข้แพ้ยารุนแรงชนิด DRESS ที่มีการเกิดโรคภูมิคุ้มกันทำลายเนื้อเยื่อตัวเอง นอกจากนี้ยังพบว่าการแสดงออกของยีนที่เกี่ยวข้องกับการทำงานของเซลล์ Tregs ก็ลดลงในกลุ่มคนไข้แพ้ยารุนแรงชนิด DRESS ที่มีการเกิดโรคภูมิคุ้มกันทำลายเนื้อเยื่อตัวเอง ซึ่งสามารถสรุปได้ว่าเซลล์ Tregs ที่ลดลง อาจใช้เป็นปัจจัยพยากรณ์โรคสำหรับภาวะแทรกซ้อนระยะยาวในกลุ่มคนไข้แพ้ยารุนแรงชนิด DRESS นี้ได้

สาขาวิชา วิทยาศาสตร์การแพทย์

ปีการศึกษา 2565

ลายมือชื่อนิสิต .....

ลายมือชื่อ อ.ที่ปรึกษาหลัก .....

ลายมือชื่อ อ.ที่ปรึกษาร่วม .....

# # 5974755630 : MAJOR MEDICAL SCIENCES

KEYWORD: Drug hypersensitivity, Drug reaction with eosinophilia and systemic symptom, Regulatory T cell, Suppressive function, NanoString technology, Autoimmune sequelae, Severe cutaneous adverse drug reaction

Suparada Khanaruksombat : Regulatory T Cell in Drug-Induced Severe Cutaneous Adverse Reactions (SCARs) During Acute and Recovery Phase. Advisor: Prof. JETTANONG KLAESONGKRAM, M.D. Co-advisor: Assoc. Prof. RANGSIMA REANTRAGOON, M.D., Ph.D.

Drug reaction with eosinophilia and systemic symptoms (DRESS) is a type of SCARs induced by various drugs. The autoimmune consequences were observed throughout the recovery phase ranging between 10 – 20 % of DRESS patients. The dynamics of regulatory T cells (Tregs) are thought to be responsible for the many symptoms of DRESS. They may be a key player in developing autoimmune sequelae in this syndrome. This study concentrated on the number and function of  $CD4^+CD25^+CD127^+FoxP3^+$  Tregs in autoimmune development in DRESS patients.  $CD4^+CD25^+CD127^+FoxP3^+$  Tregs and their immunophenotyping were characterized using peripheral blood mononuclear cells (PBMCs) from patients by Flow cytometry techniques. The suppressive function of Tregs was determined using suppression assay by co-culture between autologous Treg and effector T cells. NanoString technology was used to study mRNA profiles to explore genes associated with Tregs.  $CD4^+CD25^+CD127^+FoxP3^+$  Tregs in DRESS with autoimmune sequelae at the acute phase tended to be lower than DRESS without autoimmune sequelae, SJS/TEN patients, and in healthy controls. The immunophenotyping showed that the expression of CTLA-4, LAG-3, GITR, and IL-10 were higher in DRESS with autoimmune sequelae patients. However, the suppression of Treg on T cell proliferation was also lower in DRESS with autoimmune sequelae patients. The mRNA profile showed downregulation of genes associated with Treg function since the acute phase of DRESS with autoimmune sequelae. In conclusion, this study illustrated the regulatory functions of Tregs were altered since the acute phase after the onset of DRESS, which might be used as prognostic factors for long-term complications in DRESS subjects.

Field of Study: Medical Sciences

Student's Signature .....

Academic Year: 2022

Advisor's Signature .....

Co-advisor's Signature .....

## ACKNOWLEDGEMENTS

This study was supported by Ratchadaphiseksomphot Endowment Fund and The 100th Anniversary Chulalongkorn University for Doctoral Scholarship.

Foremost, I would like to express my sincere gratitude to my advisor, Assoc. Prof. Jettanong Klaewsongkram for his support and encouragement throughout my dissertation with his invaluable knowledge and feedback. Many gratitude to Asst.Prof.Dr. Rangsimma Reantragoon, my co-advisor, who read my numerous revisions, helped me understand the confusion and motivated me immensely.

Besides, I sincerely thank Assoc.Prof. Tanapat Palaga, Assoc. Prof. Sunchai Payungporn, and Assoc. Prof. Dr. Nipan Israsena for their kind advice and the use of their facilities for this thesis. I also appreciated Professor. Shanop Shuangshoti, Dr. Chinnachote Teerapakpinyo, and the staff from Chula GenePRO Center for their help in NanoString technology, and Associate Professor Chonlaphat Sukasem, Division of Pharmacogenomics and Personalized Medicine, Faculty of Medicine Ramathibodi Hospital, Mahidol University for his recommendations and patients recruitment. Moreover, I greatly thank Assoc. Prof. Wilai Anomasiri and Assoc. Prof. Hiroshi Chantaphakul for their noble guidance and support with full encouragement.

I am thankful to Dr. Supranee Buranapraditkul, Mr. Pattarawat Thantiworasit, and Mrs. Pungjai Mongkolpathumrat, authorities at the division of Allergy and Clinical Immunology, for their numerous support throughout my study. I also thank my colleagues from the RR team, especially Dr. Panjana Sengprasert and Dr. Nithikan Suthumchai, for their love and support, for constantly listening to me rant and talk things out, and for cracking jokes when things became too serious.

Last, thank all my precious friends and cousins for encouraging and supporting me whenever I needed them. Thank you to my little brother for always being there for me, for giving me hugs, and for telling me that I am awesome even when I do not feel that way. Lastly, I must give my wonderful mother all my honors and prizes. I realize more and more everything you do, everything you give, and everything you stand for. I love you and thank you with all my heart because you are my inspiration, and only you can light up my strength.

Suparada Khanaruksombat

## TABLE OF CONTENTS

	Page
ABSTRACT (THAI).....	iii
ABSTRACT (ENGLISH).....	iv
ACKNOWLEDGEMENTS.....	v
TABLE OF CONTENTS.....	vi
LIST OF TABLES.....	x
LIST OF FIGURES.....	xi
CHAPTER I INTRODUCTION.....	1
CHAPTER II LITERATURE REVIEW.....	3
2.1 Adverse drug reactions (ADRs).....	3
2.1.1 Gell and Coombs's classification.....	4
2.2 Severe cutaneous adverse drug reactions (SCARs).....	7
2.2 Drug reaction with eosinophilia and systemic symptoms (DRESS).....	9
2.2.1 Etiology, risk factors, and epidemiology.....	9
2.2.2 Clinical manifestation.....	10
2.2.3 Pathophysiology.....	12
2.2.4 Diagnosis.....	14
2.2.5 Management.....	15
2.2.6 Outcome and sequelae.....	16
2.3 Regulatory T cells (Tregs).....	17
2.3.1 Differentiation dynamics of Tregs.....	17
2.3.2 Tregs subsets and their immunophenotype markers.....	19

2.2.3 Functions of Tregs .....	26
2.3.4 Cell signaling of Tregs and Treg cell signaling and potential action mechanisms.....	27
2.4 Association of Treg, DRESS, and autoimmune diseases .....	29
CHAPTER III HYPOTHESIS AND OBJECTIVES .....	31
3.1 Research question.....	31
3.2 Objectives .....	31
3.3 Hypothesis .....	31
3.4 Conceptual framework.....	32
3.5 Research design and experimental framework.....	32
3.6 Expected results.....	34
3.7 The benefit of this study .....	34
CHAPTER IV METHODOLOGY .....	35
4.1 Specimen collection.....	35
4.2 Sample size determination .....	36
4.3 Inclusion criteria.....	37
4.4 Exclusion criteria .....	38
4.5 Isolation and cryopreservation of PBMC .....	39
4.6 Antibodies staining for flow cytometry.....	40
4.7 Quality control of flow cytometry.....	41
4.8 Statistical analysis for immunophenotyping characteristics of Tregs .....	41
4.9 Tregs isolation for suppression assay .....	42
4.10 Tregs and effector T cells co-culture experiments.....	43
4.11 Effector T cells proliferation analysis.....	44



4.12 Data analysis and statistical analysis of suppression assay .....	44
4.13 Tregs isolation for mRNA profiling .....	45
4.14 Total RNA extraction of Tregs.....	45
4.15 CodeSet hybridization.....	47
4.16 Post hybridization sample processes by Prep Station robot and digital analyzer .....	48
4.17 nSolver™ 4.0 analysis software and data analysis of mRNA profiling .....	49
CHAPTER V RESULTS.....	51
PART 1 PATIENT CHARACTERIZATION AND TREGS PHENOTYPING USING FLOW CYTOMETRY.....	51
5.1 Clinical characteristics .....	51
5.2 Identification of regulatory T cell frequency and their immunophenotype	54
5.2.1 CD4 <sup>+</sup> CD25 <sup>+</sup> CD127 <sup>-</sup> FoxP3 <sup>+</sup> Treg were not significantly different when compared between all groups.....	56
5.2.2 The alteration of Tregs immunophenotypic markers in the acute and recovery phases of SCARs types.....	57
PART 2 REGULATORY T CELL SUPPRESSIVE FUNCTION.....	65
5.2 The positive correlation of CD4 <sup>+</sup> CD25 <sup>+</sup> CD127 <sup>-</sup> Tregs and CD4 <sup>+</sup> CD25 <sup>+</sup> CD127 <sup>-</sup> FoxP3 <sup>+</sup> Tregs .....	65
5.3 The purity of CD4 <sup>+</sup> CD25 <sup>+</sup> CD127 <sup>-</sup> regulatory T cells and CD4 <sup>+</sup> CD25 <sup>-</sup> effector T cells after isolation.....	67
5.4 Tregs from DRESS patients could not suppress the autologous proliferation of effector T cells.....	69
PART 3 MRNA EXPRESSION PROFILE OF TREGS USING NANOSTRING TECHNOLOGY .....	73
5.5 mRNA expression profile of Tregs using NanoString Technology.....	73

CHAPTER VI DISCUSSION .....	87
CHAPTER VII CONCLUSION .....	91
REFERENCES .....	92
APPENDIX.....	103
APPENDIX A REAGENT PREPARATION.....	104
APPENDIX B CHEMICAL AND REAGENTS .....	107
APPENDIX C EQUIPMENT .....	109
APPENDIX D SUPPORTING RESULTS .....	111
VITA.....	137



## LIST OF TABLES

	<b>Page</b>
Table 1 Diagnostic criteria in the scoring system for DRESS by the RegisSCAR .....	15
Table 2 Types of Treg subsets in the immune system. ....	21
Table 3 Markers for characterization of Tregs in different actions.....	23
Table 4 Preliminary data of CD3 <sup>+</sup> CD4 <sup>+</sup> CD25 <sup>+</sup> CD127 <sup>-</sup> Tregs in DRESS and SJS/TEN patients.....	36
Table 5 The Tregs count from FAC-sorted and their yield of total RNA extraction.....	46
Table 6 Hybridization master mix for one nCounter® assay .....	48
Table 7 Clinical characteristics of DRESS patients, SJS/TEN patients, and healthy donor subjects.....	52
Table 8 The immunophenotype of Tregs from patients with DRESS, SJS/TEN, and healthy donors.....	57
Table 9 The suppressive function of Tregs shows as the percentage of inhibition. ....	71

## LIST OF FIGURES

	Page
Figure 1 Review of adverse drug reactions (ADRs).....	4
Figure 2 Types of hypersensitivity reaction.....	5
Figure 3 The interaction between inflammatory cells and the immune system in different mechanisms for small molecules or drugs. ....	9
Figure 4 The facial edema and skin rash in DRESS patients.....	12
Figure 5 Proposed pathogenic mechanisms in DRESS.....	13
Figure 6 The clinical courses of patients with DRESS.....	17
Figure 7 The differentiation dynamics of Tregs.....	20
Figure 8 The basic mechanisms of Tregs function to suppress an immune response.....	27
Figure 9 Schematic diagram of transcriptional regulation of the Foxp3 locus and cell signaling pathway of Tregs.....	29
Figure 10 The gating strategy of the complete 15-parameter staining for regulatory T cell characterization.....	55
Figure 11 The CD4 <sup>+</sup> CD25 <sup>+</sup> CD127 <sup>-</sup> FoxP3 <sup>+</sup> Treg population in PBMCs of healthy donors and SCARs patients at acute and recovery phases.....	56
Figure 12 The expression of PD-1 of CD4 <sup>+</sup> CD25 <sup>+</sup> CD127 <sup>-</sup> FoxP3 <sup>+</sup> Tregs.....	58
Figure 13 The expression of CTLA-4 of CD4 <sup>+</sup> CD25 <sup>+</sup> CD127 <sup>-</sup> FoxP3 <sup>+</sup> Tregs.....	59
Figure 14 The expression of GITR of CD4 <sup>+</sup> CD25 <sup>+</sup> CD127 <sup>-</sup> FoxP3 <sup>+</sup> Tregs.....	60
Figure 15 The expression of LAG-3 of CD4 <sup>+</sup> CD25 <sup>+</sup> CD127 <sup>-</sup> FoxP3 <sup>+</sup> Tregs.....	61
Figure 16 The expression of OX40 of CD4 <sup>+</sup> CD25 <sup>+</sup> CD127 <sup>-</sup> FoxP3 <sup>+</sup> Tregs.....	62
Figure 17 The expression of CD39 of CD4 <sup>+</sup> CD25 <sup>+</sup> CD127 <sup>-</sup> FoxP3 <sup>+</sup> Tregs.....	63
Figure 18 The expression of IL-10 of CD4 <sup>+</sup> CD25 <sup>+</sup> CD127 <sup>-</sup> FoxP3 <sup>+</sup> Tregs.....	64

Figure 19 The correlation between CD4 <sup>+</sup> CD25 <sup>+</sup> CD127 <sup>-</sup> Tregs and CD4 <sup>+</sup> CD25 <sup>+</sup> CD127 <sup>-</sup> FoxP3 <sup>+</sup> Tregs. ....	66
Figure 20 The purity of CD4 <sup>+</sup> CD25 <sup>+</sup> CD127 <sup>-</sup> Tregs in total isolated cells using flow cytometry. ....	68
Figure 21 The gating strategy for CFSE <sup>+</sup> cells to determine the proliferation cells. ....	69
Figure 22 The suppressive function of Treg was compared in the same group of donors at different effector T cells : Treg ratio, which shows the dose-dependent manner in every group. ....	70
Figure 23 Suppressive functional analysis of Tregs between DRESS and SJS/TEN patients at acute and recovery phases compared to healthy donors. ....	71
Figure 24 The variance vs. mean normalized signal plot across all targets/probes and the p-value distribution plots. ....	74
Figure 25 Differential gene expression analysis of Treg from SCARs patients compared to healthy donors. ....	76
Figure 26 Categorization of differential expressed genes (DEGs) in Tregs. ....	78
Figure 27 Gene expression profile associated with regulation of Tregs differentiation. ....	80
Figure 28 Gene expression profile associated with IL-2 mediated signaling pathway. ....	81
Figure 29 Gene expression profile associated with regulation of interleukin-10 production pathway. ....	83
Figure 30 Gene expression profile associated with JAK-STAT signaling pathway. ....	85

## LIST OF ABBREVIATIONS

ADRs	Adverse drug reactions
AGEP	Acute generalized exanthematous pustulosis
ANA	Antinuclear antibodies
APCs	antigen-presenting cells
BSA	body surface area
CD	Cluster of differentiation
CFSE	CarboxyFluorescein Succinimidyl Ester
CMV	cytomegalovirus
CTLA-4	Co-inhibitory receptor cytotoxic T lymphocyte antigen 4
CTLs	Cytotoxic T cells
DEGs	Differential expressed genes
DIHRs	Drug-induced hypersensitivity reactions
DRESS	Drug reaction with eosinophilia and systemic symptoms
EBV	Epstein-Barr virus
EM	Erythema multiforme
FACs	Fluorescence-activated cell sorting
FDE	Fixed drug eruption
FMO	Fluorescence Minus One
FoxP3	Forkhead box P3
FSC	Forward scatter
GITR	glucocorticoid-induced tumor necrosis factor receptor
GM-CSF	Granulocyte-monocyte colony-stimulating factor
GO	Gene ontology
GVHD	Graft-versus-host disease
HHV	Human herpesvirus
HLA	Human leukocyte antigens

IFN	Interferon
Ig	Immunoglobulin
IL	Interleukin
JAK	The Janus kinase
KEGG	The Kyoto Encyclopedia of Genes and Genomes
LAG3	Lymphocyte activation gene 3
MHC	Major histocompatibility complex
MPE	Maculopapular exanthema
NK cells	Natural killer cells
PBMCs	Peripheral blood mononuclear cells
pDCs	Plasmacytoid dendritic cells
RegiSCAR	The Registry of Severe Cutaneous Adverse Reaction
SCARs	Severe cutaneous adverse drug reactions
SEM	Standard error of mean
SJS	Stevens-Johnson syndrome
SLE	systemic lupus erythematosus
SSC	Side scatter
STAT	Signal transducer and activator of transcription
TCR	T-cell receptors
TEN	Toxic epidermal necrolysis
TGF	Transforming growth factor
ThaiSCARs	Thailand severe cutaneous adverse reactions
TNF	Tumor necrosis factor
Tregs	Regulatory T cells
WHO	World Health Organization

## CHAPTER I

### INTRODUCTION

Severe cutaneous adverse reactions (SCARs) are hypersensitivity reactions with potential death, that usually occur due to drug exposure which is consisted of g. It consists of Stevens-Johnson syndrome/toxic epidermal necrolysis (SJS/TEN), drug reaction with eosinophilia and systemic symptoms (DRESS), acute generalized exanthematous pustulosis (AGEP), and generalized bullous fixed drug eruptions (GBFDE). However, SJS/TEN and DRESS are symptoms that should be a concern because of their high rates of morbidity and mortality. DRESS and SJS/TEN have unique pathomechanisms, clinical courses, causative medications, and potential therapeutic approaches. Nowadays, the immunopathogenesis of DRESS and SJS/TEN remains unclear even though many hypotheses suggested include patients' genetic factors, the metabolic pathway of the drug, or even T-cell-mediated responses.

DRESS was reported to be almost 10% of the adverse drug reaction cases in Asia, with a mortality rate ranging from 3%-10%<sup>(1)</sup>. Many interesting points of DRESS have been noticed compared to SJS/TEN. Autoimmune manifestations have often been observed as long-term sequelae in the recovery phase of DRESS patients, including autoimmune thyroiditis, type 1 diabetes mellitus, systemic lupus erythematosus (SLE), and autoimmune hemolytic anemia<sup>(4)</sup>; which had no report in SJS/TEN.

The pathogenesis of DRESS is very complicated and still under investigation. But we know that both CD4 and CD8 T cells appear to be involved in the DRESS pathogenesis but play different roles. Moreover, the dynamics of regulatory T cells (Tregs) are considered to commit the diverse symptoms of DRESS due to their autoimmune sequelae during the recovery phase.



Many studies have reported that Tregs in the skin and circulation of DRESS patients were increased during the acute phase compared with other SCARs (such as SJS/TEN) and healthy donors. Whereas Tregs in the recovery phase of DRESS patients were reported dysfunctional even though there was an equal number of populations compared to SJS/TEN and healthy donors<sup>(5)</sup>. Moreover, many reports suggested Tregs were lower in number and functional properties in many autoimmune diseases from other causes<sup>(8)</sup>. Thus, the dysfunction and decrease in the population of Tregs can suggest that Tregs in DRESS can be associated with autoimmune photosynthesis in the recovery phase.

Accordingly, with the higher Tregs in the acute phase and the Treg impairment during the recovery phase of DRESS, we hypothesized that Tregs might play a significant role to caused autoimmune disease in DRESS patients during their acute and recovery phases. Therefore, this study focused on the association of Tregs immunophenotype and autoimmune sequelae of DRESS syndrome. Tregs immunophenotype in DRESS with autoimmune sequelae patients and DRESS without autoimmune sequelae patients were observed in both acute and recovery phases. Hopefully, this study will give more information about the pathogenesis of DRESS and its subsequent autoimmunity.

## CHAPTER II

### LITERATURE REVIEW

#### 2.1 Adverse drug reactions (ADRs)

The World Health Organization (WHO) has defined adverse drug reactions (ADR) as "a response to medicine which is noxious and unintended, and which occurs at doses normally used in man<sup>(9)</sup>." ADRs are common and classified into two types: on-target interaction (type A reaction) and off-target interaction (type B reaction). ADRs can occur from modulation of cellular processing after drug absorption, distribution, metabolism, and excretion, as well as drug transporter and the target receptor expression in an individual (Figure 1).

Due to the drug's pharmacological mechanism, on-target interaction can predict that a drug can interact with its intended receptor in a second tissue which is unintended tissue. This reaction occurs in about 75 - 80% of all ADRs. In contrast, off-target interaction is unpredictable and arises from other idiosyncratic reactions, including individual susceptibility (e.g., an enzyme defect) and immune-mediated ADRs, which can occur in about 20 - 25% of all ADRs<sup>(10, 11)</sup>.

There are two groups of immune-mediated ADRs: antibody-mediated (Gell-Coombs type I-III) and purely T cell-mediated (Gell-Coombs type IV).

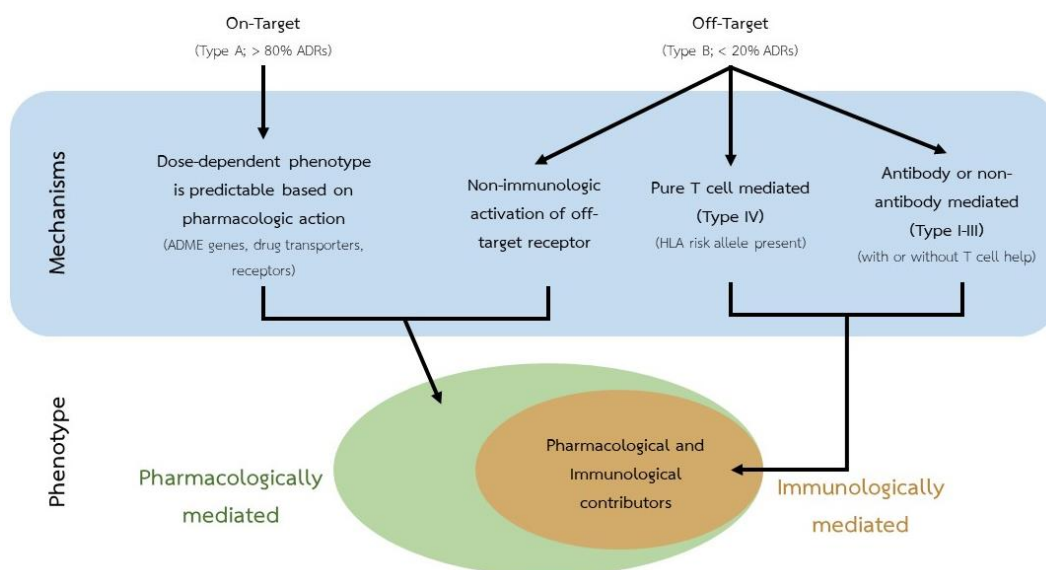


**Figure 1 Review of adverse drug reactions (ADRs).** (Modified from White, K.D., et al. 2015)<sup>(12)</sup>

### 2.1.1 Gell and Coombs's classification

The clinical symptoms of drug hypersensitivity occur from four categories of immune mechanisms proposed by Philip Gell and Robin Coombs in 1963<sup>(10, 13)</sup>, as shown in Figure 2.

Type I (IgE immediate) hypersensitivity or anaphylaxis is driven predominantly by immunoglobulin type E (IgE) produced from plasma cells bound to mast cells. This reaction usually has a short onset time, between minutes to hours. The degranulation of mast cells constantly releases many mediators (i.e., histamine) and causes vasodilation, exudative fluid outpouring, and goblet cell hyperplasia. This type of hypersensitivity may occur in only one symptom or collectively following clinical manifestation, including urticaria, angioedema, asthma, rhinitis, conjunctivitis, or even anaphylactic shock. For drug-sensitized patients, the reaction usually occurs within a few minutes to hours after receiving the suspected drug.

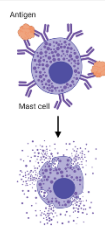
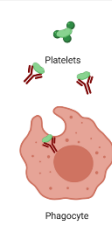
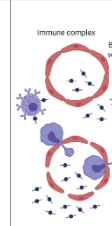
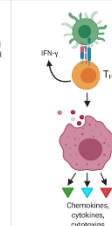
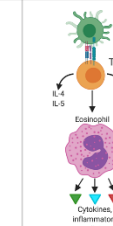
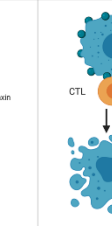
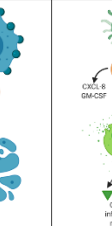
	Type I	Type II	Type III	Type IVa	Type IVb	Type IVc	Type IVd
Immune reactant	IgE	IgG	IgG	IFN- $\gamma$ , TNF- $\alpha$ (T <sub>H</sub> 1 Cells)	IL-5, IL-4/IL-13 (T <sub>H</sub> 2 Cells)	Perforin/granzyme B (CTL)	CXCL-8, IL-17, GM-CSF (T-cells)
Antigen	Soluble antigen	Cell-or matrix-associated antigen	Soluble antigen	Antigen presented by cells or direct T-cell stimulation	Antigen presented by cells or direct T-cell stimulation	Cell-associated antigen or direct T-cell stimulation	Soluble antigen presented by cell or direct T-cell stimulation
Effector	Mast cell activation 	FcR <sup>+</sup> cells (phagocytes, NK cells) 	FcR <sup>+</sup> cells complement 	Macrophage activation 	Eosinophils 	T-cells 	Neutrophils 
Example of hypersensitivity reaction	Allergic rhinitis, asthma, systemic anaphylaxis	Hemolytic anemia, thrombocytopenia (e.g., penicillin)	Serum sickness, Arthus reaction	Tuberculin reaction, contact dermatitis (with IVc)	Chronic asthma, chronic allergic rhinitis, Maculopapular exanthema with eosinophilia	Contact dermatitis, Maculopapular and bullous exanthema hepatitis	AGEP, Behcet's disease

Figure 2 Types of hypersensitivity reaction. (Modified from Sylvia (2014)<sup>(14)</sup> and created with BioRender.com).

Cytotoxic antibodies cause Type II (antibody-mediated) hypersensitivity. Cells can be damaged by IgM and IgG antibodies specific to the cells-or-matrix-associated antigen, which can bind to the cell surface of macrophages, neutrophils, and eosinophils via Fc receptors or bind to extracellular matrix antigen that activates the complement system.

Type III (immune complex-mediated) hypersensitivity occurs when antibodies (usually IgM) are specific for soluble antigens in blood-forming micro-precipitates that deposit in the blood vessel walls of various tissues, causing secondary damage to cells. This type of hypersensitivity is responsible for tissue injury in the lungs, joints, kidneys, and skin in sensitized patients. Moreover, serum sickness has also been

observed in this type and whenever the low-molecular-weight culprit drugs are administered.

For type IV (delayed) hypersensitivity, the symptoms are the results of lymphocyte stimulation, and cytokine release occurs when the allergen is presented to CD4<sup>+</sup> and CD8<sup>+</sup> T-lymphocytes by antigen-presenting cells (APCs). This type of hypersensitivity can develop the onset of symptoms in a few days to weeks and often shows skin eruptions in response to culprit drugs, cosmetics, and environmental chemicals.

The term 'drug-induced hypersensitivity reactions (DIHRs)' is in type IV hypersensitivity that accounts for 5 - 10% of all ADRs. The specific functions of drug-activated T-cells are essential for this mechanism. However, type IV reactions can be subclassified into IVa-IVd reactions according to their cytokine pattern and the different immune cells activation<sup>(15-17)</sup>.

Type IVa reaction occurs when T helper 1 (Th1) cells activate macrophages by interferon (IFN)- $\gamma$  secretion and drive the production of complement-fixing antibody isotypes (IgG1, IgG3). Moreover, the Th1 cells are co-stimulatory for pro-inflammatory responses such as tumor necrosis factor (TNF) family and interleukin (IL) – 2. They can activate CD8<sup>+</sup> T-cells, which might explain the combination of high IFN- $\gamma$  values<sup>(15)</sup>.

Type IVb reaction occurs when Th2 T-cells secrete IL-4, IL-13, and IL-5 cytokines to promote B cells to produce IgE and IgG4. Eosinophilic inflammation can be induced by IL-5, which can be observed in eosinophil-rich maculopapular exanthema and DRESS. Moreover, IL-4/IL-13 can boost IgE production, which can link to type I reaction.

Type IVc represents when the effector T cells migrate to the tissue. effector T cells can produce cytotoxic molecules (perforin, granzyme B, and FasL) to induce the death of cells, including hepatocytes or keratinocytes. This type of hypersensitivity is often the complication with type I reaction and activates the recruitment of monocyte, eosinophil, or PMN. Type IVc reaction plays a role in maculopapular or bullous skin diseases, neutrophilic inflammations, and contact dermatitis, as well as responsible for most drug-induced delayed hypersensitivity reactions found in SJS/TEN<sup>(10, 15, 18)</sup>.

Type IVd is responsible for sterile neutrophilic inflammation via T-cell-derived chemokine (C-X-C motif) ligand 8 (CXCL-8) and granulocyte-monocyte colony-stimulating factor (GM-CSF). The secretion of IL-17 and IL-22 from Th22 cells can stimulate the production of CXCL8<sup>(19)</sup>. Neutrophils can be recruited to the skin lesion by CXCL8. Additionally, the apoptosis of neutrophils can be interfered with by GM-CSF, resulting in the accumulation of neutrophils in the lesion<sup>(16, 20)</sup>.

## 2.2 Severe cutaneous adverse drug reactions (SCARs)

Skin eruptions from drug-induced hypersensitivity can range from mild skin involvement to SCARs, illustrated in Figure 3 Mild skin involvement includes maculopapular exanthema (MPE) and fixed drug eruption (FDE). MPE is usually observed as a flat rash and appears red in lighter-skinned people, and is described as an erythematous rash. It can be classified by generalized, widespread flat (macular) spots or raised bumps (papular) on the skin's surface. FDE is a skin inflammation that develops as a local annular or an oval rash that can recur at the same site after re-exposure to the same culprit drug.

SCARs comprise acute generalized exanthematous pustulosis (AGEP), DRESS, SJS, and TEN. They are considered from the extensive eruption, possibly cause systemic symptoms, and are responsible for severe chronic sequelae, which are life-threatening conditions.

AGEP is classified as one of the SCARs but less severe than others. AGEP develops numerous small pinhead-sized non-follicular pustules on an erythematous<sup>(16)</sup>. Drug-induced AGEP is about 90% of drug-induced SCARs, and antibiotics such as  $\beta$ -lactams and macrolides are the primary culprit, with approximately a 1% mortality rate<sup>(21)</sup>.

DRESS and SJS/TEN are also considered a type of SCARs that affect the skin and mucosal membrane with a life-threatening condition. SJS/TEN's mortality rate depends on the severity ranging between 10-40%<sup>(22)</sup>. Allopurinol and its metabolic form are the most common agent that causes SJS and TEN, followed by anticonvulsant drugs such as carbamazepine and phenytoin<sup>(23)</sup>.

The severity of skin lesions in SJS/TEN has been suggested in the hypothesis of cytotoxic reaction from CTLs and NK cells. Aggressive skin necrosis occurs from three major classes of cytotoxic protein, including Fas-Fas ligand (FasL), perforin/granzyme B, and granulysin<sup>(24)</sup>. The prognostic prediction can be given by the Score for Toxic Epidermal Necrolysis (SCORTEN)<sup>(25)</sup> and the algorithm for assessment of drug causality in Stevens-Johnson Syndrome and toxic epidermal necrolysis (ALDEN)<sup>(26)</sup>.

Although SCARs are rare, they can cause severe morbidity, and the mortality rate among symptoms is high. SCARs affect approximately 2% of hospitalized patients with a prevalence per year of 2-7 cases/million drug exposure cases in SJS/TEN and 1/1,000 to 1/10,000 drug exposure cases in DRESS syndrome<sup>(23, 27)</sup>.

However, many reports in epidemiology propose that age and sex have no benefit in distinguishing between DRESS and SJS<sup>(28, 29)</sup>. Since DRESS and SJS/TEN are the SCARs that affected the severe clinical manifestation and patient's motility. We focused on DRESS syndrome in our study and be reviewed below. Additionally, we used SJS/TEN patients as a comparative group because SJS/TEN is one of the SCARs phenotypes with high severity but clinical characteristics without autoimmune sequelae.

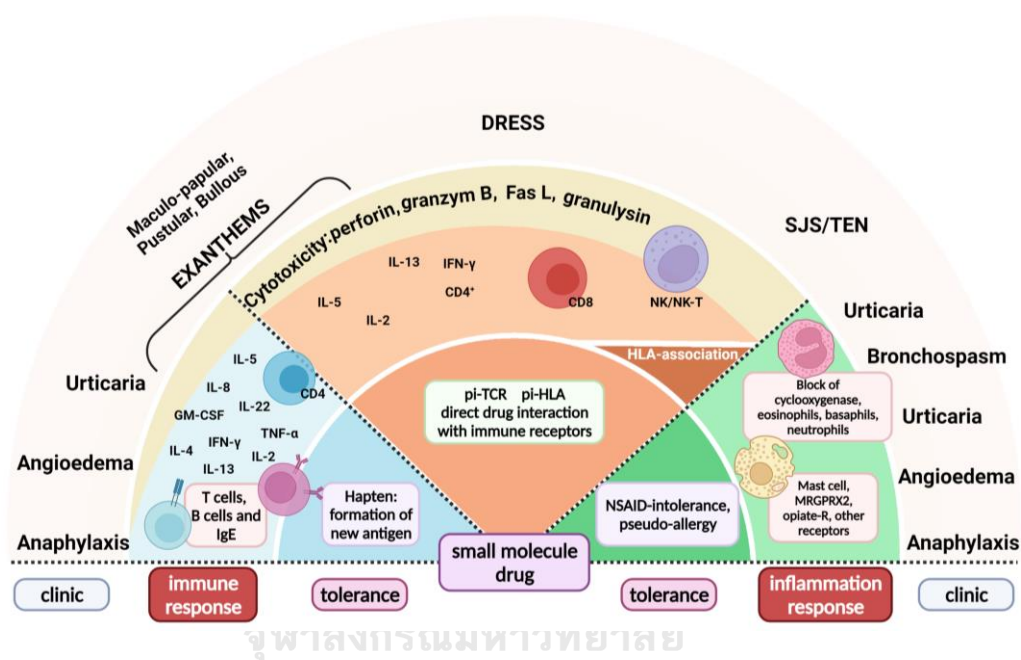


Figure 3 The interaction between inflammatory cells and the immune system in different mechanisms for small molecules or drugs. Modified from Pichler and Yerly (2018)<sup>(30)</sup> and created with BioRender.com.

## 2.2 Drug reaction with eosinophilia and systemic symptoms (DRESS)

### 2.2.1 Etiology, risk factors, and epidemiology

Many drugs are considered the cause of DRESS syndrome, but aromatic anticonvulsants, especially phenytoin, carbamazepine, and phenobarbital, are often



reported as common causes<sup>(31)</sup>. Moreover, antimicrobial, antiviral, antipyretic, and other drugs have been suggested as the causative agent of DRESS.

Although several hypotheses in the pathogenesis of DRESS have been suggested, the complete mechanism has not been clarified. Drug dosage, drug metabolism, drug antigen presentation, genetic factors such as human leukocyte antigen (HLA haplotype), host immunological properties, and environmental factors are considered to have a role in DRESS pathogenesis. The mutation of the drug detoxification enzyme leads to the gradual gathering of reactive drug metabolites, which can induce a higher risk of DRESS, especially in black patients<sup>(31)</sup>. Cytochrome P450 (CYP-450) system is responsible for several anticonvulsant agent metabolisms via epoxide hydroxylase or glutathione transferase detoxification. The mutation of epoxide hydroxylase and slow N-acetylator phenotype may gain the accumulation of toxin metabolites and evoke the immunological response<sup>(31)</sup>.

The predicted risk with the first or second prescription of an aromatic antiepileptic is roughly 1:1000-1:10,000, although this largely depends on the individual's ethnic background. The incidence rates were reported to be 3.89 per 10,000 inpatients in Spain and 0.9 per 100,000 individuals in a West Indian population. Moreover, prevalence estimates were reported to be 2.18 per 100,000 in the United States and 9.63 cases per 100,000 inpatients in Thailand<sup>(32, 33)</sup>.

### **2.2.2 Clinical manifestation**

The symptom features may appear with a long latent period ranging from 3 to 8 weeks after starting drug treatment. The clinical manifestation of DRESS syndrome is presented subsequently with high fever (38.5 °C), widespread skin rash, internal organ involvement, and possible frequent reactivation of human herpesviruses (HHVs)<sup>(4, 23)</sup>. The syndrome's onset occurs 3 weeks – 3 months after

starting drug administration<sup>(34)</sup>. The rapid onset and severity of the symptoms may increase upon re-exposure to the culprit drug. Skin lesions are usually present in 73-100% of the patients with no specific features. Still, they can spread and cover more than half of the body surface area (BSA), especially the face, which can be found in 76% of the patients<sup>(4)</sup>. Erythroderma can even be developed, but skin necrosis is rarely observed and is mainly restricted to the wrist area (Figure 4).

In the early stage of the syndrome, some patients may have the symptom of dysphagia according to the swelling of both sides of salivary glands. The enlarged lymph node is also often found in the cervical, axillary, or inguinal region<sup>(35)</sup>. The laboratory finding reported hypereosinophilia in 66-95% of patients and atypical lymphocytosis in 27-67% of the patients. These laboratory findings are considered unique features of this syndrome<sup>(36)</sup>. According to eosinophil granule proteins released, which are toxic to many tissues, multiple internal organ damage is often observed. Liver involvement is usually observed more than others and has been reported between 75-94% of the patients. Renal injury occurs in around 12-40% of the patients<sup>(4, 36)</sup>. The involvement of the other organs can be reported but not often, including pulmonary, cardiac, neurologic, gastrointestinal, and endocrine abnormalities.



**Figure 4** The facial edema and skin rash in DRESS patients. Photo of a DRESS inpatient at King Chulalongkorn Memorial Hospital. The patient had been informed and gave consent to use his picture in our study.

### 2.2.3 Pathophysiology

Significant advancements in the understanding of DRESS pathogenesis have recently been made. Although the pathophysiology of DRESS is complex and mostly unexplored, it is posited that DRESS is caused by a complicated interplay of drug (or vaccine or biologic) exposure, genetic predisposition, and viral reactivation<sup>(32, 33)</sup>. DRESS is a severe T cell-mediated drug reaction characterized as a delayed-type IVb, and occasionally IVc, hypersensitivity reaction.

The activated CD4<sup>+</sup> T cells have been proposed to have an essential role in the pathogenesis of DRESS<sup>(5)</sup>. Still, a significant decrease in the population of CD56<sup>+</sup> NK cells and CD19<sup>+</sup> B cells, as well as the level of the immunoglobulin in DRESS patients' sera at the acute phase, were observed that refer to the immunosuppressive response<sup>(37, 38)</sup>. Many cytokines such as IFN- $\gamma$  and IL-5 have been secreted from activated drug-specific T cells stimulated by an anticonvulsant agent such as carbamazepine, phenytoin, lamotrigine; and other drugs, including

sulfamethoxazole<sup>(39, 40)</sup>. Thus, the eosinophilia usually reported in DRESS patients has been responsible for IL-5 elevation.

Moreover, the CD4<sup>+</sup>CD25<sup>+</sup> FoxP3<sup>+</sup> Tregs population increased in the acute phase<sup>(5, 6)</sup>. This population of lymphocyte subset has returned to the baseline level as in the healthy control after clinical recovery. Nevertheless, the characterization of DRESS at the acute phase (days 3-10) can be considered by the expansions of totally functional Tregs corresponding with the reactivation of herpesviruses, but eventually, the progressive loss of Tregs function can be characterized in the sub-acute phase (days 11-36)<sup>(5)</sup>.

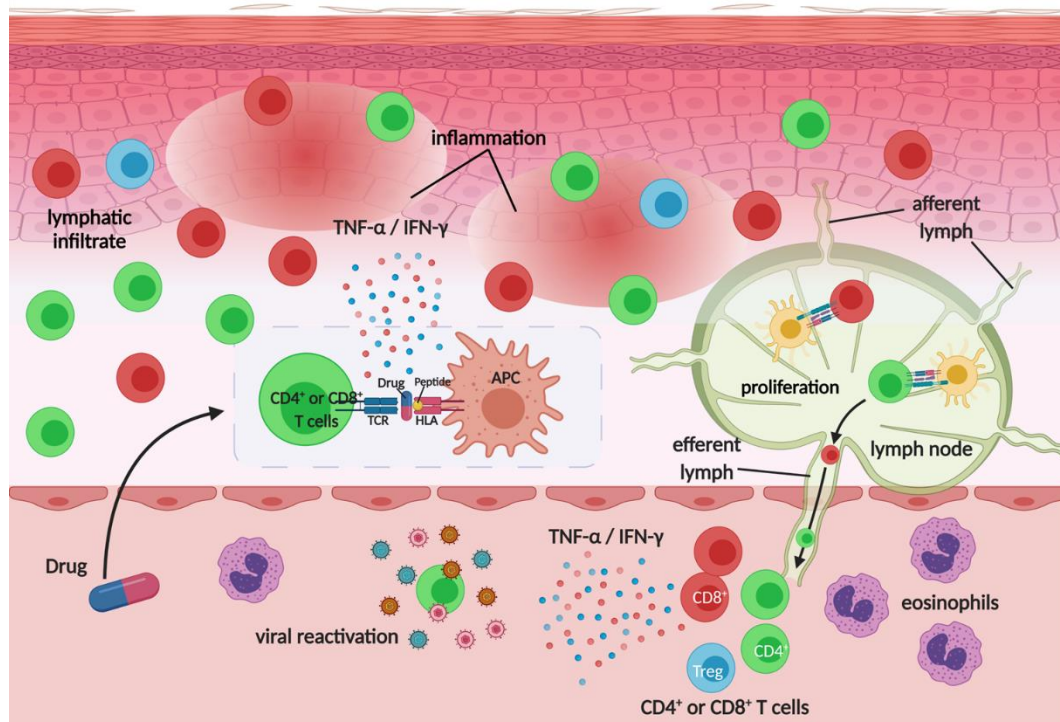


**Figure 5 Proposed pathogenic mechanisms in DRESS.** Modified from Peter et al. (2017)<sup>(41)</sup> and created with BioRender.com.

A report also showed that plasmacytoid dendritic cells (pCDs) in the circulation of DRESS patients with HHV-6 reactivation elevated the expression around

skin eruption<sup>(42)</sup>. IgG for antiviral defense has been induced by IFN- $\alpha$ , which can be produced from pDCs. So, the decrease of pDCs in the circulation of the patients can lead to the reduction of antiviral response.

Although human herpesvirus family reactivation, including cytomegalovirus (CMV), Epstein-Barr virus (EBV), HHV-6, and HHV-7, has been reported in many SCARs patients, many previous study report that HHV-6 is remark as an essential and characteristic feature with a frequency of 43-100% of DRESS patients<sup>(3, 43)</sup>. The elevated IgG anti-HHV6 and HHV-6 DNA copies showed the reactivation of the virus had usually been detected 2-3 weeks after the onset of skin rash. The study by Chen *et al.*<sup>(43)</sup> showed that pro-inflammatory cytokines and chemokines, including IL-1 $\beta$ , IL-2, IL-6, IFN- $\gamma$ , and TNF- $\alpha$ , were lower in DRESS patients with HHV-6 reactivation when compared to the patients without reactivation. In addition, Ishida *et al.*<sup>(3)</sup> showed that HHV-6 DNA copies in DRESS patients with systemic corticosteroid treatment are significantly higher than in those who had not received them.

#### 2.2.4 Diagnosis

The diagnosis of DRESS syndrome should be processed with care and attentively observation according to their very familiar presentation of many symptoms. There is also still no reliable standard for the diagnosis. Therefore, many diagnostic criteria have been developed, but the RegiSCAR group proposes the most used criteria in the scoring system (Table 1). The total score is used to diagnose the DRESS, including <2 points being considered as not DRESS case; 2-3 points as a possible case; 4-5 points as a probable case; and >5 points as a definite case<sup>(4)</sup>.

Table 1 Diagnostic criteria in the scoring system for DRESS by the RegisSCAR <sup>(44)</sup>

Items	Score			Comments
	-1	0	1	
Fever $\geq 38.5$ °C	N/U	Y		
Enlarged lymph nodes		N/U	Y	>1 cm and 2 different areas
Eosinophilia $\geq 0.7 \times 10^9/L$ or $\geq 10\%$ if WBC $< 4.0 \times 10^9/L$		N/U	Y	Score 2, when $\geq 1.5 \times 10^9/L$ or $\geq 20\%$ if WBC $< 4.0 \times 10^9/L$
Atypical lymphocytosis		N/U	Y	
Skin rash				Rash suggesting DRESS: 2 symptoms:
- Extent > 50% of BSA		N/U	Y	purpuric lesions (other than legs),
- Rash suggests DRESS	N	U	Y	infiltration, facial edema, psoriasiform desquamation
Skin biopsy suggesting DRESS	N	Y/U		
Organ involvement		N	Y	Score 1 for each organ involvement, maximal score: 2
Rash recovery $\geq 15$ days	N/U	Y		
Excluding other causes		N/U	Y	Score 1 if 3 tests of the following tests were performed and all were negative: HAV, HBV, HCV, Mycoplasma, Chlamydia, ANA, blood culture

WBC: white blood cell; ANA: antinuclear antibody; BSA: body surface area; HAV: hepatitis A virus; HBV: hepatitis B virus; HCV: hepatitis C virus; N: no; U: unknown; Y: yes.

### 2.2.5 Management

Discontinuing the suspected drug is the primary procedure to manage DRESS. The treatment with systemic corticosteroids has been used as a mainstay treatment for DRESS patients<sup>(4)</sup>. According to the prolonged symptoms in DRESS, systemic corticosteroids usually be treated over 2-3 months which can produce a higher rate of opportunistic infections and many more consequences. Intravenous immune globulin (IVIG) and antiviral treatment are other treatment options.

### 2.2.6 Outcome and sequelae

DRESS syndrome has a more extended latency than other types of SCARs, usually more than 15 days. The study of Start *et al.*<sup>(45)</sup> showed that 7 of the 32 patients (22%) had prolonged symptoms more than 90 days after onset, lasting until 6 months was 4 cases (13%) and even up to 1 year in 3 cases (9%). After all the conditions, it is quite obvious that DRESS is a life-threatening condition with a mortality rate of around 10%<sup>(4)</sup>. Long-term sequelae are reported with a rate of 10-35% within a year after the onset of DRESS<sup>(46-48)</sup> and can be divided into 2 major types according to different age groups. Elderly patients are more vulnerable to ending with organ failure due to suffering from internal organ damage between the onsets of DRESS and their recovery phase. However, young patients are prone to develop autoimmune diseases. Autoimmune thyroid diseases, including Graves' disease, Hashimoto's thyroiditis, and painless thyroiditis, are DRESS's most frequent long-term sequelae. Nevertheless, other autoimmune diseases have been reported, including Fulminant type 1 diabetes mellitus, SLE, and autoimmune hemolytic anemia<sup>(4)</sup>. Although the mechanism for the autoimmune disease development is still unknown, it has been suggested that they might be due to the dysfunctional Tregs in the recovery phase of DRESS<sup>(5)</sup> (Figure 6).

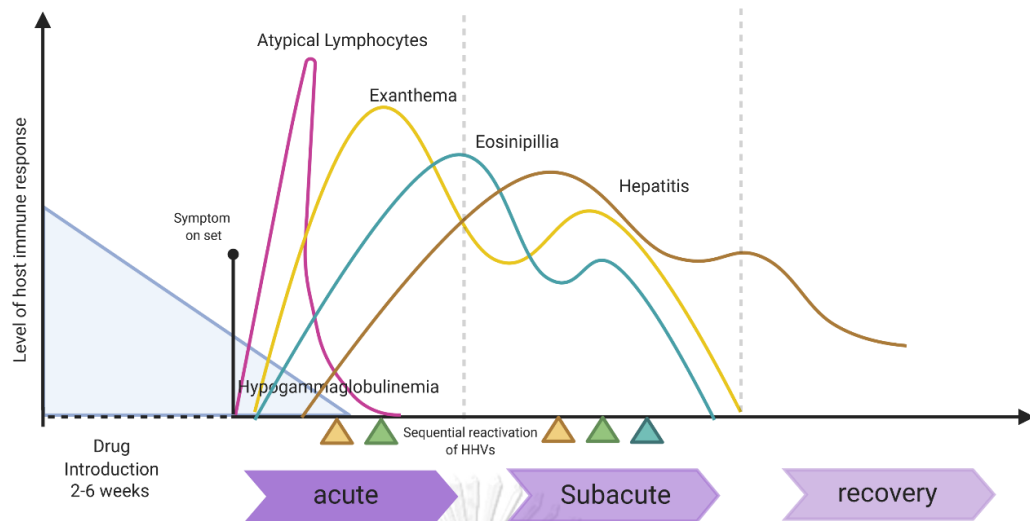


**Figure 6** The clinical courses of patients with DRESS. Modified from: Cho et al., 2017<sup>(4)</sup>; Descamps & Ranger-Rogez, 2014<sup>(32)</sup>; Criado et al., 2012<sup>(49)</sup> and created with BioRender.com.

### 2.3 Regulatory T cells (Tregs)

Regulatory T cells (Tregs) are specialized cells that are essential for immune response modulation by maintaining peripheral tolerance and immune homeostasis<sup>(50)</sup>. Tregs account for 5-10% of the CD4<sup>+</sup> T cells in healthy human peripheral blood<sup>(51)</sup>.

#### 2.3.1 Differentiation dynamics of Tregs

Tregs heterogeneity depends on their origin, differentiation, migration characteristics, and TCR specificity and affinity. The Thymic Tregs (tTregs) can develop ontogenetically in the thymus, whereas the peripheral Treg (pTregs) or Induced Treg (iTreg) can derive from effector cells. tTregs contain a T cell receptor (TCR) with sufficiently high autoaffinity with a constitutive FoxP3 expression. These cells predominate in the lymph nodes and circulatory system, essential in establishing tolerance to autoantigens. Moreover, pTregs are more frequently found in the peripheral barrier tissue, significantly limiting local inflammation when exogenous



antigens are presented<sup>(52)</sup>. The stability of FoxP3 expression in varied circumstances distinguishes tTregs from pTregs. It has been discovered that FoxP3, expressed by pTregs, is transitory during inflammation. Therefore, pTregs can differentiate into exFoxP3 effector cells with the phenotype of Th-17 lymphocytes (RORyt<sup>+</sup>), which are pathogenic for autoimmunity.

tTregs can be classified as naive cells (nTregs), central memory cells (cmTregs), effector memory cells (emTregs), and effector Treg (eTreg) lymphocytes based on their differentiation. CCR7 and CD62L molecules allow Tregs to home into secondary lymphoid organs. Tregs can function in various tissues and inflammatory areas, which is why their development is related to the acquisition of chemokine receptors and adhesion molecules involved in directed homing. For instance, CXCR3, LFA-1, VLA-4, CCR2, CCR5, CCR6, and CCR8 are essential for migration to inflammatory zones, while GPR-15 is for migration to the intestines. Moreover, future skin resident Tregs express Cxcr3 and Itgb-1 (which produce integrin-b1) since they are in the shoulder lymph nodes before migrating to the skin<sup>(52-54)</sup> (Figure 7).

Tregs and naive CD4<sup>+</sup> conventional T cells (Tconv) exhibit non-overlapping TCR repertoires, and a limited number of equal affinity TCRs are detected in both CD4<sup>+</sup> and Treg cell populations. Tregs and naive CD4<sup>+</sup> Tconv cells exhibit non-overlapping TCR repertoires, and a limited number of equal affinity TCRs are detected in both CD4<sup>+</sup> and Treg cell populations. Then, the TCR repertoires of tTregs and pTregs cells have been demonstrated to be distinct: the TCR repertoire of tTreg is oriented toward self-recognition, but TCRs generated in pTreg can detect foreign antigens with high affinity<sup>(55)</sup>. Furthermore, suppressive mechanisms of Tregs have recently been found to differ if the cells share specificity but differ in TCR affinity. High-affinity Tregs primarily increase the expression of TCR-dependent regulatory molecules such as CTLA-4, TIGIT, and IL-10, whereas cells with a low-affinity receptor

produce more Ebi3, which is responsible for IL35-mediated suppressive activity. In addition to Ebi3, Tregs with low-affinity TCR create amphiregulin, a growth factor in tissue regeneration. Nonetheless, both Tregs have suppressive potential and aid the autotolerance and immunological balance<sup>(56, 57)</sup>.

### 2.3.2 Tregs subsets and their immunophenotype markers

Although many subsets of Tregs have been identified so far<sup>(58)</sup>, the five main types of CD4<sup>+</sup> Treg have been determined, including natural Tregs (nTregs), inducible Tregs (iTregs), IL-10-producing Tregs (Tr1), transforming growth factor (TGF)- $\beta$ -producing CD4<sup>+</sup> Treg (Th3 Tregs), IL-17 producing FoxP3<sup>+</sup> Tregs and CD8<sup>+</sup> Tregs. These subsets are derived from naïve T cells under various conditions, making Tregs one of the most complicated T cell groups. The subset of Tregs is presented in Table 2. However, the new subsets of Tregs will be further investigated, and It is quite challenging to comprehend why there are so many different subsets required.

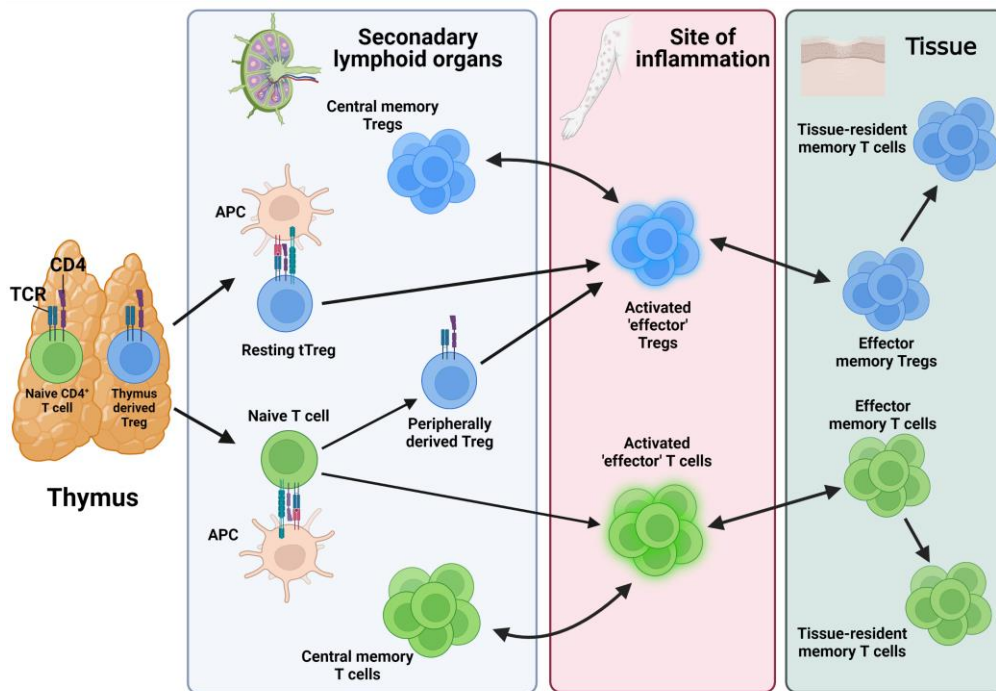


Figure 7 The differentiation dynamics of Tregs. Modified from Shevryev and Tereshchenko (2020)<sup>(52)</sup> and created with BioRender.com.

Table 2 Types of Treg subsets in the immune system. (58, 59)

Subset	Identifying Marker	Secretory product	Function	Location
Thymic Treg (tTreg)/Naive Treg (nTreg)	CD4 <sup>+</sup> CD25 <sup>+</sup> CD127 <sup>lo</sup> FoxP3 <sup>+</sup> CD45RA <sup>+</sup> CCR7 <sup>+</sup> CD62L <sup>+</sup> CTLA-4 <sup>-</sup>	IL-10, TGF- $\beta$ , Granzyme B, Perforin	Block T cell proliferation; suppression of DCs; inhibition of effector Th1, Th2, and Th17 cells; eliminate the production of allergen-specific IgE; induce IgG4 secretion; suppress mast cells, basophils, and eosinophils; interact with resident tissue cells and participate tissue remodeling	Thymus
Activated Treg (aTreg)/Effector Treg (eTreg)	CD4 <sup>+</sup> CD25 <sup>+</sup> CD127 <sup>lo</sup> FoxP3 <sup>+</sup> CD45RA <sup>+</sup> CCR7 <sup>+</sup> CD62L <sup>-</sup> CTLA-4 <sup>+</sup>	Similar to nTreg	Similar to nTreg	Peripheral/site of inflammation
Peripheral Treg (pTreg)/Induced Treg (iTreg)	CD4 <sup>+</sup> CD25 <sup>+</sup> CD127 <sup>lo</sup> FoxP3 <sup>+</sup> CD45RA <sup>+</sup> CCR7 <sup>+</sup> CD62L <sup>-</sup> CTLA-4 <sup>+</sup>	Similar to nTreg	Similar to nTreg	Peripheral/site of inflammation
Central memory Treg (cmTreg)	CD4 <sup>+</sup> CD25 <sup>+</sup> CD127 <sup>lo</sup> FoxP3 <sup>+</sup> CD45RA <sup>+</sup> CCR7 <sup>+</sup> CD62L <sup>+</sup>	To be determined (TBD)	Differentiation dynamics between eTreg	Thymus
Effector memory Treg (emTreg)	CD4 <sup>+</sup> CD25 <sup>+</sup> CD127 <sup>lo</sup> FoxP3 <sup>+</sup> CD45RA <sup>+</sup> CCR7 <sup>+</sup> CD62L <sup>-</sup> CTLA-4 <sup>+</sup>	To be determined (TBD)	Differentiation dynamics between eTreg	Peripheral tissue
Interleukin (IL)-10-producing type 1 Treg (Tr1 cell)	CD4 <sup>+</sup> CD25 <sup>+</sup> FoxP3 <sup>-</sup>	IL-10	Suppress effector Th cell migration and functions; suppress mast cells, basophils, and eosinophils	Generated from non-Treg cell precursors and home lungs and draining lymph nodes

Table 2 Types of Treg subsets in the immune system. (58, 59)

Subset	Identifying Marker	Secretory product	Function	Location
TGF- $\beta$ -producing Th3 Treg (Th3 Treg)	CD4 <sup>+</sup> CD69 <sup>+</sup> FoxP3 <sup>-</sup>	TGF- $\beta$ , IL-10	Similar to Tr1	A subset of T lymphocytes with immunoregulatory and immunosuppressive functions in peripheral tissue
IL-17-producing FoxP3 <sup>+</sup> Treg	CD4 <sup>+</sup> FoxP3 <sup>+</sup> CCR6 <sup>+</sup> RORGT <sup>+</sup>	IL-17	Inhibit the proliferation of CD4(+) effector T cells	Differentiated from CD4 <sup>+</sup> Foxp3 <sup>+</sup> CCR6 <sup>+</sup> Tregs in peripheral blood and lymphoid tissue
CD8 <sup>+</sup> Treg	CD8 <sup>+</sup> FoxP3 <sup>+</sup> CD28 <sup>+</sup> CD25 <sup>+</sup> (not for tonsil origin)	IL-10, TNF- $\alpha$ , IFN- $\gamma$ , Granzyme B	Block activation of naive or effector T cells; suppress responses; , IL-4 expression and the proliferation of CD4 <sup>+</sup> T cells.	Generated from OT-1 CD8 cells and tonsils

Table 3 Markers for characterization of Tregs in different actions. <sup>(60)</sup>

Action	Marker	Localization
Involved in the development of the Treg phenotype	FoxP3	Nucleus
	Helios	Nucleus
Involved in Tregs regulatory activity and markers of active Tregs	IL-2 receptor (CD25)	Membrane (the level of expression is crucial)
	CTLA-4	Membrane (but detectable only intracellularly)
	TGF- $\beta$	Cytoplasm
	IL-10	Cytoplasm
	Granzyme B	Cytoplasm
	Perforin	Cytoplasm
	IL-35	Cytoplasm
	E5NT (CD73)	Cytoplasm
	ENTPD1 (CD39)	Membrane
	PD-1 ligand (PD-L1)	Membrane
	Other markers of active Tregs	Membrane
Involved in tTregs differentiation	GITR (CD357)	Membrane
	T-cell Ig and mucin domain protein-3 (Tim-3)	Membrane
	Galectin-9	Membrane
	ICOS (CD278)	Membrane
	latency-associated peptide (LAP)	Membrane
	CD69 (C-type lectin receptor)	Membrane
	IL-2 receptor (CD25)	Membrane
	GITR (CD357)	Membrane
	OX40 (CD134)	Membrane

Table 3 Markers for characterization of Tregs in different actions. <sup>(60)</sup>

Action	Marker <sup>1</sup>	Localization
	TNFR2	Membrane
<b>Involved in pTregs differentiation/expansion and tTregs expansion</b>	IL-2 receptor (CD25) CD28 GITR (CD357) OX40 (CD134) ICOS (CD278) LAG-3 (CD223) Programmed cell death (PD)-1 PD-1 ligand (PD-L1) CD226 CD69 (C-type lectin receptor)	Membrane Membrane Membrane Membrane Membrane Membrane Membrane Membrane Membrane Membrane
<b>Involved in inhibition of Tregs activity</b>	GITR (CD357) OX40 (CD134) 4-1BB (CD137)	Membrane Membrane Membrane
<b>Other markers</b>	CD45R0 (memory marker) CD45RA (naïve marker) Neuropilin-1 (VEGF receptor) CD49b	Membrane Membrane Membrane Membrane
<b>Not expressed by Tregs</b>	IL-7 receptor (CD127) CD49d	Membrane Membrane

Discovering distinguishing cell-surface markers for identifying and separating Tregs has consistently been challenging. Although there are promising markers for mice Tregs, this aim for human Tregs has remained elusive. Tregs in mice and humans have traditionally been identified as CD4<sup>+</sup>CD25<sup>+</sup> (also known as IL-2R). Indeed, by staining for CD4<sup>+</sup>CD25<sup>+</sup>CD45RB<sup>low</sup> expression, mouse Tregs can be efficiently separated. However, because T cells upregulate CD25 expression when activated, the purity of isolated human Tregs has always been a concern<sup>(61)</sup>.

Soon afterward, other markers were introduced to facilitate the identification of Tregs. The CD4<sup>+</sup>CD25<sup>+</sup>FoxP3<sup>+</sup> expressions were also used to identify Tregs in humans. Even though forkhead box P3 (FOXP3) has been identified as a major regulator of Tregs formation and function in mice, many activated (non-regulatory) human T cells express FOXP3, making it ineffective as a marker for human Tregs. Moreover, a low level of CD127 expression in human Tregs was characterized and used as a marker to distinguish Tregs from Tconv<sup>(62, 63)</sup>. In addition, the co-inhibitory receptor cytotoxic T lymphocyte antigen 4 (CTLA-4) and glucocorticoid-induced tumor necrosis factor receptor (GITR) can also be used to characterize the population<sup>(8)</sup>.

Even though many studies suggest the Tregs characteristics, as mentioned in Table 3, the use of CD4, CD25, CD127, and FoxP3 are classical combined markers for Tregs characterization in the present<sup>(64)</sup>. Therefore, we would use the CD4<sup>+</sup>CD25<sup>+</sup>CD127<sup>+</sup>FoxP3<sup>+</sup> expression as Treg characterization in this study because it could represent the majority type of Tregs in the human circulatory system<sup>(58, 59)</sup>.



### 2.2.3 Functions of Tregs

Even though many subsets of Tregs are under-investigated in their function, the general activities for Treg cells have been proposed, including developing and maintaining immunologic self-tolerance, which can prevent autoimmune diseases, suppressing the hypersensitivity reactive, and suppression of weakly stimulating-induced T-cell activation.

The immune-suppressing mechanisms of Tregs have been proposed shown in Figure 8<sup>(61)</sup>. First, the secretion of inhibitory cytokines, including IL-10, IL-35, and TGF- $\beta$ , suppresses the activation and proliferation of effector T cells. Effector B cells and NK cells. The secretion of cytotoxic enzymes, including granzymes and perforin, induces the apoptosis of CD4<sup>+</sup> effector T cells. Then, the high-level expression of CD25, IL-2 receptor- $\alpha$ , empowers Tregs to devour local IL-2 and causes CD4<sup>+</sup> effector T cells death by cytokine withdrawal. Tregs are also suppressive by interrupting the metabolism of CD4<sup>+</sup> effector T cells. The expression of ectoenzyme CD39 and CD73 can generate adenosine and activate the adenosine receptor 2A (A2AR) by transferring the inhibitory cyclic AMP (cAMP) via gap junction to CD4<sup>+</sup> effector T cells. Tregs might suppress the maturation and function of DCs by expressing CTLA-4. The interaction between CTLA-4 and CD80/CD86 can activate the indoleamine 2, 3-dioxygenase (IDO) in DCs that can induce the suppression of CD4<sup>+</sup> T cells via pro-apoptotic metabolism. In addition, DCs maturation might be blocked by lymphocyte activation gene 3 (LAG3 or CD223), a CD4 homolog which high-affinity binding to MHC class II. The interaction between LAG3 and MHC class II can induce the immunoreceptor tyrosine-based activation motif (ITAM)-mediated inhibitory signaling pathway to suppress the maturation and the immunostimulatory properties of DCs. Moreover, Tregs can suppress the function of autoreactive B cells via PD-1/PD-L1 signaling (Figure 8)<sup>(52, 61, 64)</sup>.

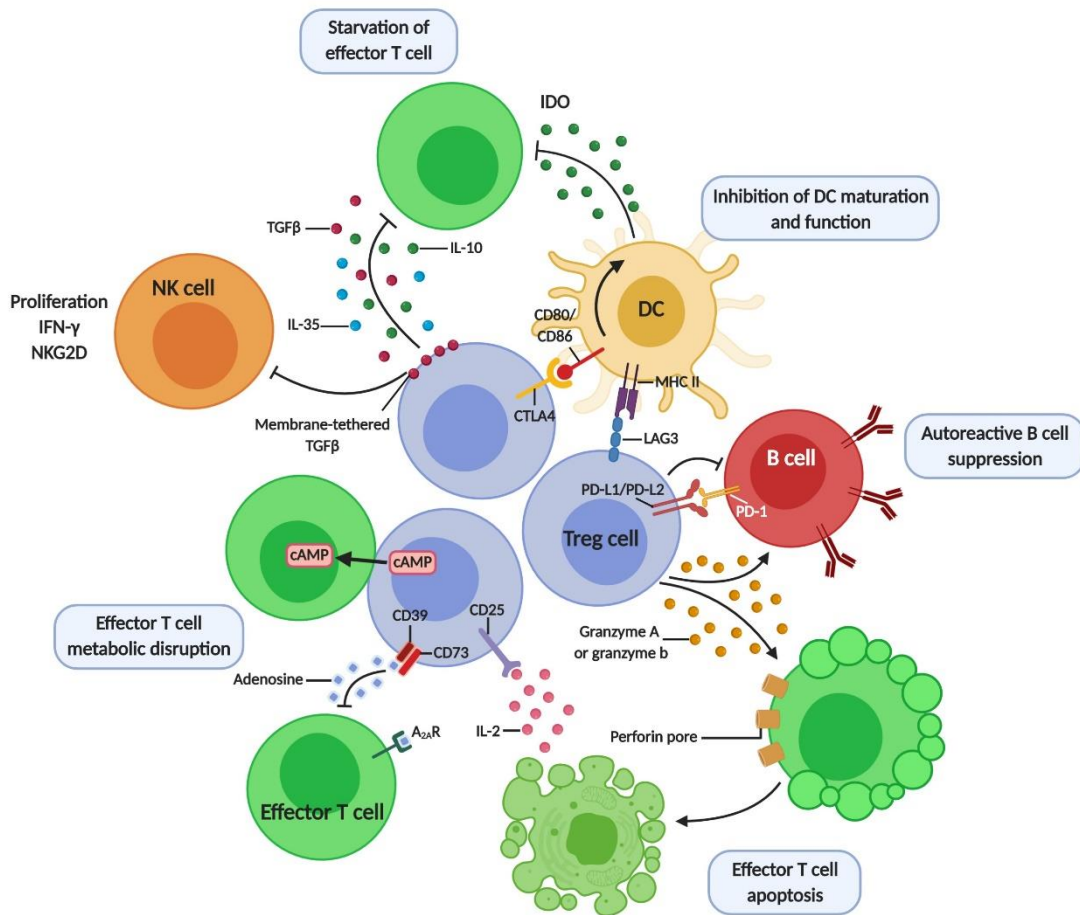


Figure 8 The basic mechanisms of Tregs function to suppress an immune response. Modified from: Romano et al., 2019<sup>(65)</sup>; Vignali et al., 2008<sup>(61)</sup> and created with BioRender.com.

### 2.3.4 Cell signaling of Tregs and Treg cell signaling and potential action mechanisms

Although the cellular signaling pathways of Tregs remain mainly uninvestigated, we can summarize the molecular mechanisms involved in their cell signaling pathway, as shown in Figure 9.

FoxP3 is a transcription factor necessary for Treg formation and function. FoxP3 not only keeps cells on the right developmental tracks toward a suppressive

phenotype but also appears required for Treg lineage stability<sup>(66)</sup>. Furthermore, FoxP3 impairment decreases Treg suppressive activity over time. The FoxP3 locus includes various conserved noncoding regions identified as CNS 0-3. Each sequence participates in a different signaling pathway. CNS0 plays a role in activating Treg-SE (specific super-enhancers) to stimulate FoxP3 expression. CNS1 includes binding sites for the nuclear factor of activated T lymphocytes and the activator protein 1, both required for TGF- signaling pathways. CNS2 can be activated by TCR expression and IL-2, which contains transcription factor binding sites for various transcription factors, including cyclic adenosine monophosphate response element-binding protein, signal transducer and activator of transcription (STAT5), and runt-related transcription factor (RUNX). The RUNX1-CBF complex binding to CNS2 is critical for maintaining a high and steady level of FoxP3 expression in Treg cells. CNS3 is a major element for FoxP3 induction during tTregs and pTregs differentiation by recruiting c-Rel and other transcription factors. In conclusion, FoxP3 is part of a vast transcriptional complex, and FoxP3 subunits can bind to several transcriptional factors to achieve Treg formation and function<sup>(67-69)</sup>.

Besides FoxP3-mediated signaling pathways, it has been reported that STAT4 is required for IL-12 to inhibit the development of TGF- $\beta$ 1-induced-expressing iTregs, even if a parallel mechanism involving T-bet exists<sup>(70)</sup>. There was reported that IL-4 supersedes Tregs function via the IL-4R $\alpha$ -STAT6 axis, which reduces FoxP3 expression in Tregs and promotes allergic inflammation. Additionally, the competing effects of IL-4-induced signaling in naive CD4<sup>+</sup> Th cells can compromise viral tolerance mediated by membrane-bound TGF- $\beta$  expression on Tregs<sup>(71-73)</sup>.

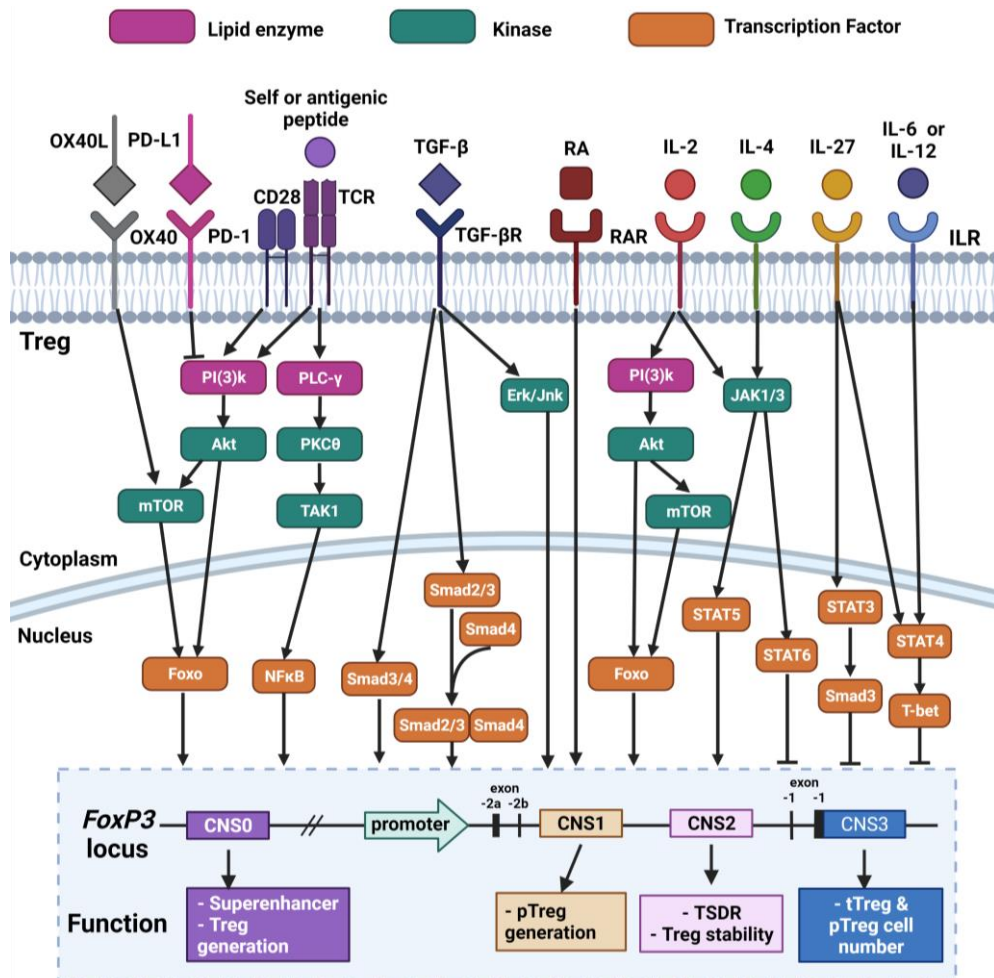


Figure 9 Schematic diagram of transcriptional regulation of the *Foxp3* locus and cell signaling pathway of Tregs. Modified from Zhang et al. (2014)<sup>(58)</sup> and Lee and Lee (2018)<sup>(74)</sup> and created with BioRender.com.

## 2.4 Association of Treg, DRESS, and autoimmune diseases

As mentioned above, Tregs are essential in immunological homeostasis by maintaining a balanced adaptive immune response. Human congenital abnormalities impair Tregs' number or function, resulting in autoimmunity, allergic dysregulation, and continuous lymphocyte infiltration in several organs, leading to disease progression and affecting patient survival.

From the clinical perspective, the mutation of FoxP3 is significantly associated with the immunological dysregulation of Tregs. Patients with a mutant FOXP3 gene suffer from autoimmune polyendocrinopathy, particularly type 1 diabetes mellitus and hypothyroidism, as well as enteropathy, which is immunodysregulation, polyendocrinopathy, enteropathy X-linked (IPEX) syndrome<sup>(75)</sup>. Moreover, decreased circulating Tregs population has been reported in patients with autoimmune diseases, including Hashimoto thyroiditis<sup>(76)</sup>, Graves' disease<sup>(77)</sup>, rheumatoid arthritis<sup>(78)</sup>, and systemic lupus erythematosus<sup>(79)</sup>. The lower circulating Treg population is also linked to increased disease activity or poor prognosis<sup>(76, 78, 79)</sup>.

When we reviewed the Tregs in DRESS, there were reported that Tregs in the skin and circulation of DRESS patients increased during the acute phase of the syndrome compared with other SCARs and healthy donors. In contrast, Tregs in the recovery phase of DRESS patients were dysfunctional even though there was an equal population level compared with other SCARs and healthy donors<sup>(5, 80)</sup>.

It is interesting to link these reports about the impairment of Tregs function in other autoimmune diseases, the defective Tregs in DRESS recovery patients, and their autoimmune sequelae. Therefore, immunophenotype and functions of Tregs at the acute and recovery phases of DRESS patients with autoimmune sequelae would give us more understanding of autoimmune sequelae in DRESS patients.

## CHAPTER III

### HYPOTHESIS AND OBJECTIVES

#### 3.1 Research question

How are the immunophenotype and functions of Tregs at the acute and recovery phases of DRESS patients with autoimmune sequelae different?

#### 3.2 Objectives

3.1.1 To characterize the regulatory T cell immunophenotype of DRESS patients with autoimmune sequelae between the acute and recovery phase.

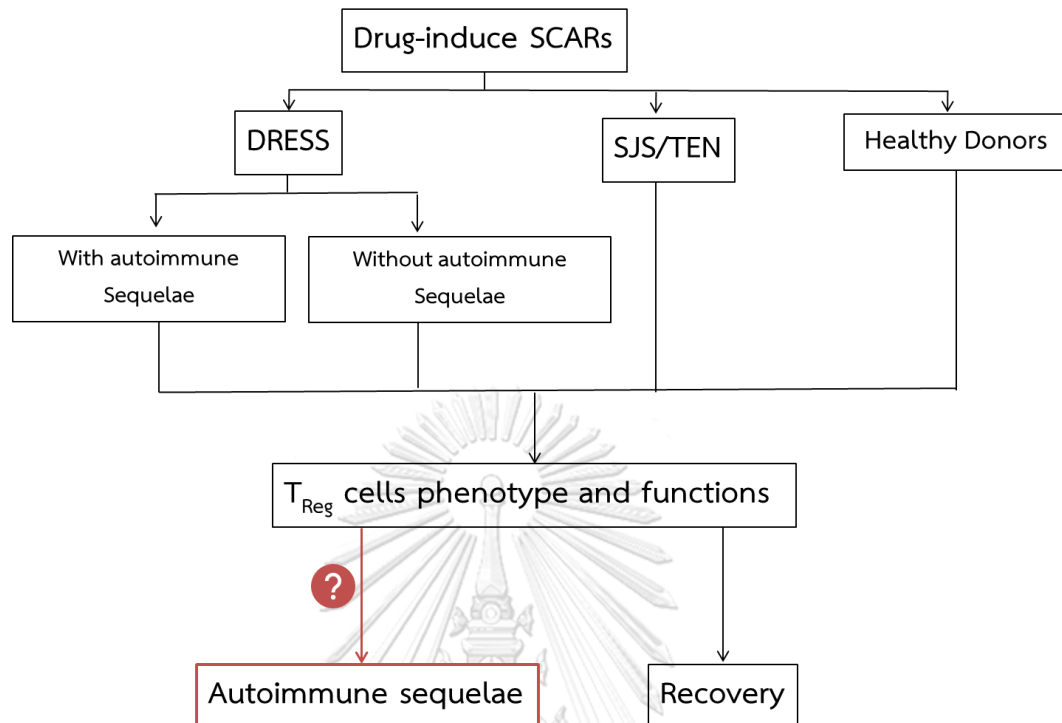
3.1.2 To investigate *in vitro* regulatory T cell suppressive function of DRESS patients with autoimmune sequelae between the acute and recovery phases.

3.1.3 To explore the gene expression profiles in Tregs from DRESS with autoimmune sequelae and control samples that might influence autoimmunity development.

#### 3.3 Hypothesis

There are differences in Tregs phenotyping between acute and recovery phases of DRESS patients with and without autoimmune sequelae

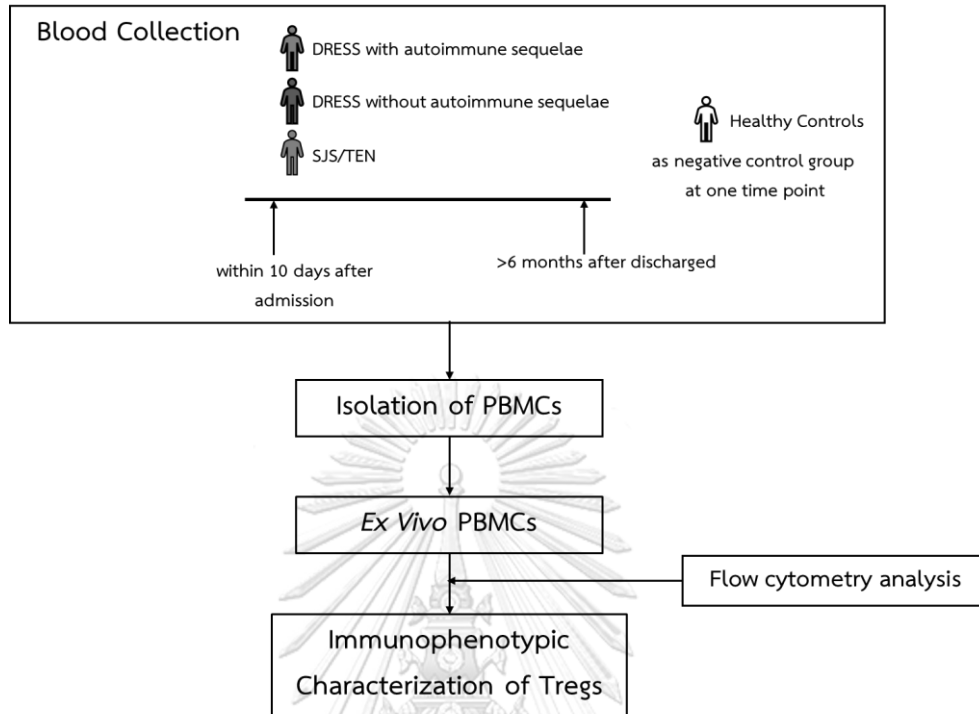
### 3.4 Conceptual framework



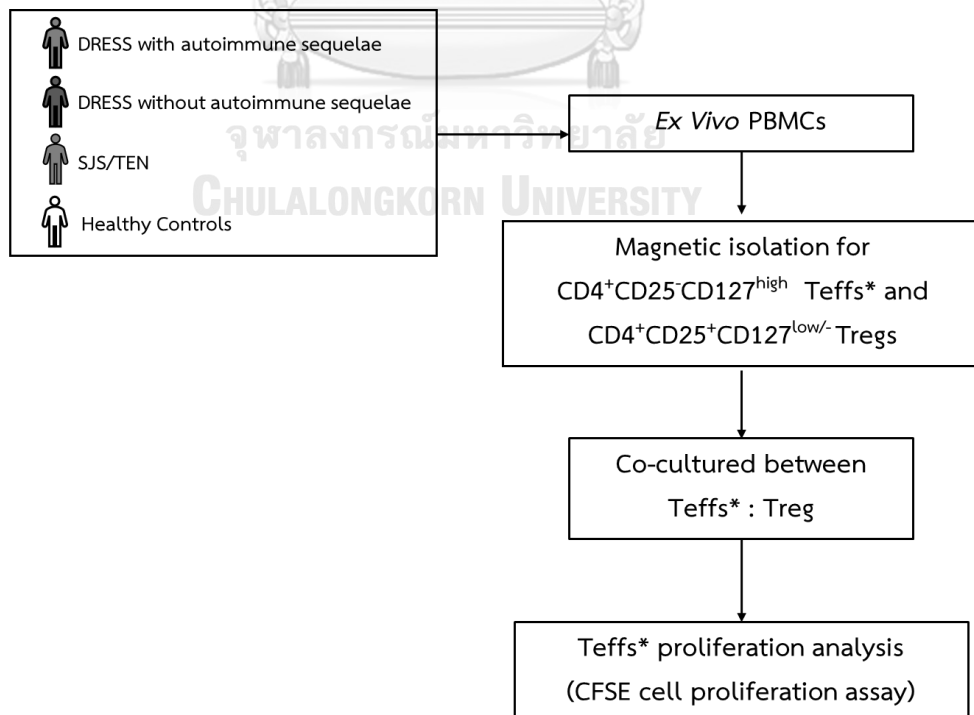
### 3.5 Research design and experimental framework

This study was a basic research study with cross-sectional observation designs. There are three parts of the experiment according to the study's objectives. This study used PBMCs from healthy donors as the negative controls for one-time points. Moreover, SJS/TEN patients were used as a comparative group because SJS/TEN is one of the SCARs phenotypes with high severity but clinical characteristics without autoimmune sequelae.

## Part 1 Characterization of the regulatory T cell immunophenotype

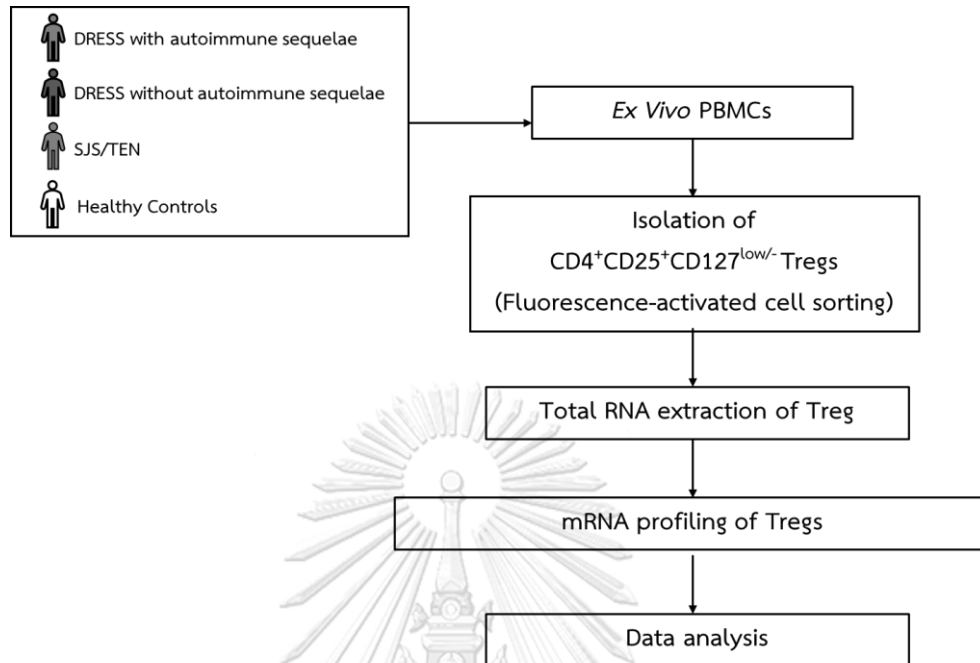


## Part 2 investigation of Tregs suppressive function *in vitro*





### Part 3 Gene expression profiles in Tregs



#### 3.6 Expected results

There are alterations in the function and number of Tregs in DRESS with autoimmune sequelae patients compared to healthy donors, DRESS without autoimmune sequelae patients, and SJS/TEN patients.

#### 3.7 The benefit of this study

3.7.1 The identification of Tregs in DRESS patients with and without autoimmune sequelae may give more information about the pathogenesis of DRESS and their subsequent autoimmunity.

3.7.2 This knowledge may help in the early diagnosis, preventing or developing future therapeutic methods for the symptoms.

## CHAPTER IV

### METHODOLOGY

#### 4.1 Specimen collection

Patients diagnosed with DRESS and SJS/TEN from drug hypersensitivity reactions were recruited from King Chulalongkorn Memorial Hospital, Bangkok, Thailand, between 2014 – 2022. All SCARs patients in this study had developed symptoms within eight weeks after initiating drug treatment. DRESS diagnoses were considered using the RegiSCAR criteria<sup>(44)</sup>. At the same time, SJS/TEN were evaluated using an algorithm for assessment of drug causality in Stevens-Johnson Syndrome and toxic epidermal necrolysis or ALDEN score<sup>(26)</sup>.

Blood samples from drug-induced SCARs patients will be obtained within ten days after admission to the hospital. They will be defined as the acute stage samples, while those obtained more than six months after the onset of the symptoms will be defined as the recovery phase samples. The criteria for blood sampling were modified from those of Takahashi *et al.* (2009)<sup>4</sup>. This study included healthy donors with no history of drug hypersensitivity as the negative controls for one-time points. Additionally, SJS/TEN patients were used as a comparative group because SJS/TEN is one of the SCARs phenotypes with high severity but clinical characteristics without autoimmune sequelae.

Before the sample collection process, all participants provided their informed consent. After consent was permitted, peripheral blood was collected by venipuncture for 30 mL (metric). All drug-induced SCAR patients were confirmed by

ELISPOT analysis with IFN- $\gamma$  released cells of more than 20 SFU/10<sup>6</sup> peripheral blood mononuclear cells (PBMCs).

All participants proceeded under a protocol approved by the Ethical Research Committee, Faculty of Medicine, Chulalongkorn University (COA No. 579/2020, IRB No.225/63). All information collected about participants during the study has been kept strictly confidential, and no identifiable personal data will be published.

#### 4.2 Sample size determination

There has never been a previous study on the Tregs immunophenotype in DRESS patients with autoimmune sequelae. But according to, preliminary results from our laboratory that compared the population of Tregs between SCAR patients at the acute phase found that there were significantly different between CD3<sup>+</sup>CD4<sup>+</sup>CD25<sup>+</sup>CD127<sup>-</sup> Tregs, as shown in Table 4.

**Table 4 Preliminary data of CD3<sup>+</sup>CD4<sup>+</sup>CD25<sup>+</sup>CD127<sup>-</sup> Tregs in DRESS and SJS/TEN patients**

SCARs phenotype	% of CD3 <sup>+</sup> CD4 <sup>+</sup> CD25 <sup>+</sup> CD127 <sup>-</sup> Tregs (n=10)		T-test
	Mean ( $\mu$ )	SD ( $\sigma$ )	
DRESS	9.600	5.8369	0.010
SJS/TEN	3.824	2.5362	

So, when using these results to predict the sample size in this research. The sample sizes required in each comparison group are given below:

$$n = \frac{(\sigma_1^2 + \sigma_2^2) \left( z_{1-\alpha/2} + z_{1-\beta} \right)^2}{\Delta^2} = \text{sample size for each group}$$

Where  $n$  is the suitable sample size in each group to have a probability of  $1-\beta$  of finding a significant difference based on a two-sided test with significance level  $\alpha$ ,  $Z_{1-\frac{\alpha}{2}} = 1.96, \alpha = 0.05$ ;  $z_{1-\beta} = 0.8, \beta = 0.2$

$\Delta = \mu_1 - \mu_2$  is the absolute value of the actual difference in means between the two groups

The means and variances of the two respective groups are  $(\mu_1, \sigma_1^2)$  and  $(\mu_2, \sigma_2^2)$

If using the above formula:

$$n = \frac{(5.8369^2 + 2.5362^2)(1.96 + 0.8)^2}{(9.600 - 3.824)^2}$$

$$n = \frac{(34.069 + 6.432)(7.618)}{33.362}$$

$$n = \frac{308.537}{33.362}$$

$$n = 9.248$$

Thus, this study recruited 40 patients who were ten patients from DRESS with autoimmune sequelae, ten patients from DRESS without autoimmune sequelae, ten patients from SJS/TEN, and ten patients as control subjects taken from healthy donors with no history of drug hypersensitivity.

#### 4.3 Inclusion criteria

- All subjects were from the Thai population and older than 18 years old.

#### For DRESS patients

- Dermatologists or allergists confirmed drug-induced DRESS subjects.
- For flow cytometry and suppressive assay, DRESS patients with autoimmune sequelae must have the Antinuclear Antibody Test (ANA) titer greater than 1:40<sup>(81)</sup> or have been diagnosed with at least one autoimmune disease or both.
- For RNA expression profile study, DRESS patients with autoimmune sequelae must have been diagnosed with at least one autoimmune disease.

#### For SJS/TEN patients

- Dermatologists or allergists confirmed drug-induced SJS/TEN subjects.

#### For healthy control subjects

- The control subjects were obtained from a healthy donor with no history of drug hypersensitivity.

#### 4.4 Exclusion criteria

- The subjects were unwilling to participate in the study.
- The subjects were unable to give informed consent.
- The subjects had unclear medical records.

#### 4.5 Isolation and cryopreservation of PBMC

Anticoagulant-treated human peripheral blood samples were collected from each group of experimental subjects. PBMCs were isolated by Ficoll-Paque™ PLUS density gradient media (GE healthcare life sciences; Chicago, IL, United States) centrifugation. Packed cells were resuspended in RF10 medium (see Appendix A for reagent details) and gently layer 10 mL of suspension cells on 4 mL of Ficoll-Paque™ PLUS in a 15 mL conical tube. Then, the tubes were centrifuged for 20 min at room temperature with a control deceleration setting as zero. The top layer was aspirated, whereas the mononuclear cell layer (lymphocytes, monocytes, and thrombocytes) remained undisturbed at the interphase. The mononuclear cell layer was carefully transferred to a new 15-mL conical tube. Then, the PBMCs were washed with RF10 media, centrifuged, and discarded the supernatant twice. The pellet was resuspended in the freezing media to yield  $1 \times 10^7$  cells/mL. Finally, The cell suspension was aliquoted 1 mL into pre-chilled cryogenic vials and subsequently placed into Mr. Frosty™ Freezing Container (Thermo Scientific™; Waltham, MA, United States) to achieve a rate of cooling close to  $-1^\circ\text{C}/\text{min}$ . The vials were transferred to liquid nitrogen for long-term storage for further use.

The cryopreserved cells were recovered from liquid nitrogen and placed cryotubes into a water bath at  $37^\circ\text{C}$  until the liquid was partially thawed. One milliliter of RF10 medium was added to the thawed cryotubes for resuspending and then transferred into a 15 mL conical tube with pre-warmed ( $37^\circ\text{C}$ ) 10 mL of RF10 media. The cell suspension was centrifuged at 1,500 rpm for 5 min at  $4^\circ\text{C}$ . The pellet was washed with 10 mL of RF10 and centrifuged again. After discarding the supernatant, the cell pellet was resuspended in 5 mL RF10 media for counting.

Cell number and viability were evaluated using a Neubauer hemocytometer in conjunction with the trypan blue exclusion assay. A 1:10 dilution of the cell suspension on 0.1% trypan blue was performed and observed under a compound light microscope. The cells were counted in a quadrant of known volume. Dead cells lost their membrane-impermeability for trypan blue, so the dye could penetrate the dead cells while the viable cells remained unstained. The following formula was used to determine the number of cells:

$$\text{number of cells per mL} = \text{mean number of cells per quadrant} \times 10^4$$

#### 4.6 Antibodies staining for flow cytometry

For surface staining, the  $1 \times 10^6$  PBMCs were surface stained and incubated for 45 min in the dark on ice with optimally concentrated surface markers by following monoclonal antibodies: CD3-PE/Cy7, CD4-APC/Cy7, CD8-AF700, CD25-PE, CD127-PerCP/Cy5.5, PD-1-BV421, CTLA-4-PE/Dazzle594, GITR-BV605, LAG-3-BV650, OX40-BV510, and CD39-BV785 (antibody detail given in Appendix A). After incubation, PBMCs were washed twice with 200 mL of cold FAC buffer. For cell fixation, cells were resuspended with 100  $\mu$ L of freshly prepared fixation/permeabilization working solution following instructions from the eBioscience™ FoxP3 Transcription Factor Staining Buffer kit to each sample. Samples were mixed gently with the pipette and incubated on ice for 60 min in the dark. Then, samples were washed twice with 1X permeabilization buffer, centrifuged, and decanted supernatant. Then, the FoxP3-AF488 and IL-10-AF647 in 1X permeabilization buffer was added for intracellular staining and incubated for 45 min in darkness at room temperature. After the surface and intracellular staining, the cells were washed, centrifugated, and resuspended before being analyzed by flow cytometry.

#### 4.7 Quality control of flow cytometry

Samples were analyzed with CytoFLEX V5-B5-R3 Flow Cytometer (13 Detectors, 3 Lasers) from Beckman Coulter Life Sciences (Indianapolis, IN, United States). Quality Control (QC) was done using CytoFLEX Daily QC Fluorospheres (Beckman Coulter Life Sciences) every time that turned on the flow cytometer to confirm that the instrument was working correctly within the specified parameters. The system reads and automatically adjusts laser delay during QC. Thresholds were set as 50,000 instead of using auto threshold setting by automated software features to ensure that most populations were analyzed. A nonionic, non-fluorescent, anti-microbial, and azide-free CytoFLEX Sheath Fluid was used to maintain the hydrodynamic focusing. Data were obtained from at least 100,000 cells gated in the forward scatter (FSC) versus side scatter plot between 10-60  $\mu\text{L}/\text{min}$  flow rate using the CytExpert software (version 2.4; Beckman Coulter Life Sciences).

FlowJo software (version 10.0.8; Tree Star, Ashland, OR, United States) was used for data analysis. Data acquired from unstained cells were used as a negative control. In addition, FMO staining results were utilized as the reference for correct gating.

#### 4.8 Statistical analysis for immunophenotyping characteristics of Tregs

Pearson's correlation coefficient was operated for the correlation analysis, and a One-way Analysis of Variance (one-way ANOVA) was used to compare the mean of all groups. Tukey's HSD (honestly significant difference) multiple comparison tests were used to follow the statistical difference between groups. Statistical data analysis was performed by IBM SPSS software (IBM; Armonk, NY, United States). *P*-values less than 0.05 (95% confidential) were considered statistically significant.



#### 4.9 Tregs isolation for suppression assay

Tregs (CD4<sup>+</sup>CD25<sup>+</sup>CD127<sup>-</sup> T cells) and effector T cells (CD4<sup>+</sup>CD25<sup>-</sup> T cells) were isolated from donor's PBMCs by EasySep Human CD4<sup>+</sup>CD127<sup>-/low</sup>CD25<sup>+</sup> Regulatory T Cell Isolation Kit (STEMCELL Technologies; Vancouver, BC, Canada) following the instruction. Briefly, PBMCs ( $1 \times 10^7$  cells) were prepared by adding 300  $\mu$ L of isolation buffer into the FACs tube. Every step was done at room temperature and must be gently mixed with the pipette. First, 25  $\mu$ L of CD25 Positive Selection Cocktail was added to the sample, mixed, and incubated for 5 min. 10  $\mu$ L of Releasable RapidSpheres and 25  $\mu$ L of CD4<sup>+</sup> T Cell Enrichment Cocktail were added to the sample to binding CD4<sup>+</sup>CD25<sup>+</sup> cells, mixed, and incubated for 5 min. 2,140  $\mu$ L of Isolation buffer was added to the cells for a complete volume of 2.5 mL. The tube (without lid) was placed into the EasySep<sup>™</sup> Magnet (STEMCELL Technologies) and incubated at room temperature for 10 min. Then, pick up the magnet and, in one continuous motion, invert the magnet and tube, pouring the supernatant into a new FAC tube. This supernatant was the CD4<sup>+</sup>CD25<sup>-</sup> and CD4<sup>-</sup> cells that would be continued isolated for CD4<sup>+</sup>CD25<sup>-</sup> effector T cells.

The cell pellet was washed twice by adding isolation buffer, incubated in EasySep<sup>™</sup> Magnet for 5 min, and discarded supernatant. The sample tube was removed from the magnet, and 300  $\mu$ L of isolation buffer was added into the tube; mix by gently pipetting up and down (be sure to collect cells off the sides of the tube. After that, 50  $\mu$ L of Release Buffer was added to the sample, vigorously pipette up and down more than five times, and 20  $\mu$ L of CD127<sup>high</sup> Depletion Cocktail was added to the sample, mixed, and incubated for 5 min. Then, Dextran RapidSpheres<sup>™</sup> (5  $\mu$ L) was added and set for 5 min. 2,125  $\mu$ L of isolation buffer was added to the cells for a complete volume of 2.5 mL. The tube (without a lid) was placed into the magnet and incubated for 5 min. Then, in one continuous motion, the magnetic tube

was inverted to pour the supernatant into a new FACs tube. Therefore, CD4<sup>+</sup>CD25<sup>+</sup>CD127<sup>-/low</sup> Tregs were contained in the new FACs tube.

From the first part, the supernatant was centrifuged into pellet cells at 1,500 rpm for 5 min and resuspended with 300  $\mu$ L of isolation buffer. Then, 45  $\mu$ L of Dextran RapidSpheres™ was added to the sample and incubated for 5 min. The tube (without a lid) was placed into the magnet and set for 5 min. Then, in one continuous motion, the magnet tube was inverted to pour the supernatant into a new FAC tube. These cells were CD4<sup>+</sup>CD25<sup>-</sup> effector T cells.

Both populations were washed with PBS buffer twice to remove excess EDTA contamination before co-culture. The frequency of CD4<sup>+</sup>CD25<sup>+</sup>CD127<sup>-/low</sup> Tregs and CD4<sup>+</sup>CD25<sup>-</sup> effector T cells were determined by flow cytometry.

#### 4.10 Tregs and effector T cells co-culture experiments

The *in vitro* Tregs suppression assay was set up following the study of Collison and Vignali (2011). After cell isolation, all Tregs were pre-activated overnight with anti-human CD3 (1  $\mu$ g/mL) and anti-human CD28 (2  $\mu$ g/mL) in a 96-well U-bottom plate. Conversely, effector T cells were rested overnight in RF10 media. Moreover, the U-bottom 96-well plated was pre-coated with soluble anti-human CD3 (10  $\mu$ g/mL) overnight and washed with PBS before being used the next day.

A carboxyfluorescein succinimidyl ester (CFSE) cell division tracker kit (BioLegend; San Diego, CA, United States) was prepared in a working solution by diluting CFSE at a 1:1000 ratio in PBS buffer. Resting effector T cells were labeled with 100  $\mu$ L of CFSE working solution and incubated in darkness at 37 °C for 8 min. Then, 500  $\mu$ L of RF10 media was added to quench the reaction. For the co-cultured experiment, CFSE-labeled effector T cells ( $1 \times 10^4$  cells) were cultured alone or with

autologous pre-activated Tregs in U-bottom 96-well plates at effector T cells/Tregs ratios ranging from 1:1 to 1:0.25. The co-cultured cells were restimulated with 2 µg/mL of soluble anti-CD28 and 200 pg/mL of recombinant Human IL-2 (carrier-free) (all from BioLegend) in RF10 media. Cells were incubated in a humidified environment at 37°C in 5% CO<sub>2</sub> for 96 hours before analysis by flow cytometry for effector T cells proliferation. The CFSE-labeled effector T cells cultured alone without stimulation were used as a negative control for gating.

#### 4.11 Effector T cells proliferation analysis

Effector T cells proliferation analyses were performed using CytoFLEX V5-B5-R3 Flow Cytometer to detect the CFSE positive effector T cells. The flow cytometer was set up as the previous methodology mentioned. In addition, the 488 nm (blue) laser was used to collect green fluorescence (CFSE) with a 525-nm band-pass filter. Data were obtained from at least 10,000 cells gated in the forward scatter (FSC) versus side scatter plot between 10-60 µL/min flow rate using the CytExpert software.

#### 4.12 Data analysis and statistical analysis of suppression assay

Data acquired from the flow cytometer were analyzed by FlowJo software. Autologous unstimulated effector T cells cultured alone were used as a negative control. Statistic data analysis was performed, as mentioned elsewhere in this chapter.

The percentage suppression was calculated using the formula:

$$\frac{\% \text{ proliferation of } T_{effs} \text{ alone} - \% \text{ proliferation of } T_{eff} \text{ co-cultured with } T_{reg}}{\% \text{ proliferation of } T_{eff} \text{ alone}} \times 100$$

#### 4.13 Tregs isolation for mRNA profiling

CD4<sup>+</sup>CD25<sup>+</sup>CD127<sup>-</sup> Tregs were sorted for mRNA profiling by flow cytometry technique. First, PBMSs ( $1 \times 10^7$  cells) were stained with CD4-PE/Cy7, CD25-PE, and CD127-PerCP/Cy5.5 as the protocol described elsewhere in this chapter.

BD FACSAria™ II Cell Sorter was used to isolate CD4<sup>+</sup>CD25<sup>+</sup>CD127<sup>-</sup> Tregs. The cytometer settings were optimized to position the cells of interest on the scattering scale and fluorescence parameters. Compensation was manually set and calculated using the Compensation Setup feature controlled by BD FACSDiva™ software. The CD4<sup>+</sup>CD25<sup>+</sup>CD127<sup>-</sup> Tregs were from multiple populations in a 5 mL FACs tube containing 1 mL of FAC buffer.

After sorting, the FACs tube containing the desired population was centrifuged at 4 °C, 1500 rpm for 5 min. Pellets were washed twice with PBS buffer for further use.

#### 4.14 Total RNA extraction of Tregs

Total RNA was extracted from each patient's Tregs using the RNeasy mini kit (QIAGEN GmbH, Hilden, Germany), following the manufacturer's instructions. Cell pellets from sorting were disrupted by adding 300  $\mu$ L of RNeasy Lysis (RLT) buffer and homogenized cells with vortex. Then, 350  $\mu$ L of 70% ethanol was added to the homogenized lysate and mixed well by pipetting. The sample, including any residue that may have formed, was transferred to an RNeasy spin column placed in a 2 mL collection tube. Close the lid gently, centrifuge for 15 sec at 8000x g, and discard the flow-through. Then, the 700  $\mu$ L of RW1 buffer was added to the RNeasy spin column. Close the lid, centrifuge to wash the spin column membrane, and discard the flow-through. After that, the column membrane was washed twice with 500  $\mu$ L of RPE

buffer, discarding the flow-through after centrifuging. Then, the RNeasy spin column was transferred to a new 1.5 ml collection tube, and 30  $\mu$ L of RNase-free water was added directly to the spin column membrane, closed the lid gently, and centrifuged for 1 min at  $\geq 8000 \times g$  to elute the RNA.

RNA quality was quantified by Qubit™ RNA High Sensitivity (HS) Assay Kits (Invitrogen, Waltham, MA, United States) via Qubit™ 4 Fluorometer (Invitrogen). In addition, RNA was quantified using a NanoDrop spectrophotometer (NanoDrop Technologies, Wilmington, DE, United States). Total RNA from

Sorted Tregs were counted and ranged between 53,588 to 709,879 cells. Then, the total RNA from Tregs was extracted with the RNeasy mini kit (QIAGEN). The yield of total RNA ranged from 2.20-42.10 ng/ $\mu$ L (Table 5).

**Table 5** The Tregs count from FAC-sorted and their yield of total RNA extraction

SCARs phenotype	Patients		Sorted Tregs (cells)	RNA Concentration (ng/ $\mu$ L)
	Initial	Phase		
Healthy donors	HD003		709,879	42.10
	HD008		233,092	17.70
	HD009		290,015	13.50
DRESS with autoimmune sequelae	PKS	Acute	204,864	29.90
	PKS	Recovery	132,509	42.00
	MJC	Acute	16,815	3.10
	MJC	Recovery	184,944	33.90
	YSP	Acute	109,822	1.80
	YSP	Recovery	117,830	6.20
	LSS	Acute	73,138	2.70
	LSS	Recovery	162,014	3.70
DRESS without autoimmune sequelae	NSS	Acute	171,518	14.50
	NSS	Recovery	287,537	17.40
	KKL	Acute	601,366	32.60

SCARs phenotype	Patients Initial	Phase	Sorted Tregs (cells)	RNA Concentration (ng/ $\mu$ L)
	KKL	Recovery	205,756	5.80
	SSD	Acute	402,087	4.20
	SSD	Recovery	96,367	14.20
SJS/TEN	JPC	Acute	134,534	3.20
	JPC	Recovery	80,933	5.90
	PTS	Acute	77,678	3.60
	PTS	Recovery	241,325	8.50
	CCP	Acute	53,588	2.60
	SPC	Recovery	62,642	2.20

#### 4.15 CodeSet hybridization

Gene expression values from CD4<sup>+</sup>CD25<sup>+</sup>CD127<sup>-</sup> Treg-sorted cells from DRESS patients, SJS patients, and healthy donors were measured using nCounter<sup>®</sup> Autoimmune Profiling Panel (NanoString Technology, WA, United States). This panel included 770 human genes involved in immune system dysfunction, including Tregs differentiation and function.

CodeSet hybridization for mRNA profiling via NanoString Technologies was performed as follows. A minimum of Total RNA (5 ng/ $\mu$ L) was added to the hybridization master mix by adding the hybridization buffer to the tube containing the Reporter CodeSet (Table 6). The tube strip was repeatedly inverted to mix and spin down with a centrifuge. Hybridization reactions were prepared using a new pipette tip at every step by adding 8  $\mu$ L of hybridization master mix to each tube of the prepared strip tube. 5  $\mu$ L of RNA sample was added to each tube containing the hybridization master mix. Then, 8  $\mu$ L of nuclease-free water was added to finalize the reaction volume to 13  $\mu$ L. Finally, 2  $\mu$ L of Capture ProbeSet was added to each tube,

tightly capped the strip tubes, and inverted the strip several times to ensure complete mixing and spin down briefly. Immediately, the tube strip was placed in the pre-heated 65°C thermal cyclers (ProFlex™ PCR System: Applied Biosystems Waltham, MA, United States) with the heated lid at 70°C. The hybridization reactions were performed for 16 hours and incubated at 4 °C on the thermal cycler following desired hybridization time before proceeding with the nCounter® system.

**Table 6** Hybridization master mix for one nCounter® assay (12 reactions + 2 reactions of dead volume).

Component	Hybridization Master Mix (μL)	Per reaction (μL)
Reporter CodeSet	42 (in the tube)	3
Hybridization Buffer	70	5
Total Volume	112	8

#### 4.16 Post hybridization sample processes by Prep Station robot and digital analyzer

After sample processing and hybridization were completed, samples were loaded onto the Prep Station robot to be purified and immobilized onto the internal surface of the sample cartridge. The Prep Station is a multi-channel pipetting robot that processes samples to prepare them for data collection on the Digital Analyzer. The instrument performs liquid transfers, magnetic bead separations, and immobilization of molecular labels on the sample cartridge surface. For Initiating a run, high sensitivity protocol was selected to increase the binding of all molecules to the sample cartridge surface. The nCounter® cartridges and Prep Plates must be at room temperature before processing. Centrifuge the Prep Plates at 2000g for 2 min to collect all liquids in the bottom of the wells before loading the Prep Plates onto the Prep Station deck. The tips and the foil piercers, the tip sheaths, the cartridge,

the empty strip tube, and hybridized sample strip tube were placed on the deck following the program setting. When the process began, the Prep Station automatically worked and took about 3-4 hours to finish.

Meanwhile, the Cartridge Definition File (CDF) template of nCounter® Autoimmune Profiling Panel was installed on the Digital Analyzer via USB flash drive (provided in the kit). The Reporter Library File (RLF) library was also created on the Digital Analyzer. The experimental data file was created by linking to CDF and RLF files. Each tube of samples was defined appropriately for the selected cartridge, and the number of images (fields of view, or FOVs) was set as 280 fov, which corresponds to the high sensitivity and high dynamic range that could be achieved.

When the mRNA-probe complexes were immobilized and aligned to the image surface on the cartridge by the Prep Station robot was completed, the cartridge was removed from the Prep Station robot and placed in the Digital Analyzer to initiate Imaging. A Reporter Code Count (RCC) file is created for each flow cell in the cartridge when the data collection had completed. The output data were grouped by cartridge into a zipped folder that contains up to 12 RCC files and could be transferred via a USB flash drive for further analysis.

#### **4.17 nSolver™ 4.0 analysis software and data analysis of mRNA profiling**

Raw data from the Digital Analyzer were processed and checked for quality using the R/Bioconductor NanoStringQCPro software package. Expression values were normalized to the geometric mean of housekeeping genes and log<sub>2</sub>-transformed. Gene expression data analysis was performed using the nSolver™ Data Analysis software with the Advanced Analysis module (NanoString Technologies).



The gene expression profiling of each sample was presented as a heatmap. The genes of interest from each condition were considered on statistical comparison between groups of the patient must be upregulated or downregulated over 1.5-fold with 95% confidence compared to healthy donor gene expression. Venn's diagram was created to represent the overlapping gene between each group of patients using InteractiVenn software (online at <https://www.interactivenn.net>)<sup>(82)</sup>. One-way Analysis of Variance (one-way ANOVA) was used to compare the mean of all groups. Tukey's HSD multiple comparison test was used for the statistical difference between groups. Data were presented as Mean±SD. *P*-values less than 0.05 were considered statistically significant.



## CHAPTER V

### RESULTS

#### PART 1 PATIENT CHARACTERIZATION AND TREGS PHENOTYPING USING FLOW CYTOMETRY

As mentioned above, Tregs have emerged as an essential component that controls allergies and autoimmune diseases. To explore how the Tregs are involved in autoimmune diseases as sequelae of DRESS. Therefore, this study investigates the immunophenotype and function of Tregs in PBMCs at the acute and recovery phases after onset between DRESS with autoimmune sequelae patients and DRESS without autoimmune sequelae patients compared with healthy patients donor subjects. And because SJS/TEN is one of the SCARs phenotypes with high severity but clinical characteristics with no report of autoimmune sequelae, patients with SJS/TEN were included as a comparison group.

##### 5.1 Clinical characteristics

In this dissertation, We used PBMCs from DRESS patients, SJS/TEN (including SJS, SJS/TEN, and TEN) patients, and healthy donors. We recruited 4, 10, and 13 patients of DRESS with autoimmune sequelae, DRESS without autoimmune sequelae, and SJS/TEN patients, respectively. Nine healthy donors were recruited as a negative control group.

**Table 7** Clinical characteristics of DRESS patients, SJS/TEN patients, and healthy donor subjects.

Characteristic	DRESS with Autoimmune sequelae (n = 4)	DRESS without Autoimmune sequelae (n = 10)	SJS/TEN (n = 13)	Healthy Donors (n = 9)
<b>Gender</b>				
Female	4 (100.0%)	4 (40.0%)	5 (38.5%)	6 (66.7%)
Male	-	6 (60.0%)	8 (61.5%)	3 (33.3%)
<b>Age (years)</b>	41.8±12.7	41.6±5.9	54.0±3.6	28.00±1.14
<b>Causative agent</b>				
IRZE	-	-	2 (15.4%)	-
Allopurinol	2 (50.0%)	1 (10.0%)	5 (38.5%)	-
Phenytoin	2 (50.0%)	4 (40.0%)	3 (23.1%)	-
Sulfa ABX	-	5 (50.0%)	3 (23.1%)	-
<b>Positive ELISpot results</b>	3 (75.0%)	90 (90.0%)	7 (53.8%)	-
<b>Corticosteroid treatment</b>	1 (25.0%)	4 (40.0%)	5 (38.5%)	-
<b>Autoimmune sequelae</b>				
Autoimmune hemolytic anemia	1 (25.0%)*	-	-	-
Grave's disease	2 (50.0%)*	-	-	-
Autoimmune hypothyroidism	2 (50.0%)	-	-	-

Note: number of subjects, n (%). Abbreviation: IRZE - Isoniazid, Rifampicin, Pyrazinamide, Ethambutol; Sulfa ABX - sulfonamide antibiotics, \*One patient has been diagnosed with 2 autoimmune sequelae.

Clinical characteristics of patients in this study are shown in Table 7 and Appendix D for details. DRESS with autoimmune sequelae patients were all female (100%), while the frequency of DRESS without autoimmune sequelae in females (40.0%) was lower than in males (60.0%). Moreover, the frequency of SJS/TEN in males (61.5%) was higher than in females (38.5%). Our findings were consistent with

those from other reports, with male subjects predominated in SJS/TEN but female subjects in DRESS<sup>(83-85)</sup>. Furthermore, the higher prevalence of females developing autoimmune sequelae in our study was also shown in the same way as the study of Mizukawa *et al*<sup>(86)</sup>.

For the age of patients, DRESS was found in their early 30s to 40s, whereas SJS//TEN was found frequently in their mid-50s. The average age of DRESS with autoimmune sequelae, DRESS without autoimmune sequelae, and SJS/TEN patients were  $41.8 \pm 12.7$ ,  $41.6 \pm 5.9$ , and  $54.0 \pm 3.6$  years old, respectively, whereas the average age of healthy donors was  $28.00 \pm 1.14$  years old.

The drugs causing DRESS with autoimmune sequelae were allopurinol (50.0%) and phenytoin (35.0%). The causative drugs in DRESS without autoimmune sequelae were sulfa (50.0%), followed by phenytoin (40.0%), and co-trimoxazole (10%). Then, SJS/TEN were allopurinol (38.5%), phenytoin (23.1%), sulfa antibodies (23.1%), and IRZE (15.4%). Thus, allopurinol and phenytoin were frequently encountered as culprit drugs in our DRESS and SJS/TEN patients.

The diagnosis of SCAR patients was evaluated by assessing drug causality and clinical history together with the RegiSCAR criteria<sup>(44)</sup> for DRESS and ALDEN score for SJS/TEN<sup>(26)</sup>. Even though dermatologists confirmed every patient as DRESS or SJS/TEN, the IFN- $\gamma$  enzyme-linked immunospot (ELISpot) assay was used to corroborate the hypersensitivity of culprit drugs in every patient. Among recruited patients, one patient from DRESS with autoimmune sequelae and one from DRESS without autoimmune sequelae showed negative IFN- $\gamma$  ELISPOT results. In SJS/TEN patients, there are six patients with negative IFN- $\gamma$  ELISPOT results. However, the IFN- $\gamma$  ELISpot assay is an alternative way to improve overall causal diagnosis performance without endangering patients<sup>(87)</sup>.

DRESS patients with autoimmune sequelae were diagnosed with at least one autoimmune disease within 6 months after the onset of DRESS. Two patients were diagnosed with autoimmune hypothyroidism (50%), and 2 patients had Grave's disease (50%). Anyway, one patient was diagnosed with autoimmune hemolytic anemia and followed with Grave's disease within 6 months after the onset of DRESS.

## 5.2 Identification of regulatory T cell frequency and their immunophenotype

In this study, Tregs were characterized by flow cytometry in total PBMCs of the patients at their acute and recovery phases between DRESS patients with and without autoimmune sequelae and SJS/TEN patients compared to the healthy donor subjects.

The gating strategy of the full 15-parameter, which includes 13-color staining, forward scatter (FSC), and side scatter (SSC) for regulatory T cell characterization, was first gated on the target lymphocytes by their size and granularity. Pseudo-color plots of FSC-A (area) and SSC-A were used to gate for lymphocytes. The single cells were gated, followed by FSC-H (height) and FSC-A. The positive expression of the CD3 staining on single cells was identified as T cells. Then, T cells were sub-grouped into CD4<sup>+</sup> and CD8<sup>+</sup> T cells. After that CD3<sup>+</sup>CD4<sup>+</sup> T cell were gated on CD25<sup>high/+</sup>CD127<sup>low/-</sup> FoxP3<sup>+</sup> cell. Therefore, Tregs in this study were defined as CD3<sup>+</sup>CD4<sup>+</sup>CD25<sup>high/+</sup>CD127<sup>low/-</sup> FoxP3<sup>+</sup> cells.

Additionally, the immunophenotype was determined by using markers including PD-1, CTLA-4, GITR, LAG-3, OX40, CD39, and IL-10 were measured in CD3<sup>+</sup>CD4<sup>+</sup>CD25<sup>high/+</sup>CD127<sup>low/-</sup> FoxP3<sup>+</sup> cells. The gating strategy is shown in Figure 10.

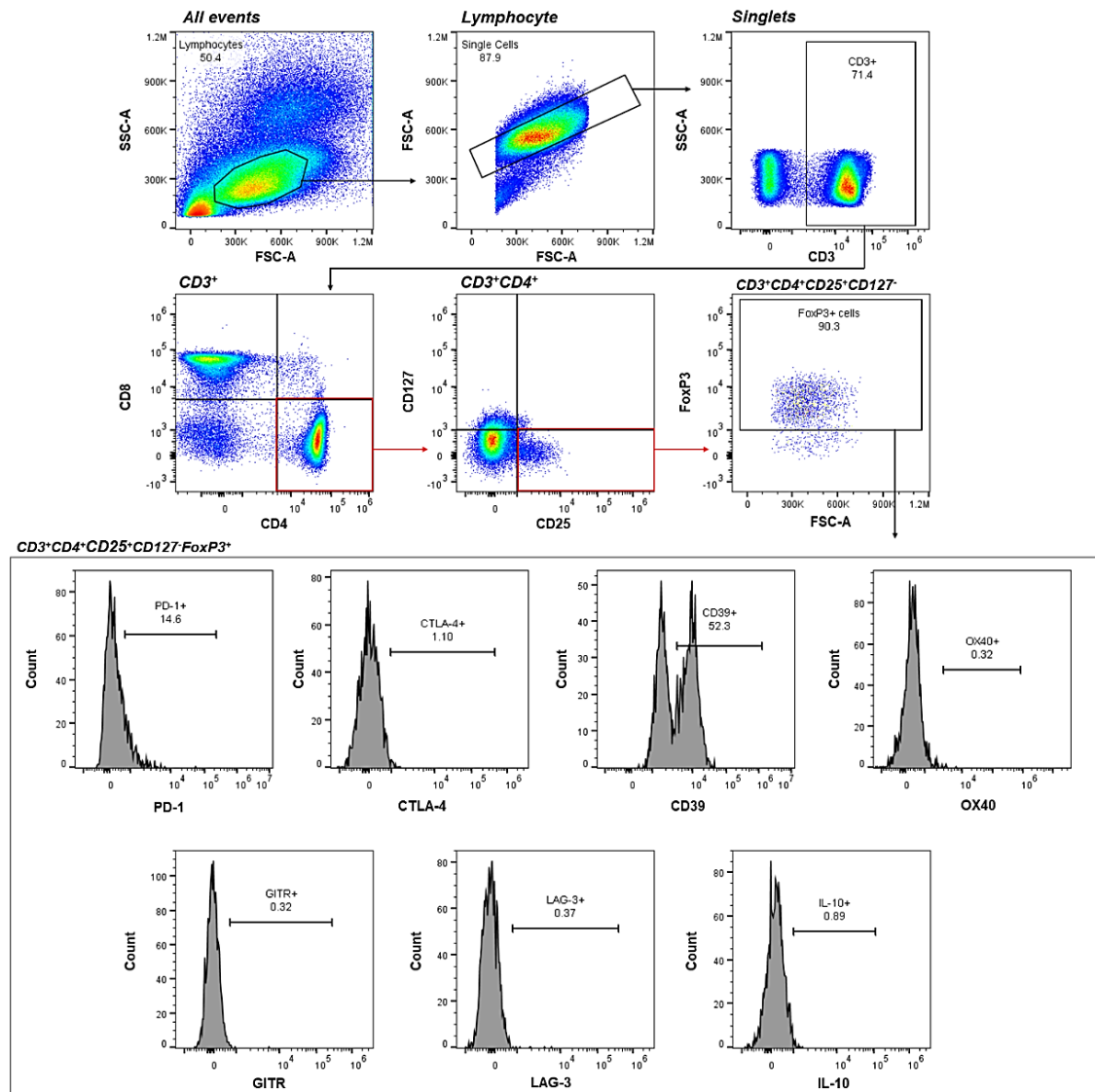
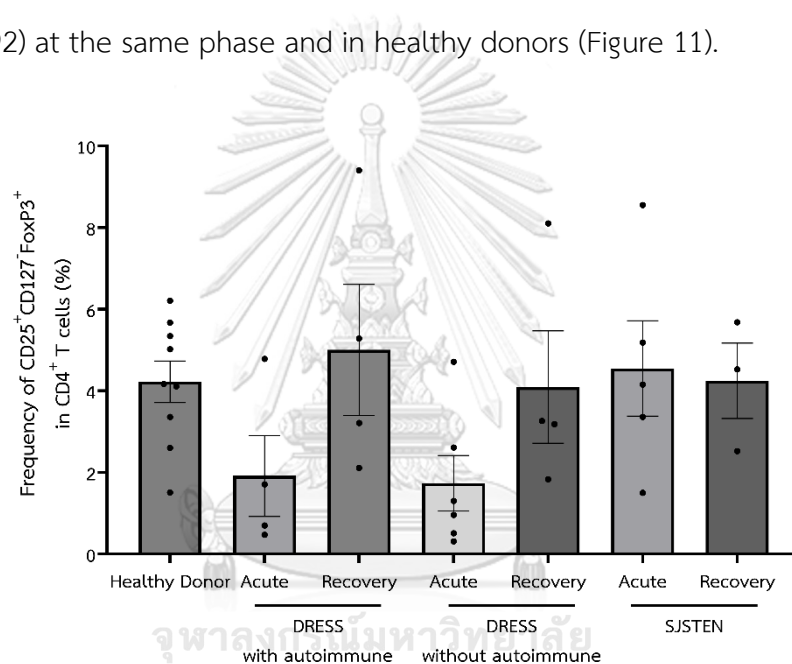


Figure 10 The gating strategy of the complete 15-parameter staining for regulatory T cell characterization. PBMCs ( $1 \times 10^6$ ) from the subjects were stained with a 13-color panel. Lymphocytes and single cell populations were gated using FCS and SSC. Tregs were gated from CD3-positive, CD4<sup>+</sup>CD8<sup>-</sup>, CD25<sup>+</sup>CD127<sup>-</sup>, and FoxP3<sup>+</sup> population, respectively. For the Treg immunophenotype, our gating strategy was anchored on the positive population of FoxP3<sup>+</sup> population in Tregs. Thus, all positive markers were expressed as a % of CD4<sup>+</sup>CD25<sup>+</sup>CD127<sup>-</sup>FoxP3<sup>+</sup> T cells.

### 5.2.1 CD4<sup>+</sup>CD25<sup>+</sup>CD127<sup>-</sup>FoxP3<sup>+</sup> Treg were not significantly different when compared between all groups

The frequency of Tregs in total CD4<sup>+</sup> T cells at the acute phase from DRESS with autoimmune sequelae ( $1.91 \pm 0.99\%$ ) and DRESS without autoimmune sequelae ( $1.74 \pm 0.58\%$ ) were not statistically different compared between all groups. However, the frequency of Treg in DRESS patients, both with and without autoimmune at the acute phase, seems to be lower than in patients with SJS/TEN ( $4.55 \pm 0.92$ ) at the same phase and in healthy donors (Figure 11).



**Figure 11** The CD4<sup>+</sup>CD25<sup>+</sup>CD127<sup>-</sup>FoxP3<sup>+</sup> Treg population in PBMCs of healthy donors and SCARs patients at acute and recovery phases. The frequency of CD25<sup>+</sup>CD127<sup>-</sup>FoxP3<sup>+</sup> cells in CD4<sup>+</sup> T cells from healthy donors, DRESS with autoimmune diseases, DRESS without autoimmune diseases, and SJS/TEN patients both in acute and recovery phases are shown. Results represent as mean  $\pm$  SEM. DRESS with autoimmune diseases (acute phase, n = 4; recovery phase, n = 4). DRESS without autoimmune diseases (acute phase, n = 6; recovery phase, n = 4), SJS/TEN (acute phase, n = 5; recovery phase, n = 3), and healthy donors (n = 9). Differences between groups were analyzed by one-way ANOVA ( $p < 0.05$ ).

## 5.2.2 The alteration of Tregs immunophenotypic markers in the acute and recovery phases of SCARs types

In addition to the number of CD4<sup>+</sup>CD25<sup>+</sup>CD127<sup>-</sup>FoxP3<sup>+</sup> Tregs between groups of subjects, It would be interesting to know whether there is any alteration of immunophenotype markers between DRESS with autoimmune sequelae patients and DRESS without autoimmune sequelae patients compared to SJS/TEN patients and healthy donor subjects. The immunophenotyping markers of CD4<sup>+</sup>CD25<sup>+</sup>CD127<sup>-</sup>FoxP3<sup>+</sup> Tregs from every group of subjects were investigated using flow cytometry analysis. Seven markers, including PD-1, CTLA-4, GITR, LAG-3, OX40, CD39, and IL-10, were identified in the total of CD4<sup>+</sup>CD25<sup>+</sup>CD127<sup>-</sup>FoxP3<sup>+</sup> T cells shown in Table 8. We chose these 7 markers because they can represent the functions of Tregs that have been reviewed elsewhere.

**Table 8** The immunophenotype of Tregs from patients with DRESS, SJS/TEN, and healthy donors.

Immuno-phenotyping markers	Healthy Donors (n = 9)	DRESS without autoimmune sequelae patients					
		DRESS with autoimmune sequelae patients		DRESS without autoimmune sequelae patients		SJS/TEN patients	
		Acute Phase (n = 4)	Recovery Phase (n = 4)	Acute Phase (n = 8)	Recovery Phase (n = 4)	Acute Phase (n = 5)	Recovery Phase (n = 3)
PD-1	17.30±1.68	32.70±7.60	31.83±6.48	40.43±9.67	33.63±13.45	39.68±9.79	40.63±5.36
CTLA-4	1.53±0.15	13.73±0.96	2.46±0.47	13.01±2.68	1.94±0.53	10.41±4.26	7.28±3.10
GITR	1.56±0.11	8.96±3.96	1.87±1.15	2.00±0.67	1.33±0.37	7.51±1.18	1.53±0.21
LAG-3	0.69±0.05	3.49±0.11	0.73±0.26	2.29±1.27	0.56±0.26	2.87±0.51	1.01±0.32
OX40	1.21±0.122	9.23±3.23	1.85±0.68	11.55±3.10	1.94±1.01	11.06±6.14	4.93±1.92
CD39	35.86±8.82	70.48±13.37	52.03±17.13	52.22±14.55	62.73±14.24	51.48±11.09	24.33±4.94
IL-10	0.74±0.06	1.94±0.30	0.77±0.10	0.93±0.22	0.50±0.06	2.39±0.34	0.30±0.17

Noted - Mean ± SEM values are shown.



PD-1 and CTLA-4 expressed on Tregs work in the same way; their binding can inhibit effector T cell proliferation, the production of inflammatory cytokines (e.g., TFN-g, TNF-a, IL-2), and affect the survival of effector T cells<sup>(88)</sup>. Our results showed that the expression of PD-1 was not significantly different when compared between all sample groups at 95% confidence. Still, it tended to be higher in SCARs patients than in healthy donors (Figure 12).

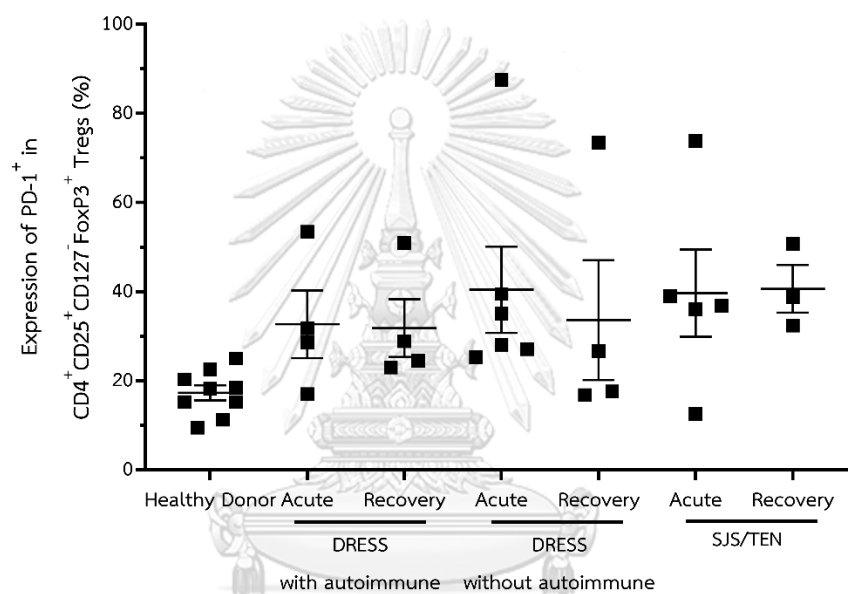


**Figure 12** The expression of PD-1 of CD4<sup>+</sup>CD25<sup>+</sup>CD127<sup>-</sup>FoxP3<sup>+</sup> Tregs. The frequency of PD-1 in CD4<sup>+</sup>CD25<sup>+</sup>CD127<sup>-</sup>FoxP3<sup>+</sup> Tregs was given as a mean±SEM value. One-way ANOVA followed by Tukey's HSD test for multiple comparisons was used to determine the significance between groups given as *P* value at 95% confidence.

The expression of CTLA-4 in CD4<sup>+</sup>CD25<sup>+</sup>CD127<sup>-</sup>FoxP3<sup>+</sup> Tregs was higher in the acute phase of DRESS with autoimmune sequelae, DRESS without autoimmune sequelae, and SJS/TEN patients when compared to the healthy donors. Moreover, CTLA-4 expression was higher in DRESS patients at the acute phase (DRESS with autoimmune sequelae and DRESS without autoimmune sequelae) compared to their recovery phase (Figure 13). However, the expression of CTLA-4 in DRESS patients with and without autoimmune sequelae during the recovery phase was not different compared to healthy donors and SJS/TEN patients during the recovery phase.

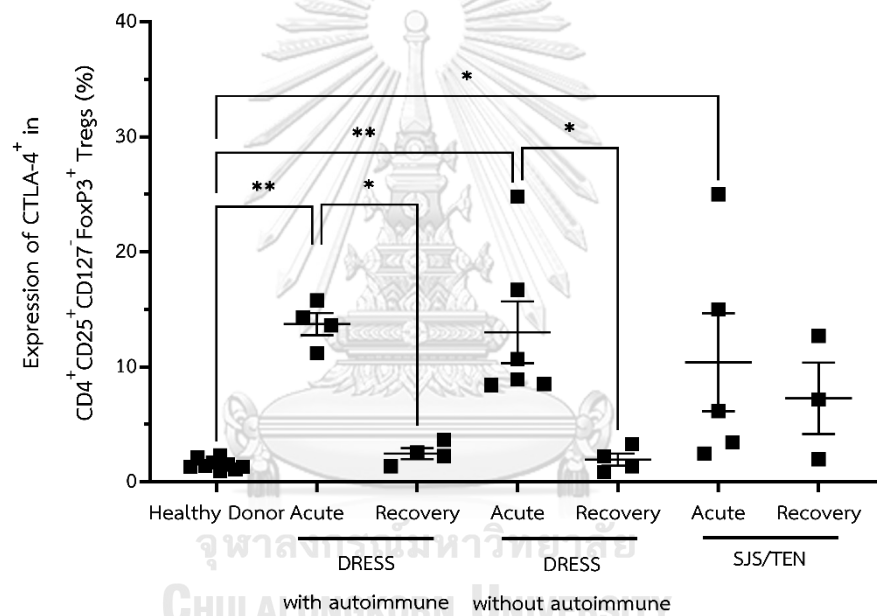


**Figure 13** The expression of CTLA-4 of CD4<sup>+</sup>CD25<sup>+</sup>CD127<sup>-</sup>FoxP3<sup>+</sup> Tregs. The frequency of CTLA-4 in CD4<sup>+</sup>CD25<sup>+</sup>CD127<sup>-</sup>FoxP3<sup>+</sup> Tregs was given as a mean±SEM value. One-way ANOVA followed by Tukey's HSD test for multiple comparisons was used to determine the significance between groups given as P value. at 95% confidence; \*P < 0.05 and \*\*P < 0.01.

The amount of GITR typically positively correlates with the immunosuppressive activity of Tregs, and the expression of GITR in Tregs can be up-regulated following activation<sup>(89, 90)</sup>. In our study, the expression of GITR in CD4<sup>+</sup>CD25<sup>+</sup>CD127<sup>-</sup>FoxP3<sup>+</sup> Tregs was higher at the acute phase of DRESS with autoimmune sequelae and SJS/TEN patients compared to healthy donors (Figure 14). These results showed that GITR expression in Tregs was higher in the acute phase of DRESS with autoimmune sequelae patients when compared to them in the recovery phase. Moreover, there are no significant differences in GITR expression at the recovery phase of DRESS patients and SJS/TEN patients compared to healthy donors.

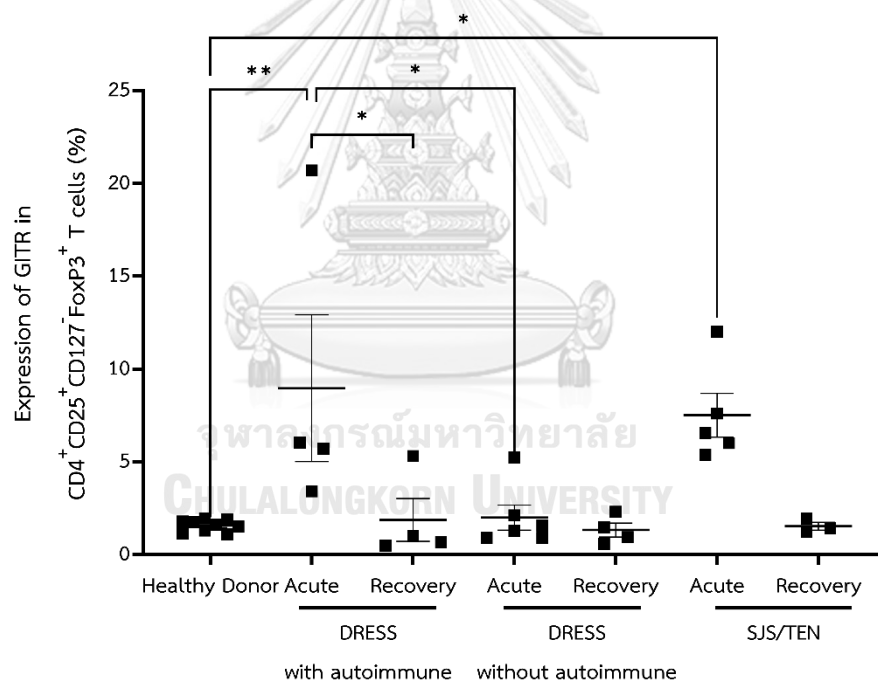


**Figure 14** The expression of GITR of CD4<sup>+</sup>CD25<sup>+</sup>CD127<sup>-</sup>FoxP3<sup>+</sup> Tregs. The frequency of GITR in CD4<sup>+</sup>CD25<sup>+</sup>CD127<sup>-</sup>FoxP3<sup>+</sup> Tregs was given as a mean±SEM value. One-way ANOVA followed by Tukey's HSD test for multiple comparisons was used to determine significance between groups given as *P* value. at 95% confidence; \**P* < 0.05 and \*\**P* < 0.01.

Several studies have shown that LAG-3 identifies Treg populations and contributes to their suppressor activity<sup>(91-93)</sup>. From our results, the LAG-3 expression in CD4<sup>+</sup>CD25<sup>+</sup>CD127<sup>-</sup>FoxP3<sup>+</sup> Tregs in DRESS with autoimmune sequelae patients was higher than in healthy donors (Figure 15). Moreover, LAG-3 tended to be higher but not statistically significant in every group of patients in the acute phase compared to their recovery phase.

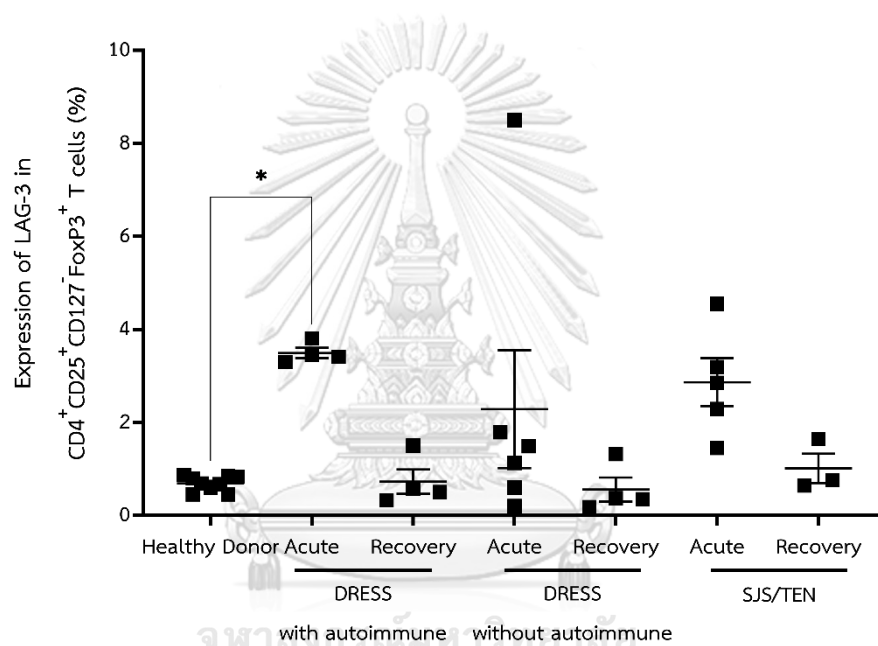


**Figure 15** The expression of LAG-3 of CD4<sup>+</sup>CD25<sup>+</sup>CD127<sup>-</sup>FoxP3<sup>+</sup> Tregs. The frequency of LAG-3 in CD4<sup>+</sup>CD25<sup>+</sup>CD127<sup>-</sup>FoxP3<sup>+</sup> Tregs was given as a mean±SEM value. One-way ANOVA followed by Tukey's HSD test for multiple comparisons was used to determine the significance between groups given as P value. at 95% confidence; \**P* < 0.05.

In 2020, Miyagawa and their colleagues reported that the upregulation of OX40 on CD4<sup>+</sup> T cells was identified in the acute phase of DRESS patients. But the expression of OX40 on Tregs has not been elucidated even though it is considered a Treg activation marker. Therefore, we would like to determine the expression of

OX40 and whether it was altered in our groups of patients. The results showed that the OX40 expression in  $CD4^+CD25^+CD127^-FoxP3^+$  Tregs was not significantly different compared between all groups. (Figure 16). However, OX40 expression seems to be higher in the acute phase of SCARs patients compared to their recovery phase and in healthy donors.

Similarly, the expression of CD39 in  $CD4^+CD25^+CD127^-FoxP3^+$  Tregs was not statistically significant between groups of patients and healthy donors. Nonetheless, it seems to be higher in the acute and recovery phase of DRESS with autoimmune sequelae and DRESS without autoimmune sequelae patients and the acute phase of SJS/TEN than in the healthy donors (Figure 17).

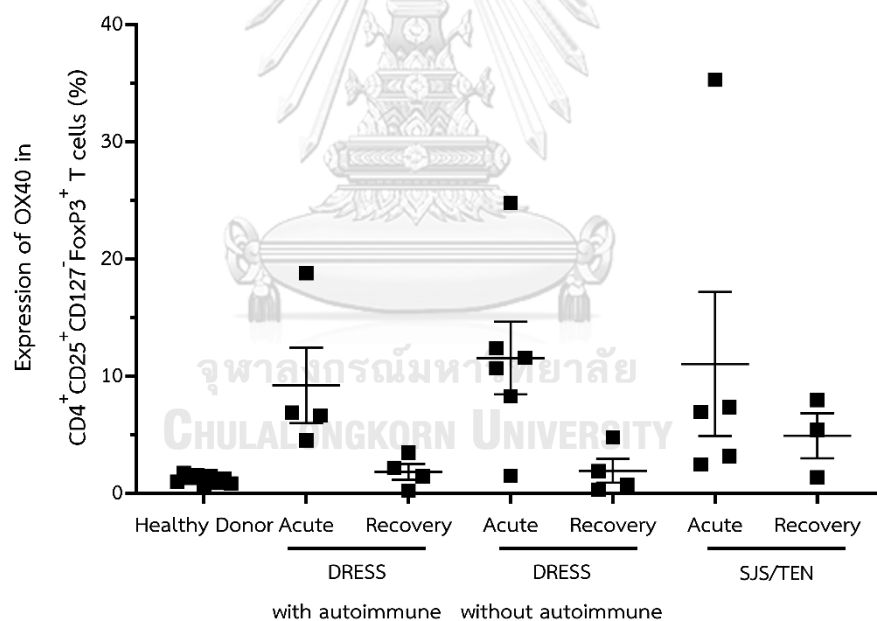


**Figure 16** The expression of OX40 of  $CD4^+CD25^+CD127^-FoxP3^+$  Tregs. The frequency of OX40 in  $CD4^+CD25^+CD127^-FoxP3^+$  Tregs was given as a mean $\pm$ SEM value. One-way ANOVA followed by Tukey's HSD test for multiple comparisons was used to determine the significance between groups given as *P* value. at 95% confidence.

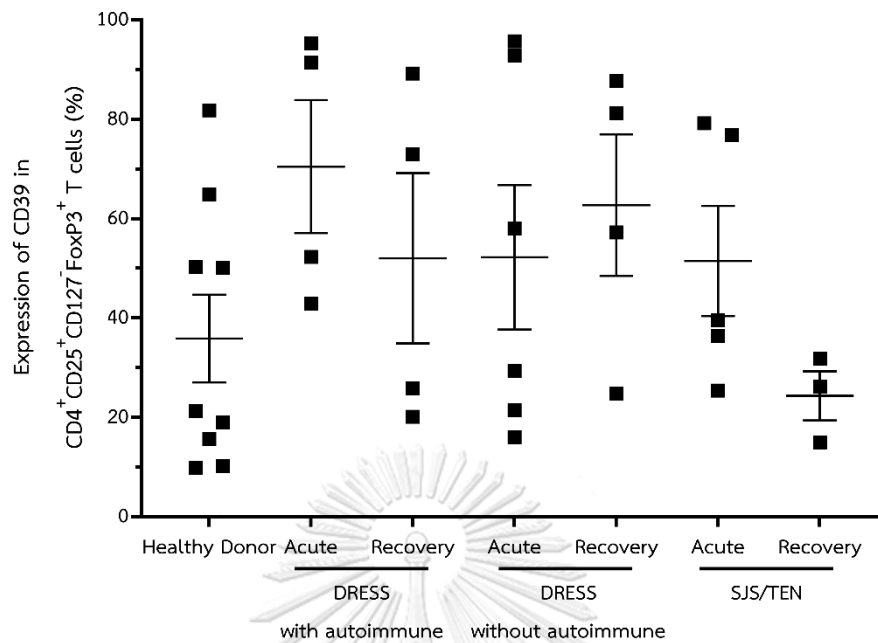


**Figure 17** The expression of CD39 of CD4<sup>+</sup>CD25<sup>+</sup>CD127<sup>-</sup>FoxP3<sup>+</sup> Tregs. The frequency of CD39 in CD4<sup>+</sup>CD25<sup>+</sup>CD127<sup>-</sup>FoxP3<sup>+</sup> Tregs was given as a mean±SEM value. One-way ANOVA followed by Tukey's HSD test for multiple comparisons was used to determine the significance between groups given as *P* value. at 95% confidence.

IL-10 is an inhibitory cytokine that is secreted prominent in Tregs. In this study, we also investigated the expression of IL-10 in CD4<sup>+</sup>CD25<sup>+</sup>CD127<sup>-</sup>FoxP3<sup>+</sup> Tregs. The results showed significantly higher IL-10 expression in patients with DRESS with autoimmune sequelae at the acute phase compared with healthy donors and lower at the recovery phase of the same group. DRESS without autoimmune sequelae at the acute phase also showed lower IL-10 expression than DRESS with autoimmune sequelae and SJS/TEN patients at the acute phase. IL-10 was also found to be higher in SJS/TEN in the acute phase than in the resolution phase and in healthy donors.

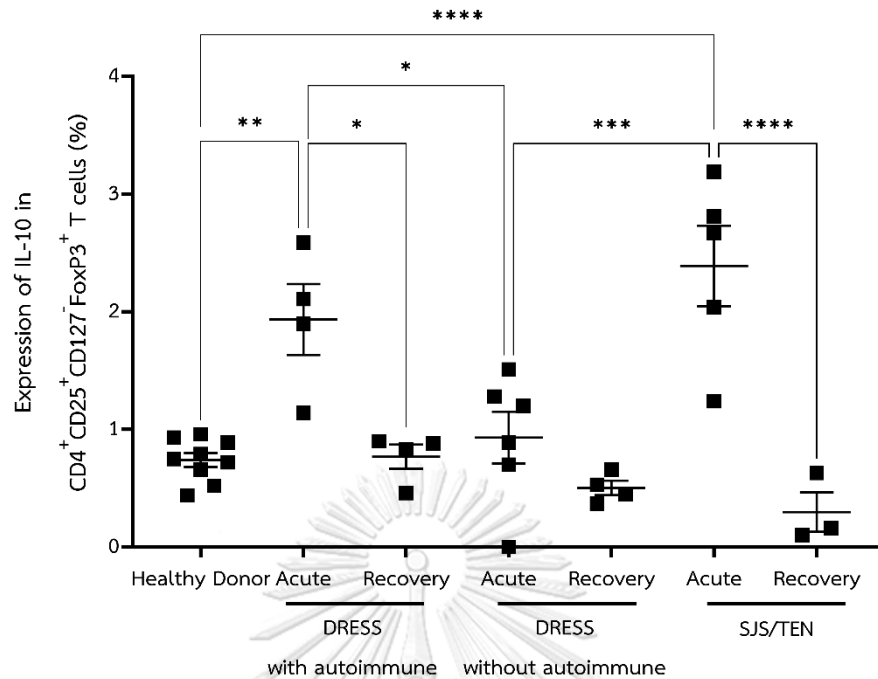


**Figure 18** The expression of IL-10 of CD4<sup>+</sup>CD25<sup>+</sup>CD127<sup>-</sup>FoxP3<sup>+</sup> Tregs. The frequency of IL-10 in CD4<sup>+</sup>CD25<sup>+</sup>CD127<sup>-</sup>FoxP3<sup>+</sup> Tregs was given as a mean±SEM value. One-way ANOVA followed by Tukey's HSD test for multiple comparisons was used to determine the significance between groups given as P value. at 95% confidence; \*P < 0.05, \*\*P < 0.01, \*\*\*P < 0.001, \*\*\*\*P < 0.0001

From our results in this part, we can suggest that the frequency of CD4<sup>+</sup>CD25<sup>+</sup>CD127<sup>-</sup>FoxP3<sup>+</sup> Tregs in DRESS patients at the acute phase tended to decrease and increases to the same level as healthy donors in their recovery phase. However, the expression of CTLA-4, GITR, LAG-3, and IL-10 was higher in the acute phase of DRESS with autoimmune sequelae when compared to their recovery phase. These indicate that Tregs might be essential in developing autoimmune disease in DRESS patients.

## PART 2 REGULATORY T CELL SUPPRESSIVE FUNCTION

The second objective of our study was to investigate the suppressive function of Treg *ex vivo*. We used the co-cultured between Tregs and Teff to evaluate the suppressive function of Tregs of DRESS with autoimmune sequelae, DRESS without autoimmune sequelae, and SJS/TEN patients.

### 5.2 The positive correlation of CD4<sup>+</sup>CD25<sup>+</sup>CD127<sup>-</sup> Tregs and CD4<sup>+</sup>CD25<sup>+</sup>CD127<sup>-</sup> FoxP3<sup>+</sup> Tregs

Since we used the FoxP3, the intracellular marker, to identify Tregs. It means that the cells must be fixed to die before intracellular staining. In this experiment, we used only CD4, CD25, and CD127 surface markers in this co-culture to identify and purify Tregs. These antibodies can bind to their markers on the cell membrane without damaging it. Thus, Tregs maintained their viability throughout the experiment.

The correlation between CD4<sup>+</sup>CD25<sup>+</sup>CD127<sup>-</sup> Tregs and CD4<sup>+</sup>CD25<sup>+</sup>CD127<sup>-</sup> FoxP3<sup>+</sup> Tregs was performed to verify whether we can use CD4<sup>+</sup>CD25<sup>+</sup>CD127<sup>-</sup> Tregs to represent CD4<sup>+</sup>CD25<sup>+</sup>CD127<sup>-</sup> FoxP3<sup>+</sup> Tregs in the suppression assay.



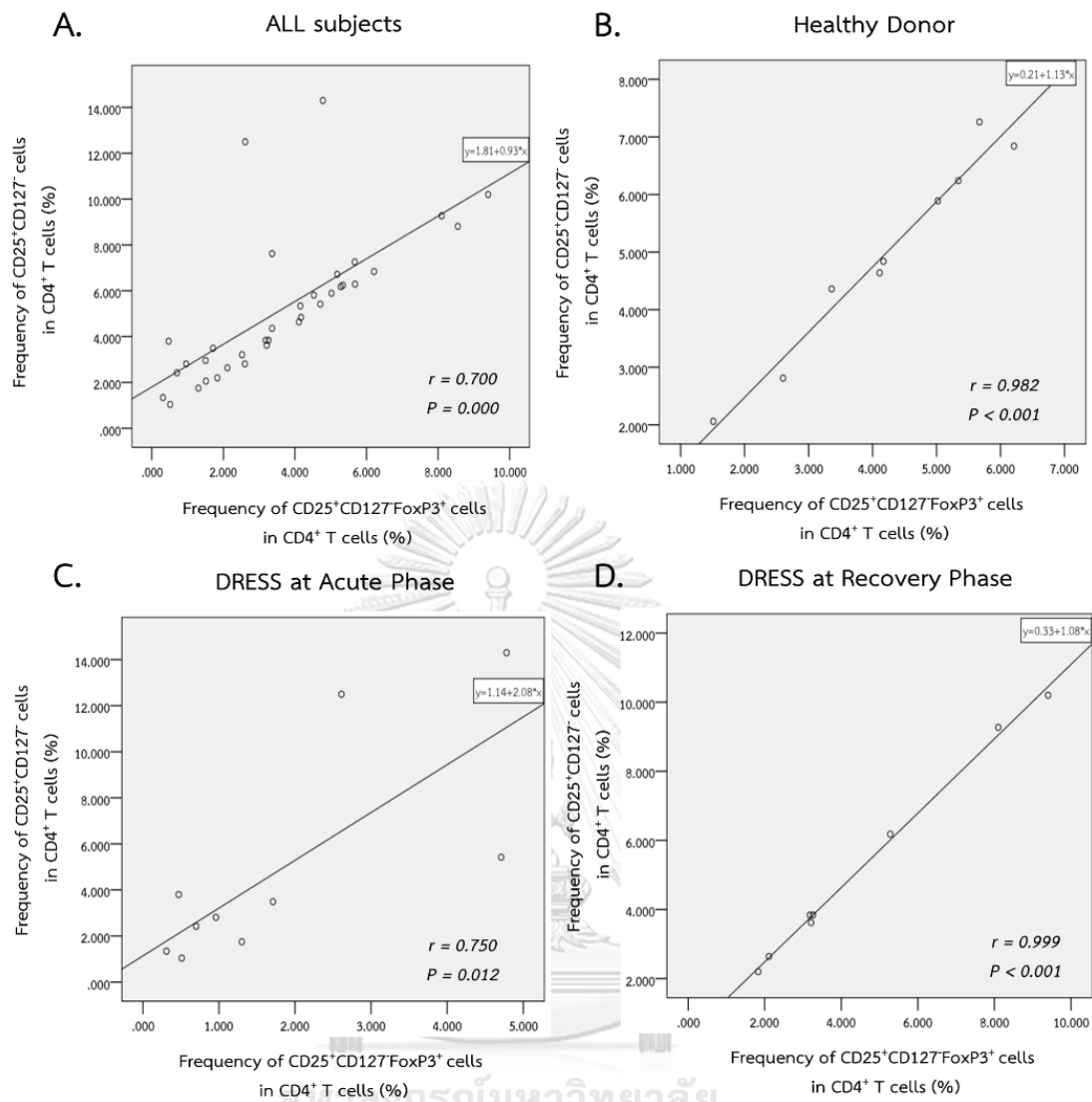


**Figure 19** The correlation between CD4<sup>+</sup>CD25<sup>+</sup>CD127<sup>-</sup> Tregs and CD4<sup>+</sup>CD25<sup>+</sup>CD127FoxP3<sup>+</sup> Tregs. (A.) From all subjects (n = 35). (B.) From healthy donors (n = 9). (C.) from DRESS patients during the acute phase (n = 10). (D.) From DRESS patients during the recovery phase (n = 8). (E.) From SJS/TEN during the acute phase (n = 5). And (F) From SJS/TEN during the acute phase (n = 3)

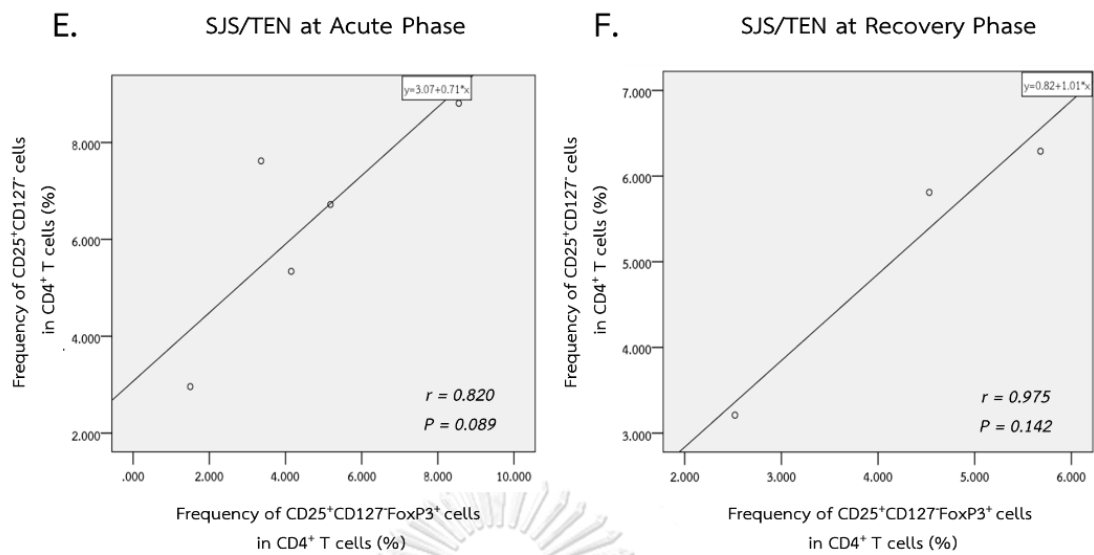


Figure 19 Continued.

A positive correlation between CD4<sup>+</sup>CD25<sup>+</sup>CD127<sup>-</sup> Tregs and CD4<sup>+</sup>CD25<sup>+</sup>CD127<sup>-</sup>FoxP3<sup>+</sup> Tregs was shown in all subjects from every group shown in Figure 19A. Moreover, when we considered the correlation in each group of patients. Every group of patients had a positive correlation between CD4<sup>+</sup>CD25<sup>+</sup>CD127<sup>-</sup> Tregs and CD4<sup>+</sup>CD25<sup>+</sup>CD127<sup>-</sup>FoxP3<sup>+</sup> as well, including healthy donors (Figure 19B), DRESS at acute phase (Figure 19C), DRESS at recovery phase (Figure 19D), SJS/TEN at acute phase (Figure 19E), and SJS/TEN at recovery phase (Figure 19F). Although the SJS/TEN groups showed no significance, which might be due to the small number of patients, these results still showed a highly positive correlation. However, we could use CD4<sup>+</sup>CD25<sup>+</sup>CD127<sup>-</sup> cells as Tregs in further suppression assay.

### 5.3 The purity of CD4<sup>+</sup>CD25<sup>+</sup>CD127<sup>-</sup> regulatory T cells and CD4<sup>+</sup>CD25<sup>-</sup> effector T cells after isolation

CD4<sup>+</sup>CD25<sup>+</sup>CD127<sup>-</sup> Tregs and CD4<sup>+</sup>CD25<sup>-</sup> effector T cells were isolated from PBMCs ( $1 \times 10^7$  cells) in the patients and healthy donors by EasySep Human CD4<sup>+</sup>CD127<sup>-</sup>CD25<sup>+</sup> Regulatory T Cell Isolation Kit (STEMCELL Technologies) as

mention in Chapter IV. Since the purpose of any cell separation process is to isolate desired cell type, the most crucial variables to consider is the purity of isolated cells.

The flow cytometry technique was used to determine the purity of isolated cells. Purity is often expressed as a ratio of the target cells to the total number of separated cells. The purity of  $CD4^+CD25^+CD127^-$  Treg after isolation was  $80.97\% \pm 7.86\%$  of whole isolated cells, while in these  $CD4^+CD25^+CD127^-$  Treg cells was expressed high frequency of FoxP3<sup>+</sup> expression ( $95.95\% \pm 1.20\%$ ), these indicate that this cells can represent the population of  $CD4^+CD25^+CD127^-$  FoxP3<sup>+</sup> Tregs. The purity of  $CD4^+CD25^-$  effector T cells after isolation was  $98.07\% \pm 0.291\%$  (Figure 5.14).

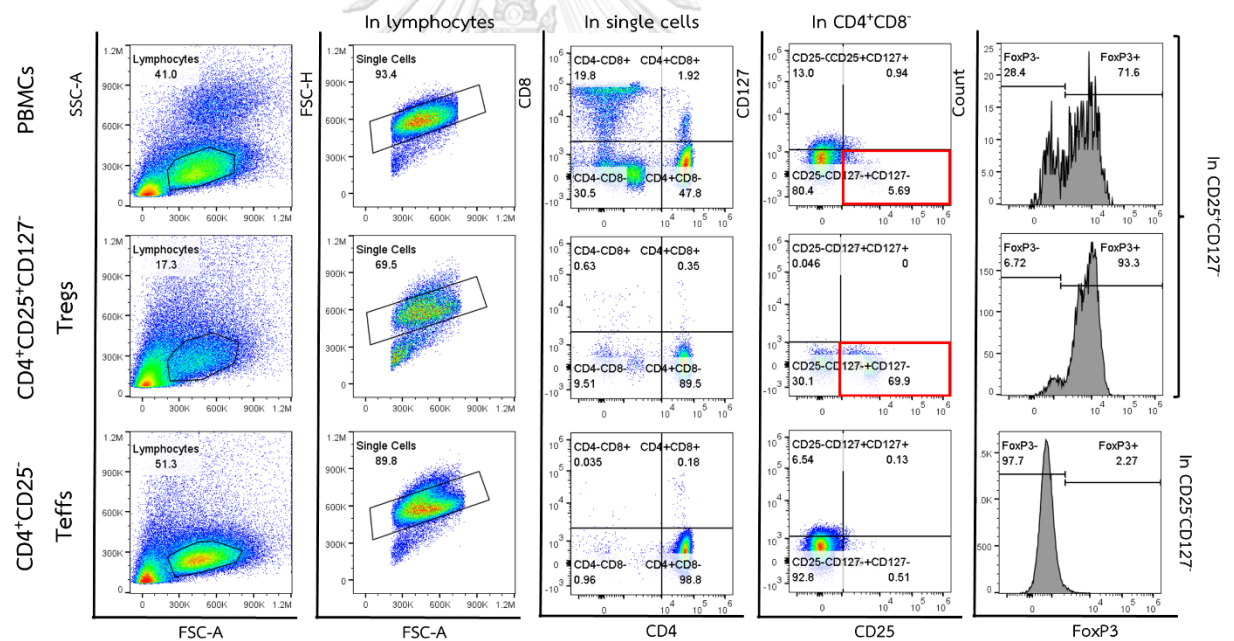


**Figure 20** The purity of  $CD4^+CD25^+CD127^-$  Tregs in total isolated cells using flow cytometry. Isolated cells were stained with CD4-APC/cy7, CD25-PE, CD127-PerCP/Cy5.5, and FoxP3-AF488 to determine  $CD4^+CD25^+CD127^-$  Treg purity and FoxP3<sup>+</sup> cells in Treg. The top row shows PBMCs before isolation. The middle row shows isolated Tregs isolated and isolated effector T are shown in the bottom row.

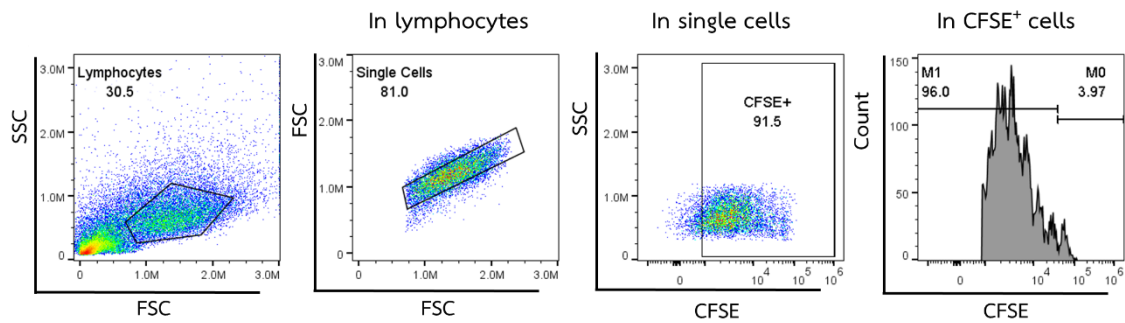


**Figure 21** The gating strategy for CFSE<sup>+</sup> cells to determine the proliferation cells.

CFSE<sup>+</sup> effector T cells were determined with the flow cytometry technique. Lymphocytes were gated from total cells using FSC and SSC plots. Then single cells were identified, and CFSE<sup>+</sup> effector T cells were gated to cut off the negative population. The initial population of effector T cells was the brightest (M0), and the resulting cell division showed a reduced CFSE signal (M1). The M1 population in the histogram represented the percentage of Teff proliferation.

#### 5.4 Tregs from DRESS patients could not suppress the autologous proliferation of effector T cells.

The suppressive function of Tregs was investigated by CFSE proliferation assay with flow cytometry. CD4<sup>+</sup>CD25<sup>+</sup>CD127<sup>-</sup> Tregs from patients and healthy donors were co-cultured with autologous CFSE-stained CD4<sup>+</sup>CD25<sup>-</sup> Teff cells at different ratios of effector T cells : Tregs ranging from 1 : 1, 1 : 0.5, 1 : 0.25, and 1 : 0. The gating strategy of flow cytometry analysis for effector T cells proliferation is shown in Figure 21.

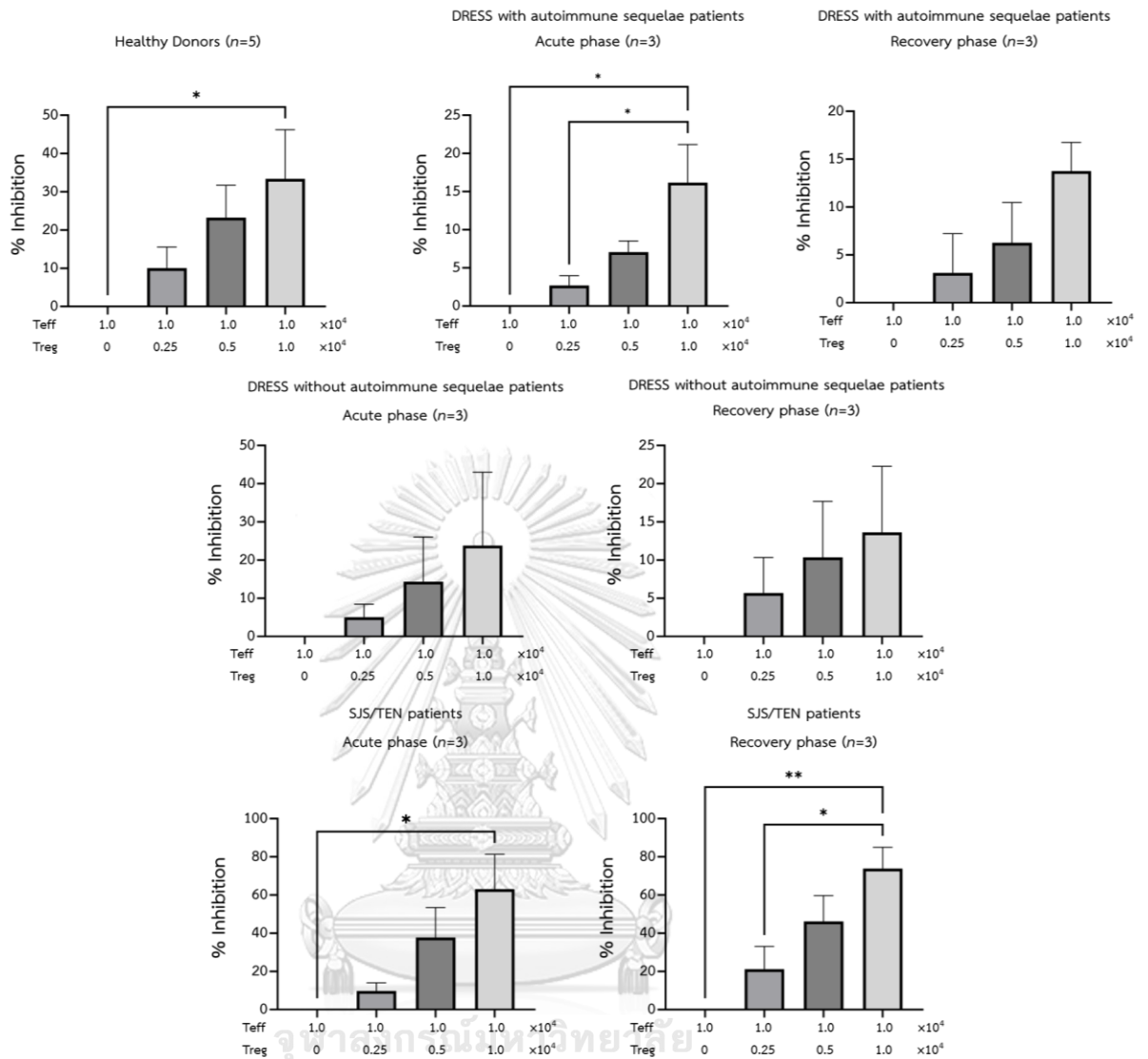
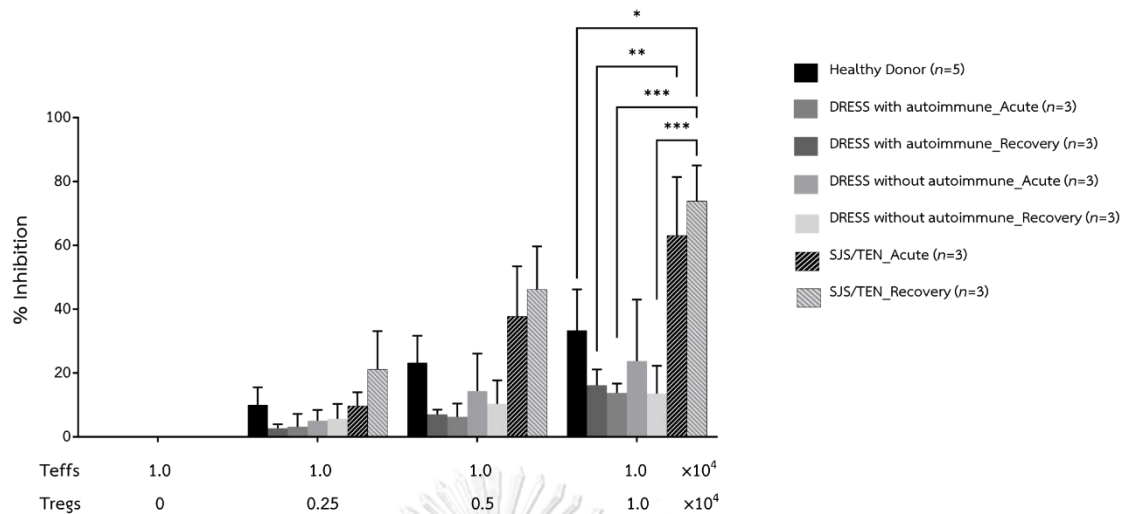


Figure 22 The suppressive function of Treg was compared in the same group of donors at different effector T cells : Treg ratio, which shows the dose-dependent manner in every group. The CFSE-stained Teff cell proliferation was analyzed using flow cytometry, and calculated the inhibition percentage by the formula given. The data were given as a mean±SEM with *P* value. at 95% confidence; \**P* < 0.05 and \*\**P* < 0.01.



**Figure 23** Suppressive functional analysis of Tregs between DRESS and SJS/TEN patients at acute and recovery phases compared to healthy donors. The CFSE-stained Teff cell proliferation was analyzed using flow cytometry, and calculated the inhibition percentage by the formula given. The suppressive function of Treg was compared between groups of donors. The suppressive functions of Tregs are presented in Mean  $\pm$  SEM values. One-way ANOVA followed by Tukey's HSD test for multiple comparisons was used to determine the significance between groups given as *P* value at 95% confidence; \**P* < 0.05, \*\**P* < 0.01, and \*\*\**P* < 0.001.

**Table 9** The suppressive function of Tregs shows as the percentage of inhibition.

Effector	Healthy Donors (n = 5)	DRESS with autoimmune sequelae patients		DRESS without autoimmune sequelae patients		SJS/TEN patients	
		Acute phase (n=3)	Recovery phase (n=3)	Acute phase (n=3)	Recovery phase (n=3)	Acute phase (n=3)	Recovery phase (n=3)
T cells :							
Tregs							
1 : 0	0	0	0	0	0	0	0
1 : 0.25	10.06 $\pm$ 5.50	2.71 $\pm$ 1.27	3.13 $\pm$ 4.09	5.07 $\pm$ 3.36	5.69 $\pm$ 4.64	9.75 $\pm$ 4.25	21.21 $\pm$ 11.95
1 : 0.5	23.26 $\pm$ 8.46	7.07 $\pm$ 1.45	6.27 $\pm$ 4.20	14.35 $\pm$ 11.73	10.37 $\pm$ 7.34	37.80 $\pm$ 15.62	46.22 $\pm$ 13.47
1 : 1	33.38 $\pm$ 12.86	16.17 $\pm$ 5.01	13.76 $\pm$ 2.99	23.80 $\pm$ 19.22	13.63 $\pm$ 8.65	63.16 $\pm$ 18.25	73.90 $\pm$ 11.16

**Noted:** The inhibition percentage of Tregs is presented in Mean  $\pm$  SEM values.

The suppressive activity of Tregs can inhibit the proliferation of effector T cells from every group of subjects by showing the inhibition percentage in a dose-dependent manner when the ratio of Tregs to effector T cells was increased (Figure 22). Especially in SJS/TEN patients in the acute and recovery phases, that inhibition percentage was dose-dependent with statistical significance at the effector T cells : Tregs ratio at 1 : 0.5 and 1 : 1.

The suppressive function of Tregs at the ratio of Tregs : effector T cells as 1 : 1 was the only concentration showing a significant difference between groups. Tregs in DRESS with and without autoimmune sequelae patients have a lower inhibitory percentage but were not statistically significant in both acute and recovery phases compared to healthy donors, as shown in Figure 23 and Table 9. Nonetheless, the suppressive function of Tregs from DRESS with autoimmune sequelae at the acute phase was significantly lower than those from SJS/TEN at the same phase. Tregs from DRESS with and without autoimmune sequelae patients at the recovery phase were significantly lower than those from SJS/TEN at the recovery phase. Moreover, the suppressive function of Tregs in SJS/TEN patients during the recovery phases was higher than the Tregs from healthy donors.

The results suggest that Tregs from DRESS with and without sequelae have lowered their ability to suppress effector T cell proliferation since the acute phase of the symptoms and still lower suppressive ability during the recovery phase. Additionally, our results were similar to the previous study of Takahashi and their colleagues<sup>(5)</sup>, which showed dysfunction of Treg cells in DIHS/DRESS since their acute stage in their suppression assay. Therefore, the decrease in the ability to suppress effector T cells might affect the pathogenesis of autoimmune sequelae in DRESS patients.

### PART 3 MRNA EXPRESSION PROFILE OF TREGS USING NANOSTRING TECHNOLOGY

In addition to investigating the Tregs population's alteration, their immunophenotypes, and the suppressive function of DRESS patients, we would like to explore the gene expression profile between Tregs of DRESS with autoimmune sequelae and DRESS without autoimmune sequelae as well.

#### 5.5 mRNA expression profile of Tregs using NanoString Technology

Sixteen internal reference genes can be used for the data normalization. In contrast, four internal reference genes were excluded due to their high expression equivalent to the endogenous genes, including PGK1, RPL4, UBB, and OAZ1 (Figure 24A). A histogram of *P*-values testing each gene's univariate association with the chosen covariate is displayed for each covariate included in the analysis (Figure 24B). Low *P*-values indicated strong evidence for an association between SCARs phenotypes and genes in the panel. This test suggested that most genes provided in the nCounter® Human Autoimmune Profiling Panel were suitable for the mRNA profiling in our study.



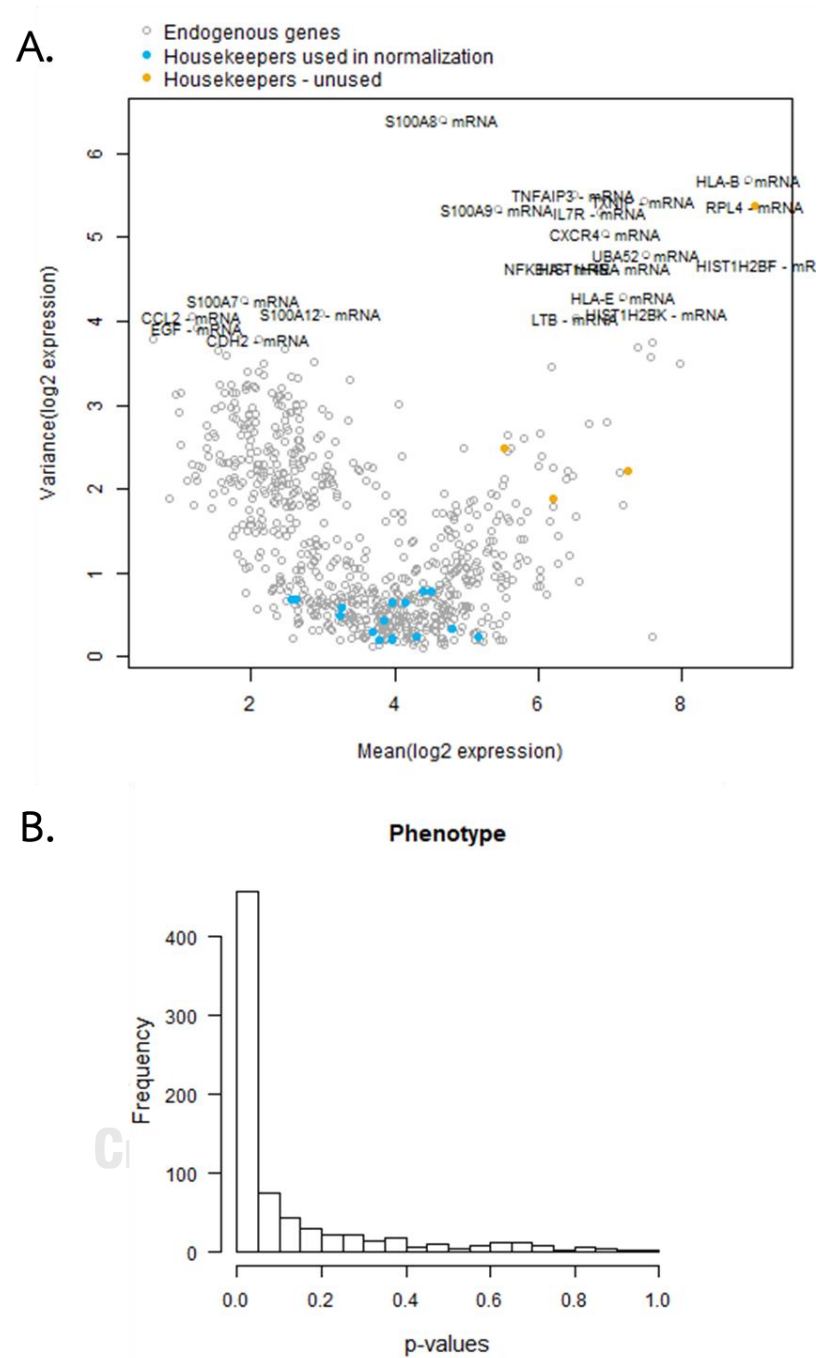


**Figure 24** The variance vs. mean normalized signal plot across all targets/probes and the p-value distribution plots. (A.) Each gene's variance in the log-scaled, normalized data is plotted against its mean value across all samples. Highly variable genes are indicated by gene name. Housekeeping genes are color-coded according to their use in (or omission from) normalization. (B.) A histogram of p-values testing each

gene's univariate association with the chosen covariate is displayed for each covariate included in the analysis. Low *P*-values indicate strong evidence for an association between genes in codeset and SCARs patients.

After normalization, the expression of each gene was calculated. Results of the number of upregulated and downregulated gene expressions are shown in Figure 5.19. Among the samples, We found 241 genes downregulating and 7 downregulating genes with DEGs value of fold change  $> 1.5$  and *p*-value  $< 0.05$  when comparing the gene expression ratio between DRESS with autoimmune sequelae patients and healthy donors. DRESS with autoimmune sequelae during the recovery phase induced DEGs were 13 upregulated genes and 4 downregulated genes compared to healthy donors. We found 4 upregulated genes and 1 downregulated gene in DRESS without autoimmune sequelae patients and 10 upregulated genes and 1 downregulated gene in DRESS without autoimmune sequelae during the recovery phase when comparing each group with healthy donors. Moreover, 2 upregulated and 8 downregulated genes were found in SJS/TEN during the acute phase. SJS/TEN during the recovery phase had 2 upregulated genes and 35 downregulated genes compared to healthy donors (Figure 25). The fold-change difference between endogenous genes in every group of samples compared to healthy donors is shown in Appendix D. These results suggested that the downregulation of 208 genes in DRESS with autoimmune sequelae patients might affect their autoimmune development.

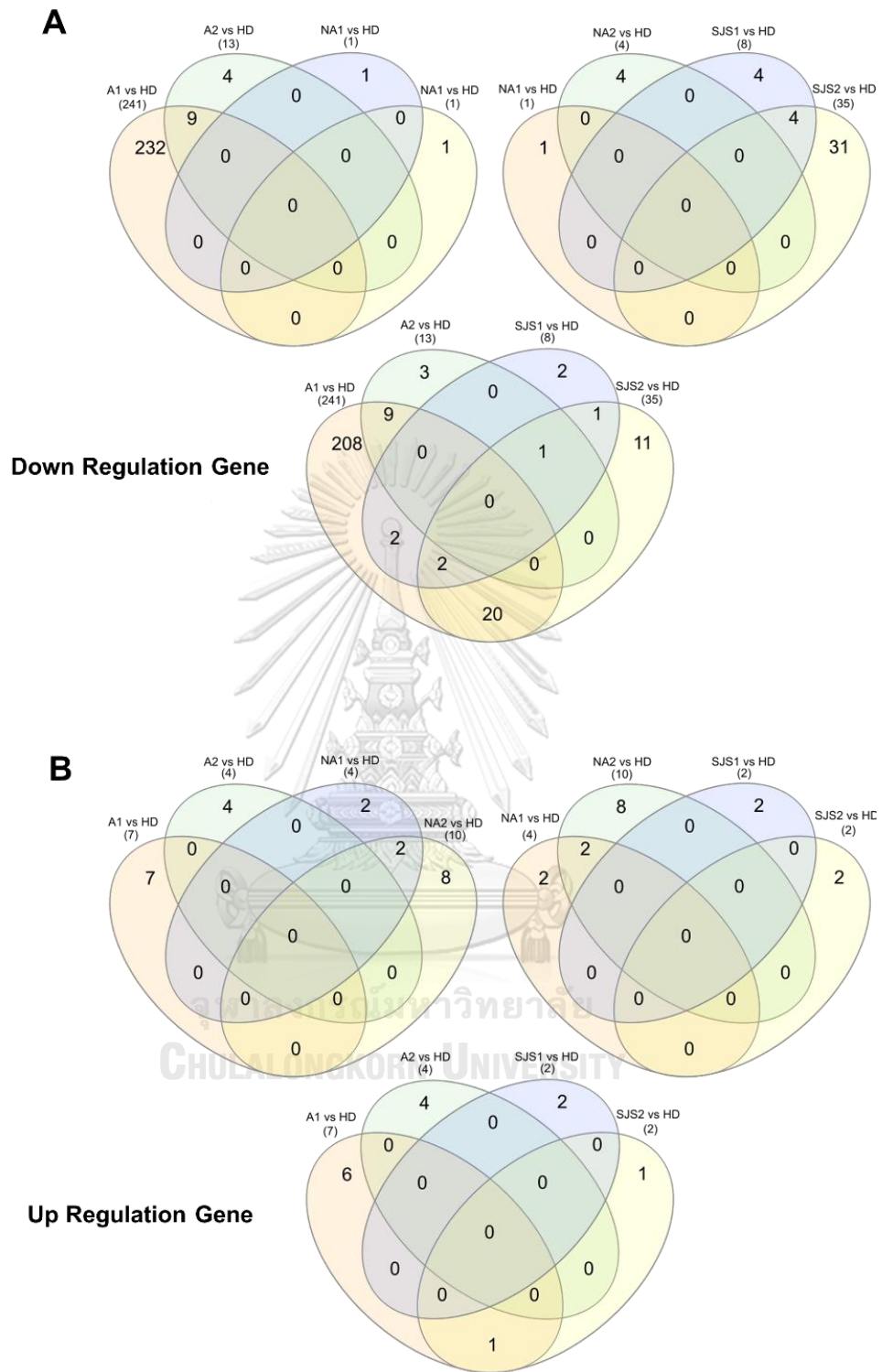


Figure 25 Differential gene expression analysis of Treg from SCARs patients compared to healthy donors. Venn diagrams showing overlapping upregulated and downregulated genes of Tregs. DRESS with autoimmune sequelae patients vs.

healthy donors (n = 3) at the acute phase (n = 4) (A1 vs. HD) and the recovery phase (n = 4) (A2 vs. HD), DRESS without autoimmune sequelae patients vs. healthy donors at the acute phase (n = 3) (NA1 vs. HD) and the recovery phase (n = 3) (NA2 vs. HD), and The SJS/TEN patients vs. healthy donors at the acute phase (n = 3) (SJS1 vs. HD) and the recovery phase (n = 3) (SJS2 vs. HD).

### 5.1 Functional categories and pathways of the expressed gene in Tregs

Next, to understand the potential role of these genes in the biological pathway of Tregs. Genes included in this analysis must have a DEGs value of fold change  $> 1.5$  and p-value  $< 0.05$  when comparing the gene expression ratio between each group, including the acute and recovery phase of DRESS with autoimmune sequelae patients, DRESS without autoimmune sequelae patients, and SJS/TEN patients as well as one time point of healthy donor subjects.

Gene Ontology (GO) Biological Process 2021 and the Kyoto Encyclopedia of Genes and Genomes (KEGG) pathway were used to identify their biological functions. However, our study selected 13 pathways related to the function of Tregs with  $-\log(P\text{-value}) > 5$ . There were 4 pathways that we focused on, including the JAK-STAT signaling pathway, regulation of interleukin-10 production (GO:0032653), regulation of regulatory T cell differentiation (GO:0045589), and interleukin-2-mediated signaling pathway (GO:0038110) (Figure 26). We chose these 4 pathways because of previously proposed mechanisms involved in FoxP3 gene expression, which is the essential transcript factor in Treg function, reviewed elsewhere.

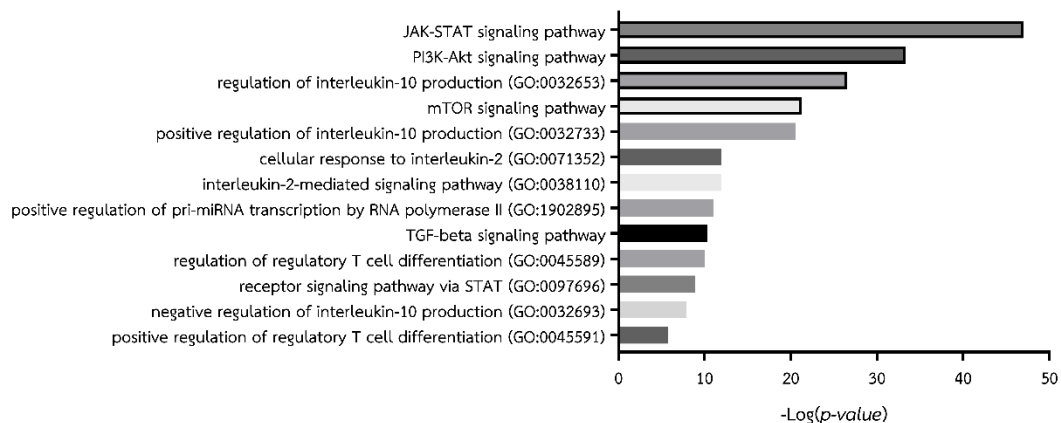


**Figure 26 Categorization of differential expressed genes (DEGs) in Tregs.**

Classification of the KEGG pathway and GO biological process pathway were generated by the Enrichr tool. Y-axis represents biological pathways, and X-axis represents  $-\log(p\text{-value})$ . The  $p$ -value is computed from the Fisher exact test, a proportion test that assumes a binomial distribution and independence for the probability of any gene belonging to any set.

To explore the expression level of genes in these pathways, we used heatmaps to represent the gene expression according to their fold change. One-way ANOVA was used to analyze the statistical difference between groups of patients. In the regulation of Tregs differentiation pathway, we found 14 DEGs (fold change > 1.5) from Treg differentiation regulation results. There are 3 genes in DRESS with autoimmune sequelae patients at the acute phase with statistical significance downregulated compared to other groups. CD46 gene, a costimulatory molecule for T cell activation, in the acute phase of DRESS with autoimmune sequelae was downregulated in DRESS with autoimmune sequelae patients at the recovery phase, DRESS without autoimmune sequelae patients at the recovery phase, SJS/TEN patients at the recovery phase, and healthy donors. LAG-3 gene, an inhibitory receptor that should be highly expressed on activated Tregs, in DRESS with autoimmune sequelae patients during the acute phase was also downregulated

compared to healthy donors. Moreover, the TNFSF4 gene encoding for OX40 in DRESS with autoimmune sequelae patients during the acute phase was significantly downregulated in DRESS without autoimmune sequelae patients during their recovery phase.

One of the markers that can be used to identify Tregs is CD25 which is an IL-2 $\alpha$  receptor. This IL-2 $\alpha$  receptor is essential in Treg survival and differentiation. Thus, the gene associated with IL-2 mediated signaling pathway should be focused on. There are 10 DEGs (fold change > 1.5) involved in the IL-2 mediated signaling pathway; the fold change of each subject is represented as Heatmap shown in Figure 28A. JAK1 gene in DRESS with autoimmune sequelae patients at the acute phase was significantly downregulated compared with healthy donors. JAK3 gene was also downregulated in DRESS with autoimmune sequelae patients at the acute phase compared to DRESS without autoimmune sequelae patients at both acute and recovery phases, SJS/TEN patients at the recovery phase, and in healthy donors.

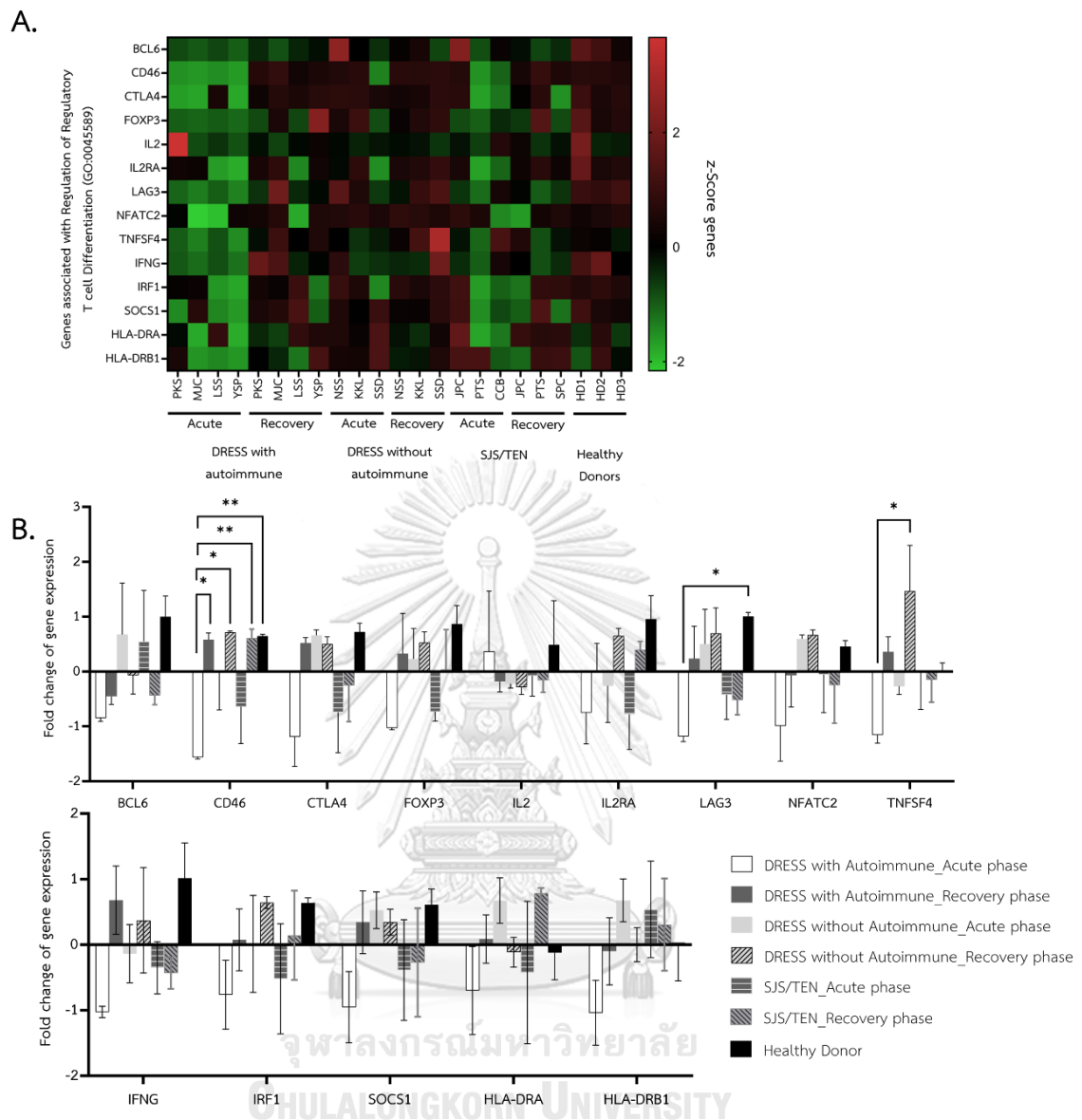


**Figure 27 Gene expression profile associated with regulation of Tregs differentiation.** A., Heatmap showing the expression level of 14 genes associated with regulation of Tregs differentiation in DRESS with autoimmune sequelae patients at the acute phase ( $n = 4$ ), DRESS with autoimmune sequelae patients at the recovery phase ( $n = 4$ ), DRESS without autoimmune sequelae patients at the acute phase ( $n = 3$ ), DRESS without autoimmune sequelae patients at the recovery phase ( $n = 3$ ), SJS/TEN patients at the acute phase ( $n = 3$ ), SJS/TEN patients at the recovery phase ( $n = 3$ ), and healthy donors ( $n = 3$ ). B., Graph showing fold change of genes associated with regulation of Tregs differentiation, compared between groups of subjects. The significance between groups given as  $P$  value at 95% confidence;  $*P < 0.05$  and  $**P < 0.01$ .

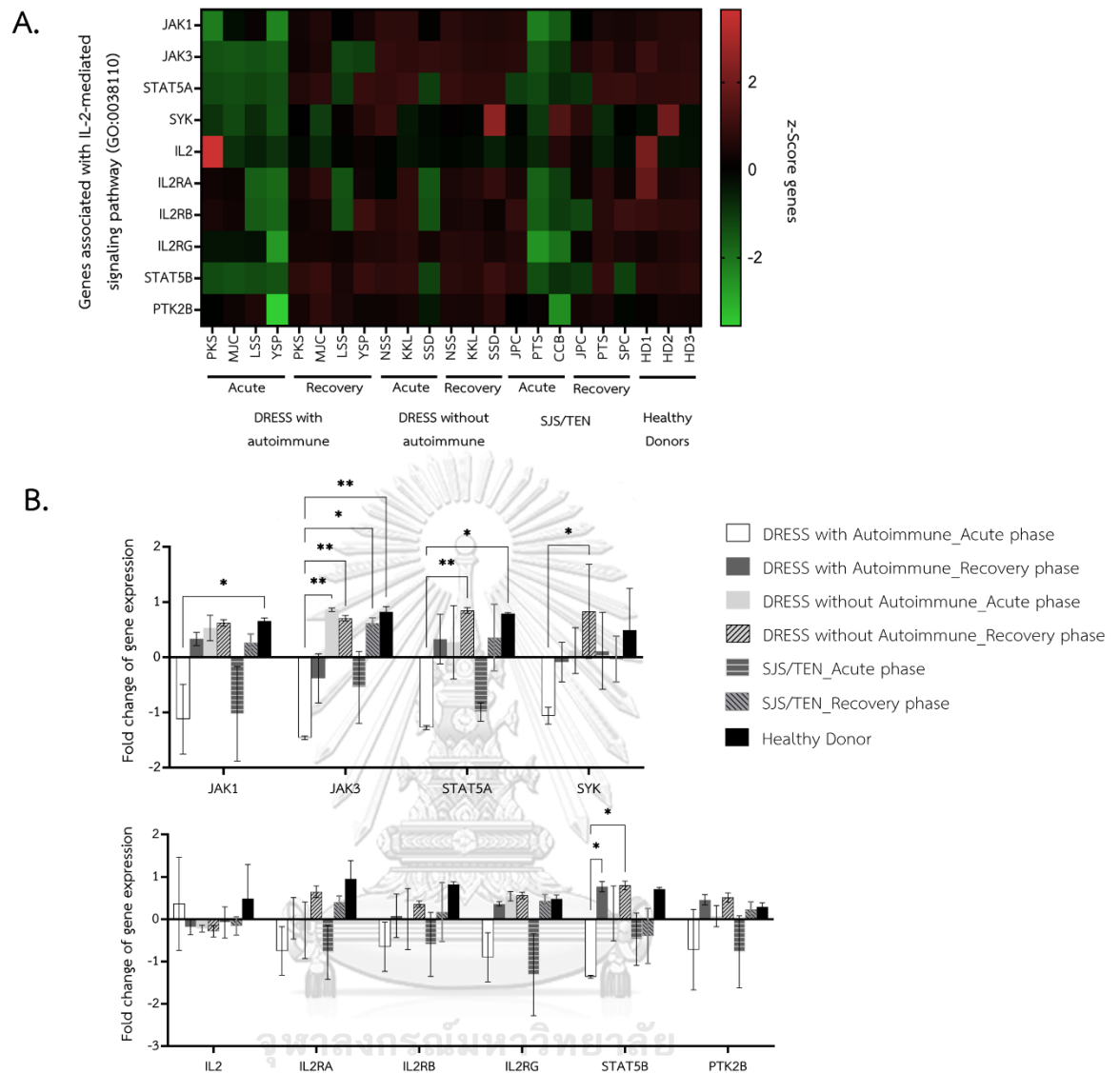


**Figure 28 Gene expression profile associated with IL-2 mediated signaling pathway.**

A., Heatmap showing the expression level of 10 genes associated with IL-2 mediated signaling pathway in DRESS with autoimmune sequelae patients at the acute phase ( $n = 4$ ), DRESS with autoimmune sequelae patients at the recovery phase ( $n = 4$ ), DRESS without autoimmune sequelae patients at the acute phase ( $n = 3$ ), DRESS without autoimmune sequelae patients at the recovery phase ( $n = 3$ ), SJS/TEN patients at the acute phase ( $n = 3$ ), SJS/TEN patients at the recovery phase ( $n = 3$ ), and healthy donors ( $n = 3$ ). B., Graph showing fold change of genes associated with IL-2 mediated signaling pathway, compared between groups of subjects. The significance between groups given as  $P$  value at 95% confidence;  $*P < 0.05$  and  $**P < 0.01$ .



Since the cytokine IL-10, the inhibitory cytokine is mostly secret from Tregs to help in suppressive function. The gene expression profile that regulates the IL-10 production pathway should be explored to determine whether the suppressive role of IL-10 inhibition has an alteration in DRESS patients with autoimmune sequelae. The Heatmap shows the expression level of 13 genes related to regulating the IL-10 production pathway (Figure 29A). Eight genes were significantly downregulated in DRESS with autoimmune sequelae patients at the acute phase compared to the group of healthy donors. One gene (TLR4 gene) was upregulated in DRESS with autoimmune sequelae patients at the acute phase compared to the healthy donors' group (Figure 29B).

ISG15 gene, interferon-stimulated gene 15, in DRESS with autoimmune sequelae patients at the acute phase was significantly downregulated in every group except in SJS/TEN patients at the recovery phase. We also found that the JAK3 and STAT3 genes were downregulated in DRESS patients with autoimmune sequelae compared to DRESS patients without autoimmune sequelae and in healthy donors. These results suggest that ISG15, JAK3, and STAT3 genes were downregulating and might be affected in DRESS patients in the development of their autoimmune sequelae. However, we found that the TLR4 gene, a toll-like receptor 4 gene, in DRESS with autoimmune sequelae patients at the acute phase was higher than in SJS/TEN patients at the recovery phase and in healthy donors.

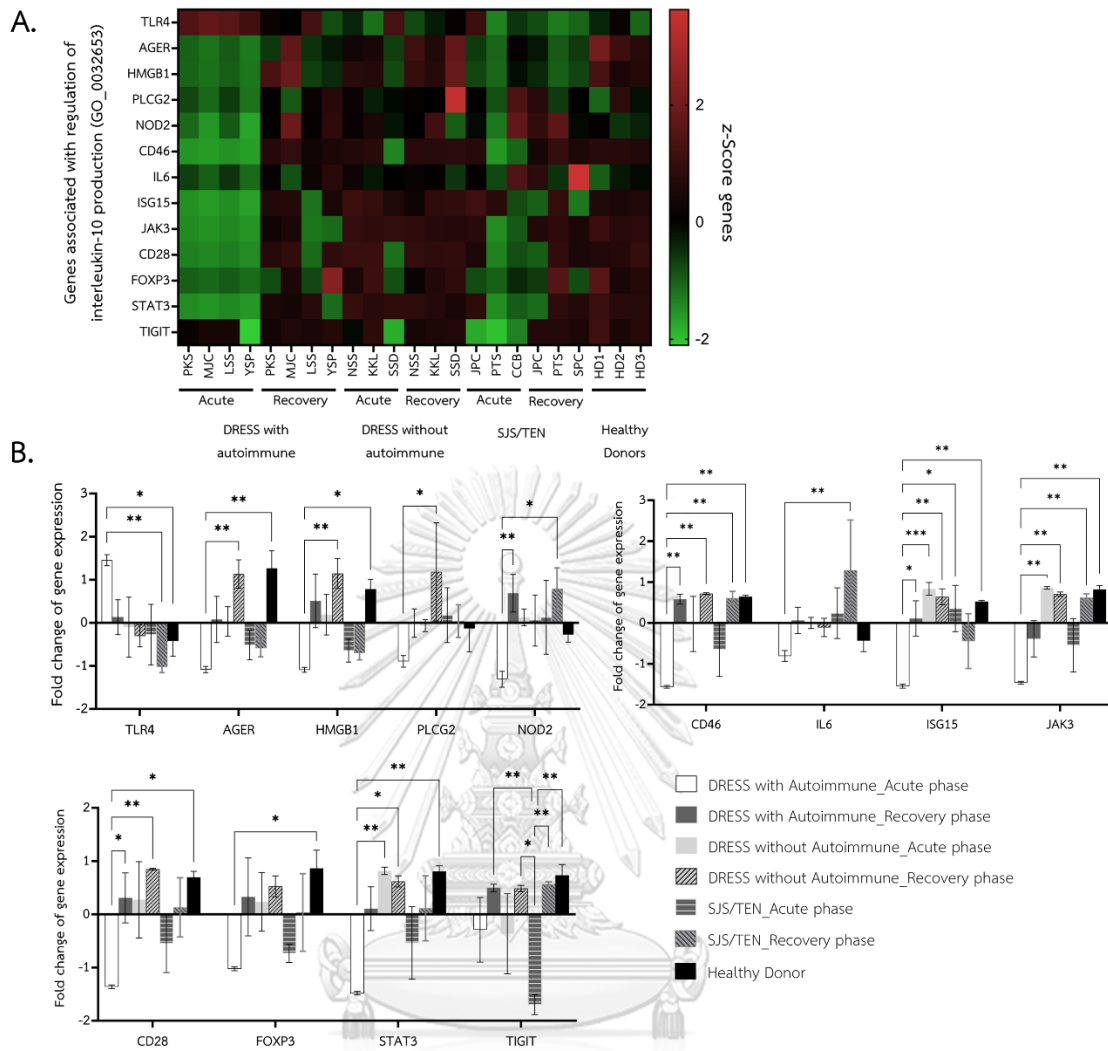


**Figure 29 Gene expression profile associated with regulation of interleukin-10 production pathway.** A., Heatmap showing the expression level of 13 genes associated with regulation of interleukin-10 production pathway in DRESS with autoimmune sequelae patients at the acute phase (n = 4), DRESS with autoimmune sequelae patients at the recovery phase (n = 4), DRESS without autoimmune sequelae patients at the acute phase (n = 3), DRESS without autoimmune sequelae patients at the recovery phase (n = 3), SJS/TEN patients at the acute phase (n = 3), SJS/TEN patients at the recovery phase (n = 3), and healthy donors (n = 3). B., Graph showing fold change of genes associated with regulation of interleukin-10 production pathway, compared between groups of subjects. The significance between groups given as P value at 95% confidence; \*P < 0.05 and \*\*P < 0.01.

Previous results showed that genes, including JAK1, JAK3, STAT3, STAT5A, and STAT5B, were downregulated in DRESS patients with autoimmune sequelae at their acute phase. Therefore we are interested in characterizing the gene expression profile associated with the IL-2/JAK3/STAT-5 signaling pathway, which is crucial in initiating and maintaining the transcription factor Foxp3 in Tregs mentioned elsewhere. Moreover, it has been associated with the demethylation of the intronic Conserved Non-Coding Sequence-2 (CNS2)<sup>(94)</sup>. The Heatmap shows the expression level of 28 genes associated with the JAK-STAT signaling pathway in every group of subjects Figure 30A. Our results showed that genes related to JAK-STAT signaling pathway, including CREBBP, IL12RB1, IL6ST, STAT1, STAT3, IL7R, JAK3, STAT5A, STAT5B, and GRB2 genes in DRESS with autoimmune sequelae patients at the acute phase were significantly downregulated compared to DRESS patients with autoimmune sequelae and in healthy donors. Nevertheless, we found that only one gene, IFNA1, in DRESS patients with autoimmune sequelae at the acute phase was significantly upregulated compared with every other group.

These findings indicate that most of the genes associated with the function of Tregs were downregulated during the acute phase of DRESS with autoimmune sequelae patients. We can suggest that these alterations might occur in the genes associated with the IL-2-mediated signaling pathway and regulation of the IL-10 production pathway. Moreover, the JAK-STAT signaling pathway might play an essential role in subsequent to the dysfunction of Tregs in DRESS with autoimmune sequelae patients.

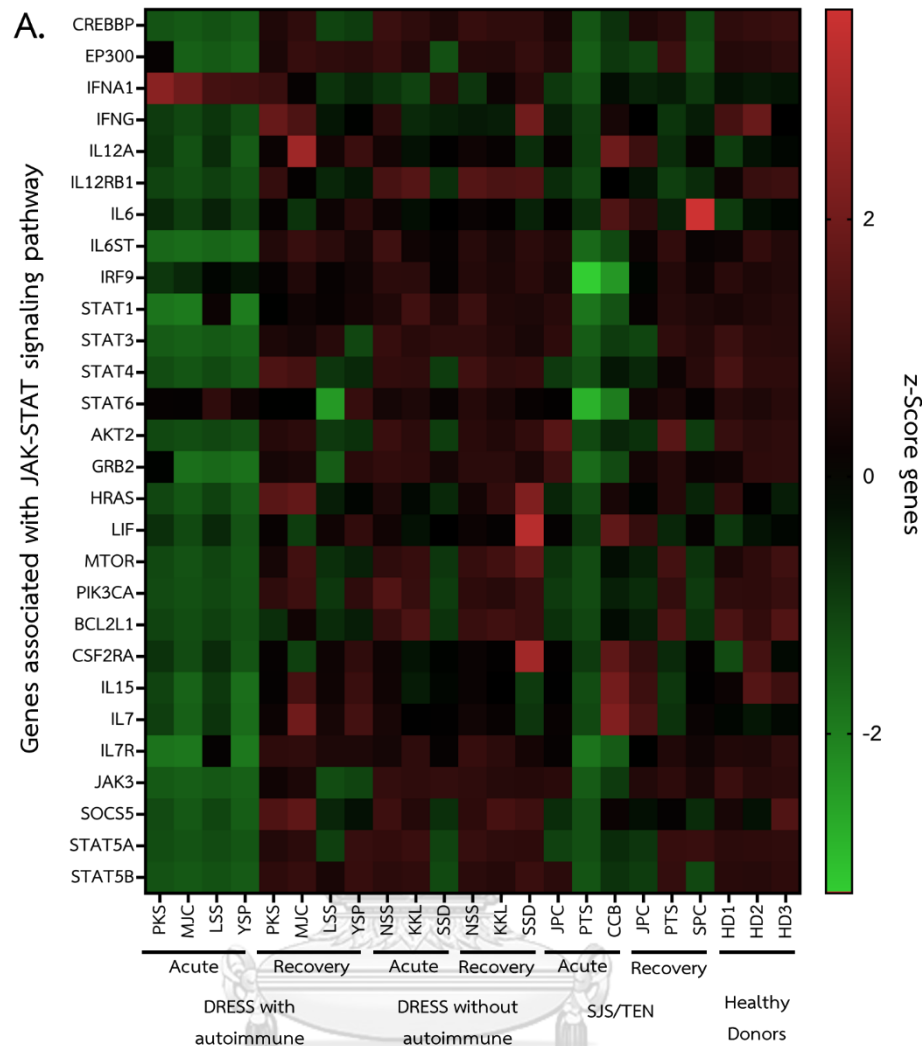


**Figure 30 Gene expression profile associated with JAK-STAT signaling pathway.**

A., Heatmap showing the expression level of 28 genes associated with JAK-STAT signaling pathway in DRESS with autoimmune sequelae patients at the acute phase (n = 4), DRESS with autoimmune sequelae patients at the recovery phase (n = 4), DRESS without autoimmune sequelae patients at the acute phase (n = 3), DRESS without autoimmune sequelae patients at the recovery phase (n = 3), SJS/TEN patients at the acute phase (n = 3), SJS/TEN patients at the recovery phase (n = 3), and healthy donors (n = 3). B., Graph showing fold change of genes associated with regulation of JAK-STAT signaling pathway, compared between groups of subjects. The significance between groups given as P value at 95% confidence; \*P < 0.05, \*\*P < 0.01, and \*\*\*P < 0.001

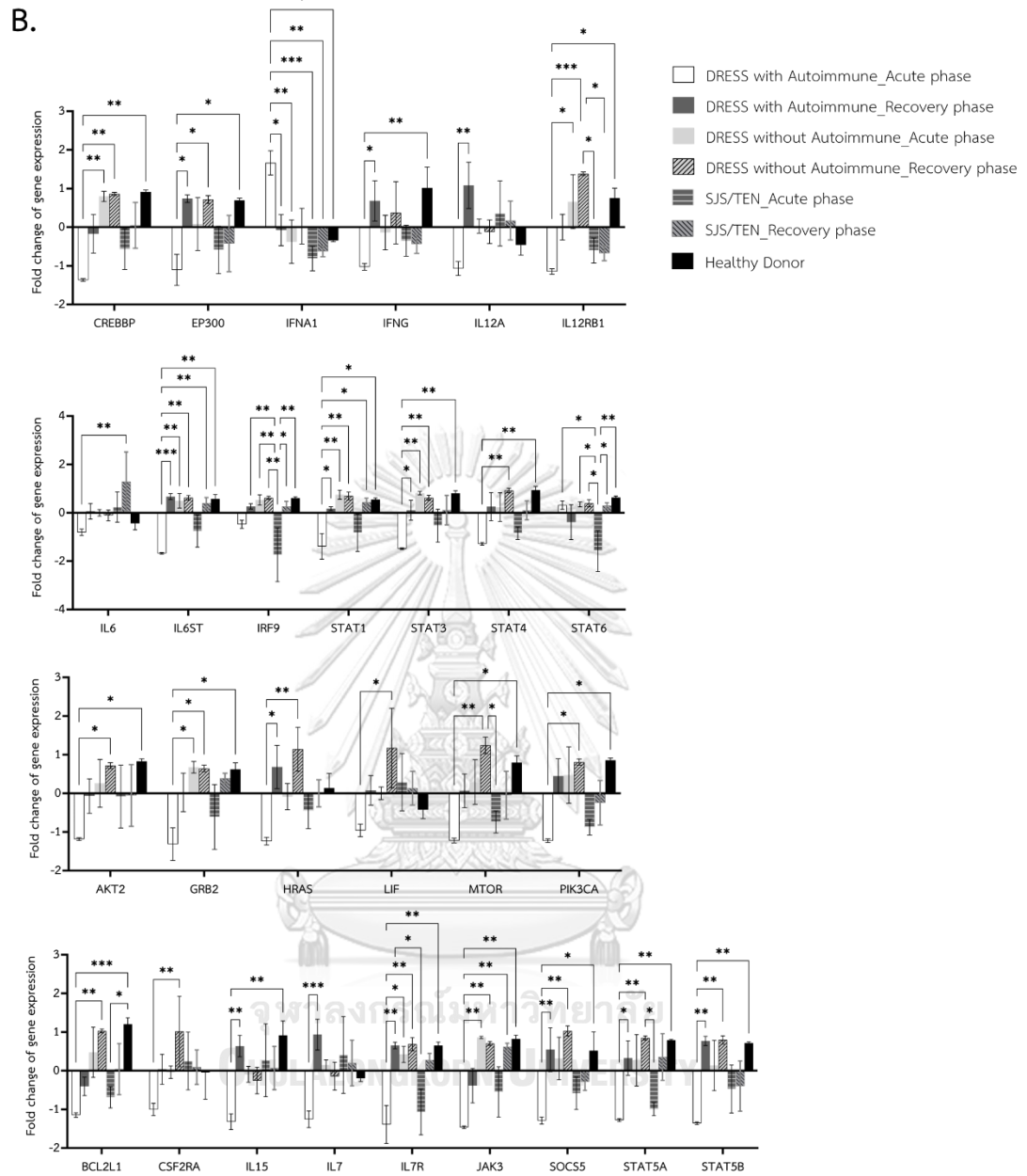


Figure 30 Continued.

## CHAPTER VI

### DISCUSSION

Drug-induced eosinophilia and systemic symptoms (DRESS) have accounted for about 10% of all SCARs cases in Thailand<sup>(1)</sup>. Autoimmune diseases have been observed as long-term sequelae in about 10-20% of the recovery phase of DRESS patients<sup>(4, 46, 47)</sup>. Consequently, the dynamics of Tregs (Tregs) are thought to be responsible for the many symptoms of DRESS<sup>(5, 6, 80)</sup>. We hypothesized that there might be differences in Treg phenotyping between acute and recovery phases of DRESS patients with and without autoimmune sequelae. Therefore, this study focused on the relationship between Treg immunophenotype and DRESS disease autoimmune sequelae. Treg immunophenotype was characterized in both acute and recovery stages of DRESS patients with autoimmune sequelae and DRESS patients without autoimmune sequelae.

We characterized Tregs by their CD4<sup>+</sup>CD25<sup>+</sup>CD127<sup>-</sup>FoxP3<sup>+</sup> expression in PBMCs from DRESS with autoimmune sequelae patients, DRESS without autoimmune sequelae, SJS/TEN patients, and healthy donors. SJS/TEN patients in this study were used as a comparative group because SJS/TEN is one of the SCAR phenotypes with a high mortality rate. Still, clinical characteristics were reported without autoimmune sequelae after recovery. Our results found that the number of Tregs was not different between groups of subjects, even though it tended to be lower in DRESS patients at the acute phase compared to SJS/TEN patients and healthy donors. Our results differed from the Japanese scientists' previous study that showing a significantly higher CD4<sup>+</sup>CD25<sup>+</sup>FoxP3<sup>+</sup> Tregs population in DRESS at the acute phase compared with healthy donors and SJS/TEN patients at the same phase<sup>(5, 80)</sup>. These may be due to the late hospitalization of our patients. The clinical history of our

patients showed the onset of some symptoms about 5 – 7 days before emergency admission to the hospital. Thus, the blood withdrawal for the patients might be delayed which might affect the dynamic of Treg population. Moreover, our observations did not exclude the potential of immunosuppressant that was administered to some patients, which may have promoted the frequency and functionality of Treg cells during the acute phase. However, the study by European scientists has shown similar results as ours; there was no significant difference in CD4<sup>+</sup>CD25<sup>+</sup>FoxP3<sup>+</sup> in healthy donors and SCARs patients<sup>(95)</sup>.

The expression of other markers that represented Tregs functions was also investigated. CTLA-4, GITR, LAG-3, and IL-10 were significantly higher in DRESS with autoimmune sequelae at the acute phase than in other groups and seemed to be the crucial markers in Tregs function. An increasing number of these molecules have been proven to participate in the Treg-mediated suppression mechanism<sup>(66)</sup>. Moreover, our results showed up-regulation of CD39 on the CD4<sup>+</sup>CD25<sup>+</sup>CD127<sup>-</sup>FoxP3<sup>+</sup> Tregs population which had the same trend as Gu *et al.* (2017) that suggested up-regulation of CD39 on CD4<sup>+</sup>Foxp3<sup>+</sup> Tregs in the activation environment. They indicated that CD39 expression could maintain the suppressive function of Tregs. However, the suppressive function of Tregs was not different compared to the group of DRESS with autoimmune sequelae both in the acute and recovery phase, DRESS without autoimmune sequelae at the acute and recovery phase, and even in healthy donors.

Nevertheless, when compared to SJS/TEN patients, we found that the suppressive function of Tregs was significantly lower than those in DRESS patients, both with autoimmune sequelae and without autoimmune sequelae. In our experiment, the co-cultures between Tregs and effector T cells were performed *in vitro*. Accordingly, the modulation of Treg function might depend on more than

soluble mediators derived from Tregs and these inhibitory receptors on Tregs' surface membrane, which can occur in the actual situation in the body.

Additionally, we used NanoString technology to investigate mRNA profiling in Tregs. DRESS with autoimmune sequelae patients at the acute phase showed signature 232 genes that were downregulated compared to healthy donors, including CTLA-4, LAG-3, and IL-10, which contradicted our flow cytometry results. Nevertheless, systematic research on transcripts and proteins at genomic scales revealed the significance of factors other than transcript concentration contributing to determining a protein's expression level, including translation rate modulation<sup>(96)</sup>. Moreover, the biological function identified by GO Biological Process 2021 and the KEGG pathway showed that these 232 genes in DRESS with autoimmune sequelae patients were most associated with the IL-2/JAK3/STAT-5 signaling pathway. IL-2 signaling is necessary for early FoxP3 induction via activation of STAT5, which directly binds to promoter and enhancer sites to activate its expression<sup>(97)</sup>. Notably, deletion of STAT5A/B results in a significant reduction in mouse FoxP3<sup>+</sup> Th cells *in vivo*<sup>(98)</sup>. In humans, this mechanism might become STAT5B specific, as STAT5B impairments result in decreased Foxp3 expression and Tregs suppressive activity even in the presence of normal STAT5A expression and are consequently sufficient to trigger autoimmune diseases<sup>(99)</sup>. However, our results cannot thoroughly explain the role of Tregs in developing autoimmune sequelae in DRESS patients because several mechanisms might work together in the actual situation.

Our study has some limitations. First, patient specimens were limited and could not match patients between the acute and recovery phases. This problem may be because SJS/TEN and DRESS are not common drug hypersensitivity. Moreover, we cannot contact patients after they are discharged from the hospital, which may be due to the change of contact information without notifying the



hospital and some patients being refused to participate in our projects. Our first limitation led to a limited number of Tregs isolated from the patient's PBMCs, which is essential for studying the suppressive function and mRNA profiling. Second, we examined only Tregs in patients' peripheral blood because we could not recruit patients for the skin biopsy. The last limitation is funding and time limitations by the program.

In conclusion, our findings found that  $CD4^+CD25^+CD127^{\text{low}}FoxP3^+$  Tregs were not different in number between DRESS with autoimmune sequelae patients, DRESS without autoimmune patients, and SJS/TEN patients in both the acute and recovery phase as well as in the healthy donors. However, the suppressive function of Tregs in DRESS patients was lower than those in SJS/TEN patients. Thus, the dynamics of the Treg population and their function might play an essential role in DRESS patients developing autoimmune sequelae after recovery. To improve our study, it is necessary to investigate more patients because a small sample size may prevent extrapolating findings. According to the mRNA profiling results, Treg function can be affected by many genes in various pathways. We suggested that IL-2/JAK3/STAT5 pathway may be the next interesting point to investigate.

Notwithstanding the defective regulation of Tregs on autoimmunity development; a combination of genetic and environmental factors still be the factor that affects autoimmunity development. In order to completely understand the immunopathogenesis of autoimmune in DRESS patients, other perspectives should be considered. Thus, further studies could include mechanism studies on the efficiency of Tregs in DRESS as well as others immune cells and factors that may be involved in autoimmunity development to improve our understanding of their autoimmune sequelae pathogenesis.

## CHAPTER VII

### CONCLUSION

CD4<sup>+</sup>CD25<sup>+</sup>CD127<sup>-</sup> Tregs can be one of the essential players in developing autoimmune sequelae in DRESS recovery patients. The regulatory/suppressive functions of Tregs in DRESS during the acute phase were subsequently diminished compared to SJS/TEN when followed up during the recovery phase. The comparative analyses of Treg mRNA profiles in the Treg-involved pathway during the acute phase were found down-regulated in DRESS patients who developed autoimmune sequelae compared to healthy individuals. Thus, it can be suggested that Treg in DRESS with autoimmune diseases showed a lower number and regulatory/suppressive functions of Tregs early during the acute phase. Moreover, we can suggest that Treg from DRESS patients who developed autoimmune consequences might be dysfunctional since the acute phase via many pathways including the JAK-STAT signaling pathway.

Therefore, the functional analysis by pathway should be developed to prove their mechanism in the future. There are differences in the suppressive function of Tregs in DRESS and SJS/TEN patients. The downregulation of genes associated with Treg function in DRESS patients at the acute phase may affect their pathogenesis of autoimmune diseases in the recovery phase.

The study of Tregs phenotypes and function may better understand the pathophysiology of these symptoms and their subsequent autoimmunity. Additionally, they may aid in developing new strategies for diagnosis and treatment.

## REFERENCES



จุฬาลงกรณ์มหาวิทยาลัย  
**CHULALONGKORN UNIVERSITY**

1. Hiransuthikul A, Rattananupong T, Klaewsongkram J, Rerknimitr P, Pongprutthipan M, Ruxrungtham K. Drug-induced hypersensitivity syndrome/drug reaction with eosinophilia and systemic symptoms (DIHS/DRESS): 11 years retrospective study in Thailand. 2016;65(4):432-8.
2. Miyashita K, Miyagawa F, Nakamura Y, Ommori R, Azukizawa H, Asada H. Up-regulation of Human Herpesvirus 6B-derived microRNAs in the Serum of Patients with Drug-induced Hypersensitivity Syndrome/Drug Reaction with Eosinophilia and Systemic Symptoms. *Acta Derm Venereol*. 2018;98(6):612-3.
3. Ishida T, Kano Y, Mizukawa Y, Shiohara T. The dynamics of herpesvirus reactivations during and after severe drug eruptions: their relation to the clinical phenotype and therapeutic outcome. *Allergy*. 2014;69(6):798-805.
4. Cho YT, Yang CW, Chu CY. Drug Reaction with Eosinophilia and Systemic Symptoms (DRESS): An Interplay among Drugs, Viruses, and Immune System. *International journal of molecular sciences*. 2017;18(6).
5. Takahashi R, Kano Y, Yamazaki Y, Kimishima M, Mizukawa Y, Shiohara T. Defective Tregs in patients with severe drug eruptions: timing of the dysfunction is associated with the pathological phenotype and outcome. *J Immunol*. 2009;182(12):8071-9.
6. Morito H, Ogawa K, Fukumoto T, Kobayashi N, Morii T, Kasai T, et al. Increased ratio of FoxP3+ Tregs/CD3+ T cells in skin lesions in drug-induced hypersensitivity syndrome/drug rash with eosinophilia and systemic symptoms. *Clin Exp Dermatol*. 2014;39(3):284-91.
7. Hashizume H, Fujiyama T, Tokura Y. Reciprocal contribution of Th17 and Tregs in severe drug allergy. *Journal of dermatological science*. 2016;81(2):131-4.
8. Pellerin L, Jenks JA, Begin P, Bacchetta R, Nadeau KC. Tregs and their roles in immune dysregulation and allergy. *Immunologic research*. 2014;58(2-3):358-68.
9. Organization WH. Safety of Medicines - A Guide to Detecting and Reporting Adverse Drug Reactions - Why Health Professionals Need to Take Action Geneva, Switzerland: World Health Organization; 2002 [Available from: <http://apps.who.int/medicinedocs/en/d/Jh2992e/2.html>].
10. Pichler WJ. Drug hypersensitivity. Basel ; New York: Karger; 2007. ix, 438 p. p.

11. Riedl MA, Casillas AM. Adverse drug reactions: types and treatment options. *Am Fam Physician*. 2003;68(9):1781-90.
12. White KD, Chung WH, Hung SI, Mallal S, Phillips EJ. Evolving models of the immunopathogenesis of T cell-mediated drug allergy: The role of host, pathogens, and drug response. *The Journal of allergy and clinical immunology*. 2015;136(2):219-34; quiz 35.
13. Coombs RRAG, P.G.H. Classification of allergic reactions responsible for drug hypersensitivity reactions. In: Coombs RRAG, P.G.H., editor. *Clinical Aspects of Immunology*. Davis, Philadelphia: Oxford: Blackwell Scientific Publications; 1968. p. 575- 96.
14. Sylvia LM. Chapter 22. Allergic and Pseudoallergic Drug Reactions. In: DiPiro JT, Talbert RL, Yee GC, Matzke GR, Wells BG, Posey LM, editors. *Pharmacotherapy: A Pathophysiologic Approach*, 9e. New York, NY: The McGraw-Hill Companies; 2014.
15. Adam J, Pichler WJ, Yerly D. Delayed drug hypersensitivity: models of T-cell stimulation. *Br J Clin Pharmacol*. 2011;71(5):701-7.
16. Posadas SJ, Pichler WJ. Delayed drug hypersensitivity reactions - new concepts. *Clin Exp Allergy*. 2007;37(7):989-99.
17. Pichler WJ, Adam J, Daubner B, Gentinetta T, Keller M, Yerly D. Drug hypersensitivity reactions: pathomechanism and clinical symptoms. *Med Clin North Am*. 2010;94(4):645-64, xv.
18. Pichler WJ, Hausmann O. Classification of Drug Hypersensitivity into Allergic, p-i, and Pseudo-Allergic Forms. *Int Arch Allergy Immunol*. 2016;171(3-4):166-79.
19. Eyerich S, Traidl-Hoffmann C, Behrendt H, Cavani A, Schmidt-Weber CB, Ring J, et al. Novel key cytokines in allergy: IL-17, IL-22. *Allergol Select*. 2017;1(1):71-6.
20. Uzzaman A, Cho SH. Chapter 28: Classification of hypersensitivity reactions. *Allergy and asthma proceedings*. 2012;33 Suppl 1:96-9.
21. Roujeau JC, Bioulac-Sage P, Bourseau C, Guillaume JC, Bernard P, Lok C, et al. Acute generalized exanthematous pustulosis. Analysis of 63 cases. *Archives of dermatology*. 1991;127(9):1333-8.
22. Duong TA, Valeyrie-Allanore L, Wolkenstein P, Chosidow O. Severe cutaneous adverse reactions to drugs. *Lancet (London, England)*. 2017;390(10106):1996-2011.

23. Chung WH, Wang CW, Dao RL. Severe cutaneous adverse drug reactions. *The Journal of dermatology*. 2016;43(7):758-66.
24. Sukasem C, Katsila T, Tempark T, Patrinos GP, Chantratita W. Drug-Induced Stevens-Johnson Syndrome and Toxic Epidermal Necrolysis Call for Optimum Patient Stratification and Theranostics via Pharmacogenomics. *Annu Rev Genomics Hum Genet*. 2018;19:329-53.
25. Schwartz RA, McDonough PH, Lee BW. Toxic epidermal necrolysis: Part II. Prognosis, sequelae, diagnosis, differential diagnosis, prevention, and treatment. *Journal of the American Academy of Dermatology*. 2013;69(2):187.e1-16; quiz 203-4.
26. Sassolas B, Haddad C, Mockenhaupt M, Dunant A, Liss Y, Bork K, et al. ALDEN, an algorithm for assessment of drug causality in Stevens-Johnson Syndrome and toxic epidermal necrolysis: comparison with case-control analysis. *Clin Pharmacol Ther*. 2010;88(1):60-8.
27. Cranga TA, Simpson MA, Featherstone P. Acute generalised exanthematous pustulosis (AGEP)-a potential pitfall for the acute physician. *Acute medicine*. 2016;15(3):140-4.
28. Loo CH, Tan WC, Khor YH, Chan LC. A 10-years retrospective study on Severe Cutaneous Adverse Reactions (SCARs) in a tertiary hospital in Penang, Malaysia. *The Medical journal of Malaysia*. 2018;73(2):73-7.
29. Grando LR, Schmitt TA, Bakos RM. Severe cutaneous reactions to drugs in the setting of a general hospital. *Anais brasileiros de dermatologia*. 2014;89(5):758-62.
30. Pichler WJ, Yerly D. Drug hypersensitivity: We need to do more. *The Journal of allergy and clinical immunology*. 2018;141(1):89-91.
31. Husain Z, Reddy BY, Schwartz RA. DRESS syndrome: Part I. Clinical perspectives. *Journal of the American Academy of Dermatology*. 2013;68(5):693.e1-14; quiz 706-8.
32. Descamps V, Ranger-Rogez S. DRESS syndrome. *Joint Bone Spine*. 2014;81(1):15-21.
33. Stirton H, Shear NH, Dodiuk-Gad RP. Drug Reaction with Eosinophilia and Systemic Symptoms (DReSS)/Drug-Induced Hypersensitivity Syndrome (DIHS)-Readdressing the DReSS. *Biomedicines*. 2022;10(5).

34. Shiohara T, Kano Y. Drug reaction with eosinophilia and systemic symptoms (DRESS): incidence, pathogenesis and management. *Expert opinion on drug safety*. 2017;16(2):139-47.
35. Shiohara T, Mizukawa Y. Drug-induced hypersensitivity syndrome (DiHS)/drug reaction with eosinophilia and systemic symptoms (DRESS): An update in 2019. *Allergol Int*. 2019.
36. Kardaun SH, Sekula P, Valeyrie-Allanore L, Liss Y, Chu CY, Creamer D, et al. Drug reaction with eosinophilia and systemic symptoms (DRESS): an original multisystem adverse drug reaction. Results from the prospective RegiSCAR study. *The British journal of dermatology*. 2013;169(5):1071-80.
37. Yazicioglu M, Elmas R, Turgut B, Genchallac T. The association between DRESS and the diminished numbers of peripheral B lymphocytes and natural killer cells. *Pediatric allergy and immunology : official publication of the European Society of Pediatric Allergy and Immunology*. 2012;23(3):289-96.
38. Kano Y, Seishima M, Shiohara T. Hypogammaglobulinemia as an early sign of drug-induced hypersensitivity syndrome. *Journal of the American Academy of Dermatology*. 2006;55(4):727-8.
39. Ben m'rad M, Leclerc-Mercier S, Blanche P, Franck N, Rozenberg F, Fulla Y, et al. Drug-induced hypersensitivity syndrome: clinical and biologic disease patterns in 24 patients. *Medicine*. 2009;88(3):131-40.
40. Mockenhaupt M. Severe drug-induced skin reactions: clinical pattern, diagnostics and therapy. *Journal der Deutschen Dermatologischen Gesellschaft = Journal of the German Society of Dermatology : JDDG*. 2009;7(2):142-60; quiz 61-2.
41. Peter JG, Lehloenya R, Dlamini S, Risma K, White KD, Konvinse KC, et al. Severe Delayed Cutaneous and Systemic Reactions to Drugs: A Global Perspective on the Science and Art of Current Practice. *J Allergy Clin Immunol Pract*. 2017;5(3):547-63.
42. Sugita K, Tohyama M, Watanabe H, Otsuka A, Nakajima S, Iijima M, et al. Fluctuation of blood and skin plasmacytoid dendritic cells in drug-induced hypersensitivity syndrome. *The Journal of allergy and clinical immunology*. 2010;126(2):408-10.

43. Chen YC, Chiang HH, Cho YT, Chang CY, Chen KL, Yang CW, et al. Human herpes virus reactivations and dynamic cytokine profiles in patients with cutaneous adverse drug reactions --a prospective comparative study. *Allergy*. 2015;70(5):568-75.
44. Sasidharanpillai S, Ajithkumar K, Jishna P, Khader A, Anagha KV, Binitha MP, et al. RegiSCAR DRESS (Drug Reaction with Eosinophilia and Systemic Symptoms) Validation Scoring System and Japanese Consensus Group Criteria for Atypical Drug-Induced Hypersensitivity Syndrome (DIHS): A Comparative Analysis. *Indian Dermatol Online J*. 2022;13(1):40-5.
45. Tetart F, Picard D, Janela B, Joly P, Musette P. Prolonged evolution of drug reaction with eosinophilia and systemic symptoms: clinical, virologic, and biological features. *JAMA dermatology*. 2014;150(2):206-7.
46. Chen YC, Chang CY, Cho YT, Chiu HC, Chu CY. Long-term sequelae of drug reaction with eosinophilia and systemic symptoms: a retrospective cohort study from Taiwan. *Journal of the American Academy of Dermatology*. 2013;68(3):459-65.
47. Matta JM, Flores SM, Cherit JD. Drug reaction with eosinophilia and systemic symptoms (DRESS) and its relation with autoimmunity in a reference center in Mexico. *Anais brasileiros de dermatologia*. 2017;92(1):30-3.
48. Aota N, Hirahara K, Kano Y, Fukuoka T, Yamada A, Shiohara T. Systemic lupus erythematosus presenting with Kikuchi-Fujimoto's disease as a long-term sequela of drug-induced hypersensitivity syndrome. A possible role of Epstein-Barr virus reactivation. *Dermatology*. 2009;218(3):275-7.
49. Criado PR, Criado RF, Avancini JM, Santi CG. Drug reaction with Eosinophilia and Systemic Symptoms (DRESS) / Drug-induced Hypersensitivity Syndrome (DIHS): a review of current concepts. *Anais brasileiros de dermatologia*. 2012;87(3):435-49.
50. Nishizuka Y, Sakakura T. Thymus and reproduction: sex-linked dysgenesis of the gonad after neonatal thymectomy in mice. *Science (New York, NY)*. 1969;166(3906):753-5.
51. Mason GM, Lowe K, Melchiotti R, Ellis R, de Rinaldis E, Peakman M, et al. Phenotypic Complexity of the Human Regulatory T Cell Compartment Revealed by Mass Cytometry. *J Immunol*. 2015;195(5):2030-7.



52. Shevryev D, Tereshchenko V. Treg Heterogeneity, Function, and Homeostasis. *Frontiers in immunology*. 2019;10:3100.
53. Gratz IK, Truong HA, Yang SH, Maurano MM, Lee K, Abbas AK, et al. Cutting Edge: memory Tregs require IL-7 and not IL-2 for their maintenance in peripheral tissues. *J Immunol*. 2013;190(9):4483-7.
54. Miragaia RJ, Gomes T, Chomka A, Jardine L, Riedel A, Hegazy AN, et al. Single-Cell Transcriptomics of Tregs Reveals Trajectories of Tissue Adaptation. *Immunity*. 2019;50(2):493-504 e7.
55. Wyss L, Stadinski BD, King CG, Schallenberg S, McCarthy NI, Lee JY, et al. Affinity for self antigen selects Treg cells with distinct functional properties. *Nat Immunol*. 2016;17(9):1093-101.
56. Sprouse ML, Shevchenko I, Scavuzzo MA, Joseph F, Lee T, Blum S, et al. Cutting Edge: Low-Affinity TCRs Support Regulatory T Cell Function in Autoimmunity. *J Immunol*. 2018;200(3):909-14.
57. Wei X, Zhang J, Gu Q, Huang M, Zhang W, Guo J, et al. Reciprocal Expression of IL-35 and IL-10 Defines Two Distinct Effector Treg Subsets that Are Required for Maintenance of Immune Tolerance. *Cell Rep*. 2017;21(7):1853-69.
58. Zhang H, Kong H, Zeng X, Guo L, Sun X, He S. Subsets of Tregs and their roles in allergy. *J Transl Med*. 2014;12:125.
59. Kosten IJ, Rustemeyer T. Generation, subsets and functions of inducible Tregs. *Antiinflamm Antiallergy Agents Med Chem*. 2015;13(3):139-53.
60. Ronchetti S, Ricci E, Petrillo MG, Cari L, Migliorati G, Nocentini G, et al. Glucocorticoid-induced tumour necrosis factor receptor-related protein: a key marker of functional Tregs. *J Immunol Res*. 2015;2015:171520.
61. Vignali DA, Collison LW, Workman CJ. How Tregs work. *Nat Rev Immunol*. 2008;8(7):523-32.
62. Liu W, Putnam AL, Xu-Yu Z, Szot GL, Lee MR, Zhu S, et al. CD127 expression inversely correlates with FoxP3 and suppressive function of human CD4+ T reg cells. *J Exp Med*. 2006;203(7):1701-11.

63. Simonetta F, Chiali A, Cordier C, Urrutia A, Girault I, Bloquet S, et al. Increased CD127 expression on activated FOXP3+CD4+ Tregs. *Eur J Immunol*. 2010;40(9):2528-38.
64. Corthay A. How do Tregs work? *Scand J Immunol*. 2009;70(4):326-36.
65. Romano M, Fanelli G, Albany CJ, Giganti G, Lombardi G. Past, Present, and Future of Regulatory T Cell Therapy in Transplantation and Autoimmunity. *Frontiers in immunology*. 2019;10:43.
66. Zhao H, Liao X, Kang Y. Tregs: Where We Are and What Comes Next? *Frontiers in immunology*. 2017;8:1578.
67. Fontenot JD, Gavin MA, Rudensky AY. Foxp3 programs the development and function of CD4+CD25+ Tregs. *Nat Immunol*. 2003;4(4):330-6.
68. Gavin MA, Rasmussen JP, Fontenot JD, Vasta V, Manganiello VC, Beavo JA, et al. Foxp3-dependent programme of regulatory T-cell differentiation. *Nature*. 2007;445(7129):771-5.
69. Hori S, Nomura T, Sakaguchi S. Control of regulatory T cell development by the transcription factor Foxp3. *Science (New York, NY)*. 2003;299(5609):1057-61.
70. O'Malley JT, Sehra S, Thieu VT, Yu Q, Chang HC, Stritesky GL, et al. Signal transducer and activator of transcription 4 limits the development of adaptive Tregs. *Immunology*. 2009;127(4):587-95.
71. Mahmud SA, Manlove LS, Farrar MA. Interleukin-2 and STAT5 in regulatory T cell development and function. *JAKSTAT*. 2013;2(1):e23154.
72. Pillemer BB, Qi Z, Melgert B, Oriss TB, Ray P, Ray A. STAT6 activation confers upon T helper cells resistance to suppression by Tregs. *J Immunol*. 2009;183(1):155-63.
73. Wang Y, Souabni A, Flavell RA, Wan YY. An intrinsic mechanism predisposes Foxp3-expressing Tregs to Th2 conversion in vivo. *J Immunol*. 2010;185(10):5983-92.
74. Lee W, Lee GR. Transcriptional regulation and development of Tregs. *Exp Mol Med*. 2018;50(3):e456.
75. Dejaco C, Duftner C, Grubeck-Loebenstien B, Schirmer M. Imbalance of Tregs in human autoimmune diseases. *Immunology*. 2006;117(3):289-300.

76. Hu Y, Zhang L, Chen H, Liu X, Zheng X, Shi H, et al. Analysis of Regulatory T Cell Subsets and Their Expression of Helios and PD-1 in Patients with Hashimoto Thyroiditis. *Int J Endocrinol*. 2019;2019:5368473.
77. Pan D, Shin YH, Gopalakrishnan G, Hennessey J, De Groot LJ. Tregs in Graves' disease. *Clin Endocrinol (Oxf)*. 2009;71(4):587-93.
78. van Amelsfort JM, Jacobs KM, Bijlsma JW, Lafeber FP, Taams LS. CD4(+)CD25(+) Tregs in rheumatoid arthritis: differences in the presence, phenotype, and function between peripheral blood and synovial fluid. *Arthritis Rheum*. 2004;50(9):2775-85.
79. Liu MF, Wang CR, Fung LL, Wu CR. Decreased CD4+CD25+ T cells in peripheral blood of patients with systemic lupus erythematosus. *Scand J Immunol*. 2004;59(2):198-202.
80. Ushigome Y, Mizukawa Y, Kimishima M, Yamazaki Y, Takahashi R, Kano Y, et al. Monocytes are involved in the balance between Tregs and Th17 cells in severe drug eruptions. *Clin Exp Allergy*. 2018;48(11):1453-63.
81. Kavanaugh A, Tomar R, Reveille J, Solomon DH, Homburger HA. Guidelines for clinical use of the antinuclear antibody test and tests for specific autoantibodies to nuclear antigens. American College of Pathologists. *Arch Pathol Lab Med*. 2000;124(1):71-81.
82. Heberle H, Meirelles GV, da Silva FR, Telles GP, Minghim R. InteractiVenn: a web-based tool for the analysis of sets through Venn diagrams. *BMC Bioinformatics*. 2015;16:169.
83. Frey N, Jossi J, Bodmer M, Bircher A, Jick SS, Meier CR, et al. The Epidemiology of Stevens-Johnson Syndrome and Toxic Epidermal Necrolysis in the UK. *J Invest Dermatol*. 2017;137(6):1240-7.
84. Sasidharanpillai S, Riyaz N, Khader A, Rajan U, Binitha MP, Sureshan DN. Severe cutaneous adverse drug reactions: a clinicoepidemiological study. *Indian J Dermatol*. 2015;60(1):102.
85. Syu FK, Pan HY, Chuang PC, Huang YS, Cheng CY, Cheng FJ. Incidence of Stevens-Johnson syndrome following combination drug use of allopurinol,

carbamazepine and phenytoin in Taiwan: A case-control study. *The Journal of dermatology*. 2018;45(9):1080-7.

86. Mizukawa Y, Aoyama Y, Takahashi H, Takahashi R, Shiohara T. Risk of Progression to Autoimmune Disease in Severe Drug Eruption: Risk Factors and the Factor-Guided Stratification. *J Invest Dermatol*. 2022;142(3 Pt B):960-8 e9.
87. Porebski G, Piotrowicz-Wojcik K, Spiewak R. ELISpot assay as a diagnostic tool in drug hypersensitivity reactions. *J Immunol Methods*. 2021;495:113062.
88. Buchbinder EI, Desai A. CTLA-4 and PD-1 Pathways: Similarities, Differences, and Implications of Their Inhibition. *Am J Clin Oncol*. 2016;39(1):98-106.
89. Ephrem A, Epstein AL, Stephens GL, Thornton AM, Glass D, Shevach EM. Modulation of Treg cells/T effector function by GITR signaling is context-dependent. *Eur J Immunol*. 2013;43(9):2421-9.
90. Tian J, Zhang B, Rui K, Wang S. The Role of GITR/GITRL Interaction in Autoimmune Diseases. *Frontiers in immunology*. 2020;11:588682.
91. Do JS, Visperas A, Sanogo YO, Bechtel JJ, Dvorina N, Kim S, et al. An IL-27/Lag3 axis enhances Foxp3+ regulatory T cell-suppressive function and therapeutic efficacy. *Mucosal Immunol*. 2016;9(1):137-45.
92. Huang CT, Workman CJ, Flies D, Pan X, Marson AL, Zhou G, et al. Role of LAG-3 in Tregs. *Immunity*. 2004;21(4):503-13.
93. Workman CJ, Vignali DA. The CD4-related molecule, LAG-3 (CD223), regulates the expansion of activated T cells. *Eur J Immunol*. 2003;33(4):970-9.
94. Goldstein JD, Burlion A, Zaragoza B, Sendeyo K, Polansky JK, Huehn J, et al. Inhibition of the JAK/STAT Signaling Pathway in Tregs Reveals a Very Dynamic Regulation of Foxp3 Expression. *PLoS One*. 2016;11(4):e0153682.
95. Daubner B, Groux-Keller M, Hausmann OV, Kawabata T, Naisbitt DJ, Park BK, et al. Multiple drug hypersensitivity: normal Treg cell function but enhanced in vivo activation of drug-specific T cells. *Allergy*. 2012;67(1):58-66.
96. Liu Y, Beyer A, Aebersold R. On the Dependency of Cellular Protein Levels on mRNA Abundance. *Cell*. 2016;165(3):535-50.
97. Jones DM, Read KA, Oestreich KJ. Dynamic Roles for IL-2-STAT5 Signaling in Effector and Regulatory CD4(+) T Cell Populations. *J Immunol*. 2020;205(7):1721-30.

98. Yao Z, Kanno Y, Kerenyi M, Stephens G, Durant L, Watford WT, et al. Nonredundant roles for Stat5a/b in directly regulating Foxp3. *Blood*. 2007;109(10):4368-75.
99. Jenks JA, Seki S, Kanai T, Huang J, Morgan AA, Scalco RC, et al. Differentiating the roles of STAT5B and STAT5A in human CD4+ T cells. *Clin Immunol*. 2013;148(2):227-36.





APPENDIX

จุฬาลงกรณ์มหาวิทยาลัย  
**CHULALONGKORN UNIVERSITY**

APPENDIX A  
REAGENT PREPARATION

1. Cell culture

1.1 SC solution (Supplement Complete)

Component	Final Volume
RPMI media	220 ml
Non-essential amino acid solution (NEAA)	100 ml
Penicillin-Streptomycin (10,000 U/ml)	80 ml
HEPES	11.9 g
L-glutamine	100 ml or 3 g
$\beta$ -mercaptoethanol	35 $\mu$ l
Total	500 ml

1.2 Fetal bovine serum (FBS)

Heat-inactivated at 56°C for 30 minutes and store at -20°C

1.3 RF10 media

Component	Final Volume
Heat-inactivated FBS	60 ml
SC solution	30 ml
RPMI media	500 ml
Total	590 ml

#### 1.4 Freezing media

Component	Final Volume
Heat-inactivated FBS	90 ml
Dimethyl sulfoxide (DMSO)	10 ml
Total	100 ml

## 2. Flow cytometry

#### 2.1 FACS buffer

Component	Final Volume
Phosphate buffer saline	95 ml
Fetal bovine serum (final conc. Is 5% v/v)	6 ml
Total	100 ml

#### 2.2 Fixation buffer

Component	Final Volume
Phosphate buffer saline	92.2 ml
Fetal bovine serum (final conc. Is 5% v/v)	6 ml
Formaldehyde (final conc. 2% v/v)	2.8 ml
Total	100 ml



### 3. Tregs isolation by magnetic bead

#### 3.1 Isolation buffer

Component	Final Volume
Phosphate buffer saline	97.8 ml
Fetal bovine serum (final conc. is 2% v/v)	2 ml
500 mM EDTA (final conc. 1 mM)	0.2 ml
Total	100 ml



**APPENDIX B**  
**CHEMICAL AND REAGENTS**

4-(2-Hydroxyethyl)-1-piperazineethanesulfonic acid (HEPES)	Applichem	Germany
anti-human CD127 Ab - PerCP/Cy5.5 (Clone: A019D5)	Biologend	USA
anti-human CD25 Ab - PE (Clone: BC96)	Biologend	USA
anti-human CD3 Ab - Alexa Fluor® 488 (Clone: UCHT1)	Biologend	USA
anti-human CD3 AB - APC (Clone: UCHT1)	Biologend	USA
anti-human CD3 Ab - Brilliant Violet 421™ (Clone: OKT3)	Biologend	USA
anti-human CD3 Ab - Brilliant Violet 510™ (Clone: UCHT1)	Biologend	USA
anti-human CD3 Ab - Brilliant Violet 785™ (Clone: OKT3)	Biologend	USA
anti-human CD3 Ab - FITC (Clone: UCHT1)	Biologend	USA
anti-human CD3 Ab - PE/Cy7 (Clone: UCHT1)	Biologend	USA
anti-human CD3 Ab - PE/Dazzle™ 594 (Clone: OKT3)	Biologend	USA
anti-human CD357 (GITR) Ab - Brilliant Violet 605™ (Clone: 108-17)	Biologend	USA
anti-human CD39 Ab - Brilliant Violet 785™ (Clone: A1)	Biologend	USA
anti-human CD4 Ab - Brilliant Violet 650™ (Clone: RPA-T4)	Biologend	USA
anti-human CD4 Ab - PE/Cyanine5 (Clone: RPA-TA)	Biologend	USA
anti-human CD8 Ab - Alexa Fluor® 700 (Clone: SK1)	Biologend	USA
anti-human CD8 Ab - Brilliant Violet 605™ (Clone: SK1)	Biologend	USA
anti-human CTLA-4 Ab - PE/Dazzle™ 594 (Clone: BNI3)	Biologend	USA
anti-human FOXP3 Ab - Alexa Fluor® 488 (Clone: 206D)	Biologend	USA
anti-human LAG-3 Ab - Brilliant Violet 650™ (Clone: 11C3C65)	Biologend	USA
anti-human OX40 Ab - Brilliant Violet 510™ (Clone: Ber-ACT35)	Biologend	USA
anti-human PD-1 Ab - Brilliant Violet 421™ (Clone: EH12.2H7)	Biologend	USA
Beta-mercaptoethanol	Sigma-Aldrich	Germany
CFSE Cell Division Tracker Kit	Biologend	USA
CytoFLEX Sheath Fluid	Beckman Coulter	USA
Dimethyl sulfoxide (DMSO)	Applichem	Germany
EasySep Human CD4 <sup>+</sup> CD127 <sup>low</sup> CD25 <sup>+</sup> Regulatory T Cell Isolation Kit	STEMCELL	Canada
eBioscience™ Foxp3 / Transcription Factor Staining Buffer Set	Invitroge	USA
Fetal bovine serum (FBS)	Gibco	USA
Ficoll® Paque Plus	GE Healthcare	Sweden
Improved Minimum Essential Medium (IMEM)	Gibco	USA

L-Glutamine solution	Gibco	USA
nCounter® Autoimmune Profiling Panel	NanoString	USA
Non-essential amino acid (NEAA)	Gibco	USA
Penicillin Streptomycin Solution (Pen-Strep)	Gibco	USA
Phosphate buffer saline (PBS)	Serva	Germany
Qubit™ RNA High Sensitivity (HS) Assay Kits	Invitrogen	USA
Recombinant Human IL-2 (carrier-free)	Biologend	USA
RNeasy mini kit	QIAGEN	Germany
Ultra-LEAF™ Purified anti-human CD28 Ab (Clone: CD28.2)	Biologend	USA
Ultra-LEAF™ Purified anti-human CD3 Ab (Clone: OKT3)	Biologend	USA



## APPENDIX C EQUIPMENT

### Equipment

BD FACSAria™ II Cell Sorter	BD Biosciences	USA
Biological Safety Cabinet class II		
Centrifuge (5427 R)	Eppendorf	Germany
Centrifuge (Allegra X-14/R)	Beckman Coulter	USA
CO2 incubator	Thermo scientific	USA
EasySep™ Magnet	STEMCELL	Canada
Flow Cytometer (CytoFLEX V5-B5-R3)	Beckman Coulter	USA
Mr. Frosty™ Freezing Container	Thermo Scientific	USA
NanoDrop spectrophotometer	NanoDrop	USA
NanoString nCounter MAX Analyzer	NanoString	USA
Phase contrast fluorescence microscope	Olympus	Japan
Qubit™ 4 Fluorometer	Invitrogen	USA
Thermal cyclers (ProFlex™ PCR System)	Applied Biosystems	USA
Vortex mixer	Scientific Industries	USA
Water bath	Grant Instruments	UK

### Plasticware and glassware

Autopipette 1,000, 200, 50 and 10 ul

Conical tube 15 mL (Sterile)

Conical tube 50 mL (Sterile)

Coverslip

Cryo Tubes 2.0 mL

Disposable plastic transfer pipettes

Eppendorf tube 0.2 mL

Eppendorf tube 0.6 mL

Eppendorf tube 1.5 mL

FAC tube 5 mL

Hemocytometer

Multichannel pipette 20-200  $\mu$ l

Polystyrene flat-bottom plate 96 well

Polystyrene U-bottom plate 96 well

Polystyrene V-bottom plate 96 well

VACUETTE® TUBE 4 mL K3E K3EDTA

VACUETTE® TUBE 4 mL LH Lithium Heparin

### Softwares

GraphPad Prism 9.0

Dotmatics USA

EndNote X10

Clarivate USA

FlowJo V.10.0.8

Flow LLC USA

SPSS 22

IBM USA

nSolver™ 4.0 analysis

NanoString USA



## APPENDIX D

### SUPPORTING RESULTS

#### Clinical characteristics of SJS/TEN and DRESS patients

\* Age at the development of SCARs, F: Female, M: Male, SJS: Stevens-Johnson syndrome, TEN: Toxic epidermal necrolysis, DRESS: Drug reaction with eosinophilia and systemic symptoms, IRZE: Isoniazid, Rifampicin, Pyrazinamide, Ethambutol, ND: Non-identified

- Part 1 Identification of the regulatory T cell immunophenotype
- Part 2 investigation of Tregs suppressive function in vitro
- Part 3 Gene expression profiles in Tregs



ThaiSCA R code	Gender	Age (Years at onset)	Drug	Allergy	ELIspot	Steroid	sequelae	ANA	time point	Part 1	Part 2	Part 3
PKS112	F	17	Phenytoin	DRESS	Positive (124spots)	No	Autoimmune hypothyroid	ANA(+) >=1280	Acute Recovery	✓ ✓	✓ ✓	✓ ✓
LSS142	F	50	Allopurinol	DRESS	Negative	No	Drug-induced autoimmune hemolytic anemia and grave's disease	ANA(+) >=1280	Acute Recovery	✓ ✓	✓ ✓	✓ ✓
YSP250	F	74	Allopurinol	DRESS	Positive (20 spots)	Prednisolone	Grave's Disease	Antithyroid peroxidase	Acute Recovery	✓ ✓	- -	✓ ✓
MUC089	F	17	Phenytoin	DRESS	Positive	N/A	Hypothyroidism		Acute Recovery	✓ ✓	✓ ✓	✓ ✓
NSS681	M	19	Phenytoin	DRESS	Positive	No			Acute Recovery	✓ ✓	✓ ✓	✓ ✓
SSL120	M	63	Phenytoin	DRESS	Positive (431 spots)	Prednisolone			Acute Recovery	✓ -	- -	- -
CSP383	F	47	Efavirenz	DRESS	Positive	Prednisolone			Acute Recovery	✓ ✓	- -	- -
KKL708	M	38	Sulfasalazine	DRESS	Positive	No			Acute Recovery	- -	- -	✓ ✓
SSD711	M	37	CO-trimoxazole	DRESS	Positive	No			Acute Recovery	- -	✓ ✓	✓ ✓

ThaiSCA R code	Gender	Age (Years at on set)	Drug	Allergy	ELIspot	Steroid	sequelae	ANA	time point	Part 1	Part 2	Part 3
KTP017	F	27	Phenobarbital	DRESS	Negative	No			Acute Recovery	✓ -	- -	- -
KTN171	F	74	Allopurinol	DRESS	Positive	Prednisolone			Acute Recovery	✓ -	- -	- -
TSM363	M	17	co- trimoxazole	DRESS	Positive	Yes			Acute Recovery	✓ ✓	✓ ✓	- -
UCC025	F	36	Phenytoin	DRESS	Positive (83 spots)	Yes			Acute Recovery	✓ -	- -	- -
PJB309	M	57	co- trimoxazole	DRESS	Positive (554 spots)	No			Acute Recovery	- ✓	- -	- -
SUU046	M	68	Allopurinol	SJS	Positive	ND			Acute Recovery	- ✓	- -	- -
TTK223	M	55	IRZE	SJS	Positive	No			Acute Recovery	- -	✓ -	- -
PED394	F	64	Co- trimoxazole	SJS	Pos	ND			Acute Recovery	✓ -	- -	- -
PTS409	M	51	Allopurinol	SJS/TEN	Pos	ND			Acute Recovery	✓ ✓	- ✓	✓ ✓
SPC405	M	59	Co- trimoxazole	SJS	Positive	No			Acute Recovery	- -	- ✓	- ✓

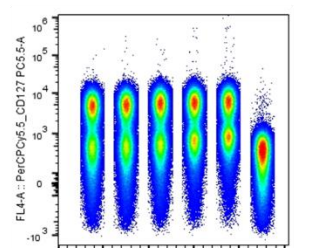


ThaiSCA R code	Gender	Age (Years at onset)	Drug	Allergy	ELISpot	Steroid	sequelae	ANA	time point	Part 1	Part 2	Part 3
JPC470	M	31	Allopurinol	SJS	ND	ND			Acute Recovery	- -	- √	- √
JES302	M	38	IRZE	SJS	Positive	No			Acute Recovery	√ -	- -	- -
KJP407	M	67	amoxiclav	SJS/TEN	Negative	No			Acute Recovery	- -	√ -	- -
SKC414	F	66	Phenytoin,	SJS/TEN	ND	ND			Acute Recovery	- -	√ -	- -
UKV391	F	67	Allopurinol	SJS	ND	Dexamethasone			Acute Recovery	√ √	- -	- -
VIK151	F	32	Phenytoin	SJS/TEN	Negative	Dexamethasone			Acute Recovery	√ -	- -	- -
SNT065	M	55	phenytoin	SJS	Positive (52 spots)	No			Acute Recovery	√ -	- -	- -
CCP374	F	50	celecoxib	SJS	Negative	No			Acute Recovery	- -	- -	√ -

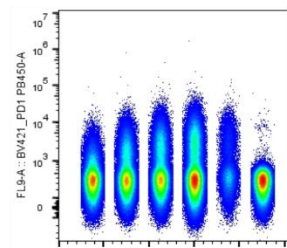
### Antibodies titration

We titrated new 8 antibodies that do not know their optimal concentration.

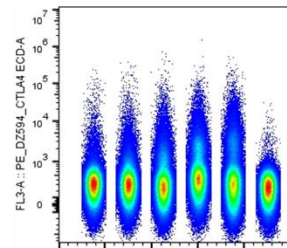
From the results, we used the optimal concentration as follows:



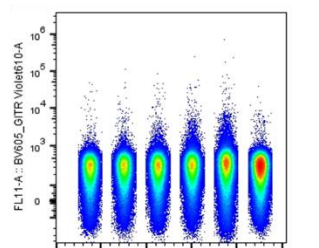
Ab Amt 0.31 0.62 1.25 2.5 5 Neg (uL)  
SI 11.0 11.4 11.6 11.6 10.9 -



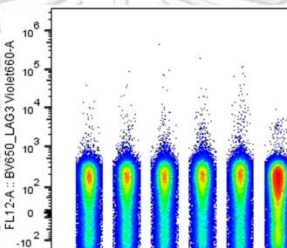
Ab Amt 0.31 0.62 1.25 2.5 5 Neg (uL)  
SI 5.39 7.79 10.3 11.9 11.1 -



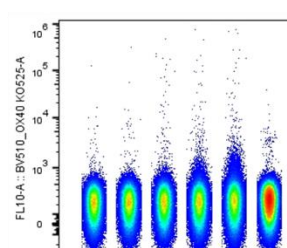
Ab Amt 0.31 0.62 1.25 2.5 5 Neg (uL)  
SI 9.77 9.97 7.66 7.36 10.5 -



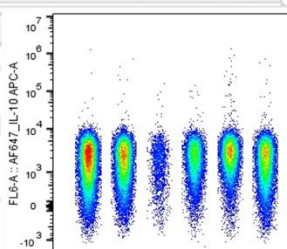
Ab Amt 0.31 0.62 1.25 2.5 5 Neg (uL)  
SI 8.03 8.18 7.24 7.63 6.11 -



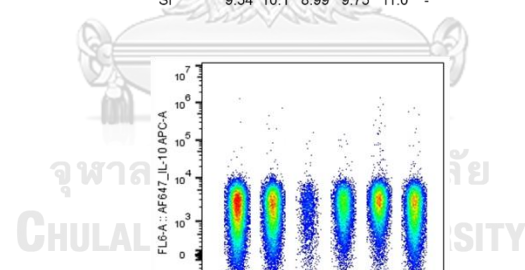
Ab Amt 0.31 0.62 1.25 2.5 5 Neg (uL)  
SI 9.54 10.1 8.99 9.75 11.0 -



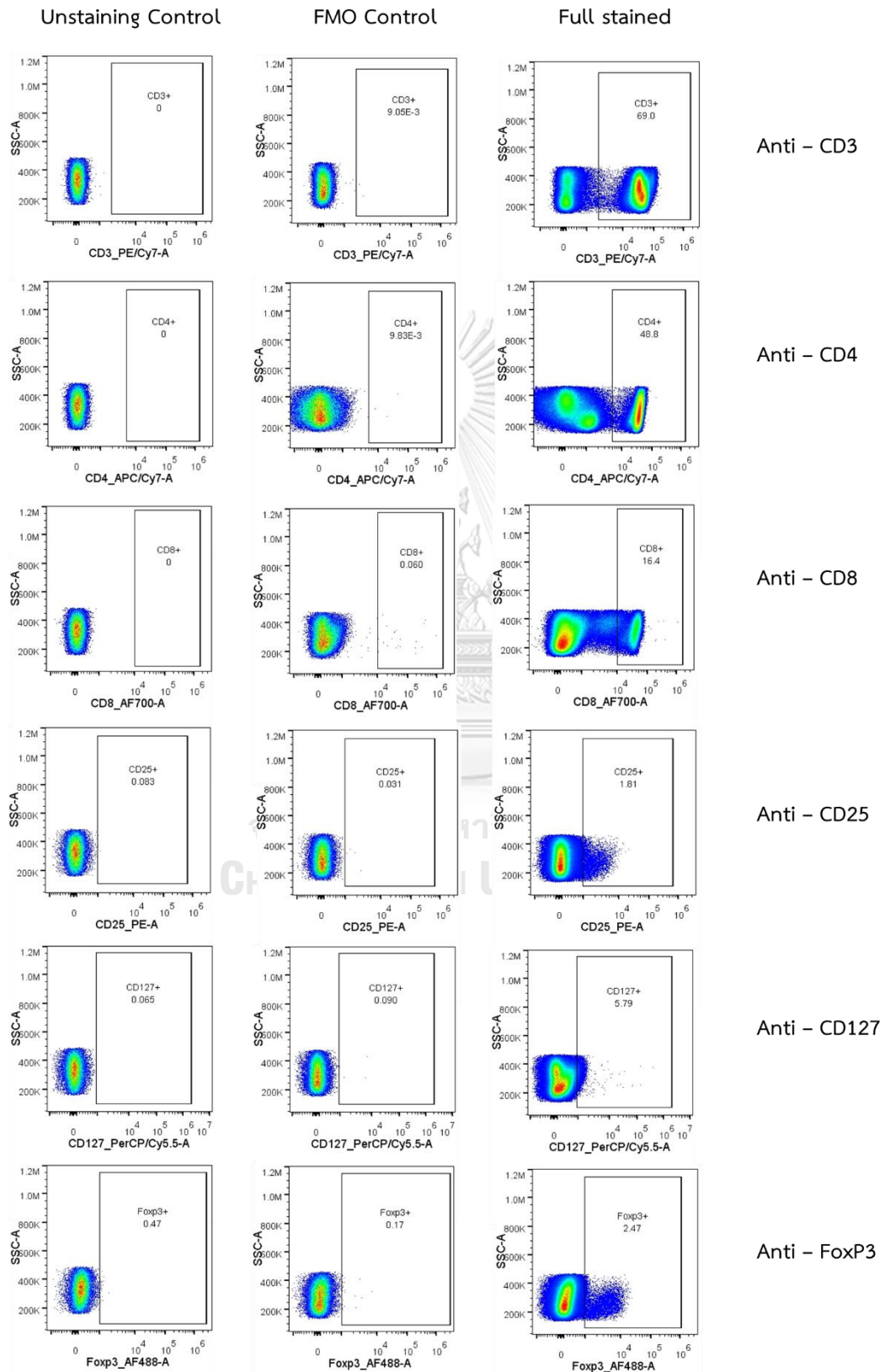
Ab Amt 0.31 0.62 1.25 2.5 5 Neg (uL)  
SI 9.29 4.08 4.88 5.76 6.54 -

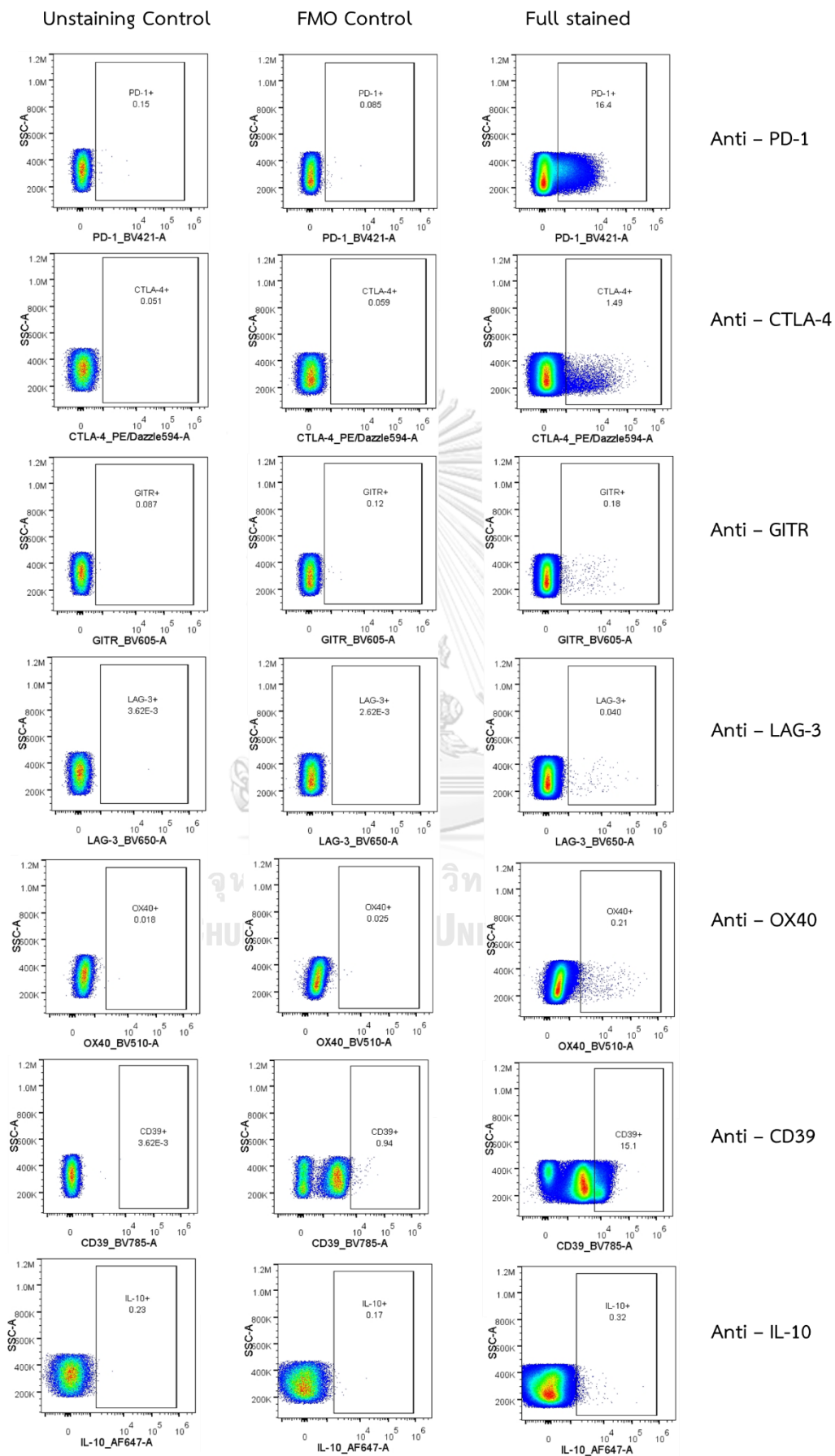


Ab Amt 0.31 0.62 1.25 2.5 5 Neg (uL)  
SI 4.68 5.43 6.54 7.19 8.33 -



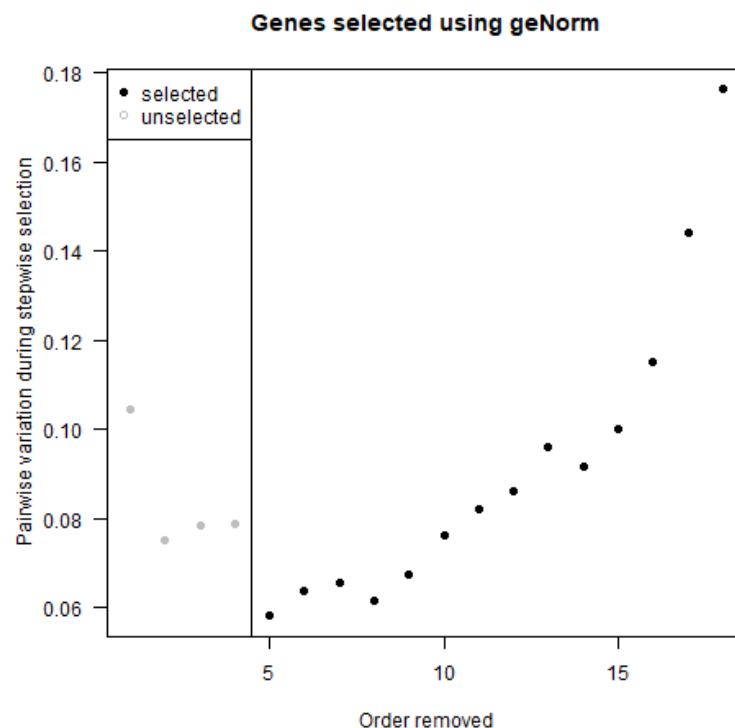
FMO control





### Genes normalization Pairwise Variance during HK Selection

Displays the geNorm pairwise variation statistic after successive genes are removed. This statistic cannot be computed for the final two genes, which are therefore not displayed. The ideal normalization gene set will minimize the pairwise variation statistic.

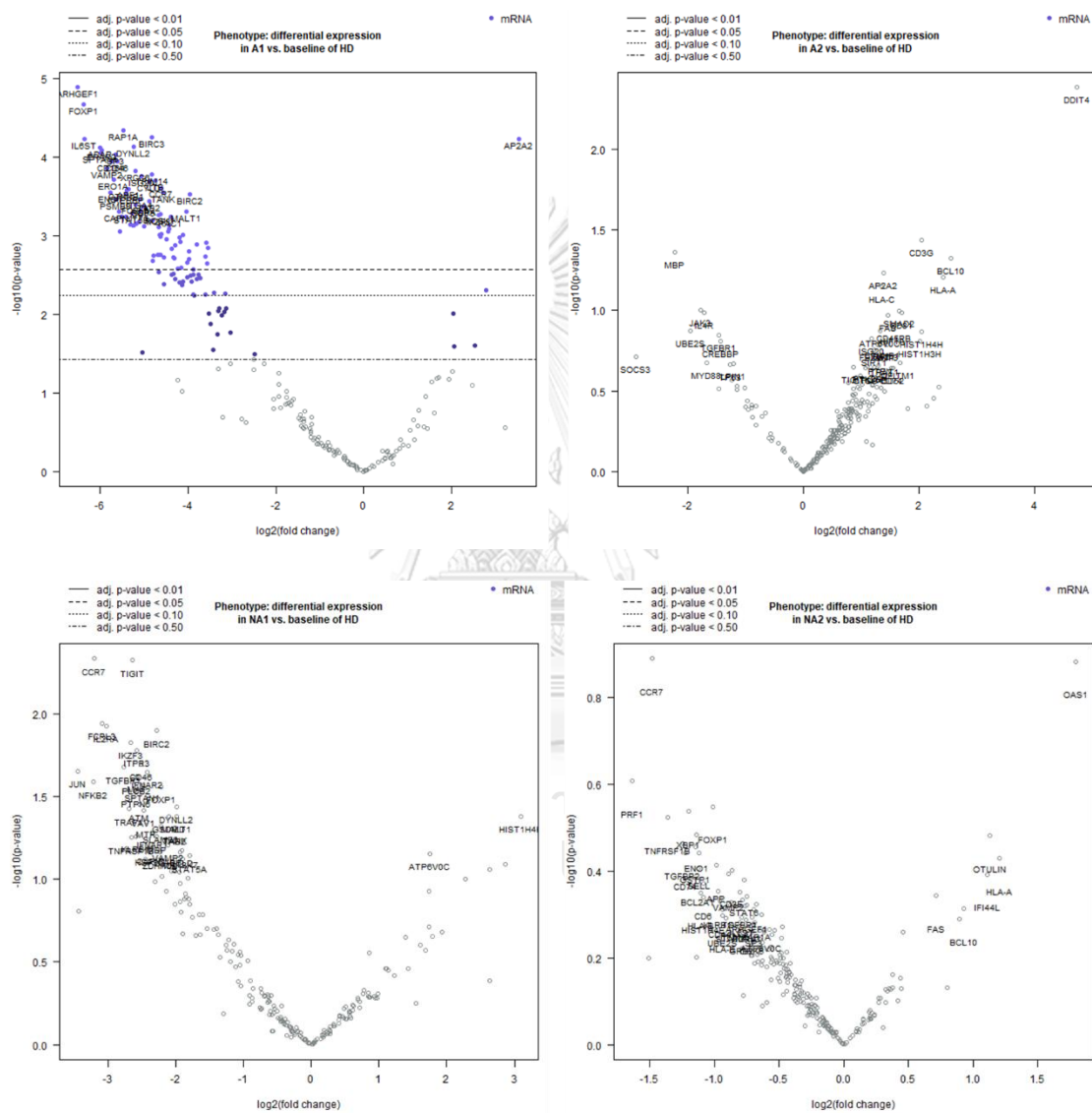


### CHULALONGKORN UNIVERSITY

Moreover, genes are tested for differential expression in response to each selected covariate. A single linear regression is fit for each gene using all selected covariates to predict expression. This approach eliminates confounding due to measured covariates and isolates the independent association of each covariate with gene expression, measuring each variable's association with a gene after holding all other variables constant.

Volcano plot displaying each gene's  $-\log_{10}(\text{p-value})$  and  $\log_2$  fold change with the selected covariate. Highly statistically significant genes fall at the top of the plot above the horizontal lines, and highly differentially expressed genes fall to either side. Horizontal lines indicate various False Discovery Rate (FDR) thresholds or p-

value thresholds if there is no adjustment to the p-values. Genes are colored if the resulting p-value is below the given FDR or p-value threshold. The 40 most statistically significant genes are labeled in the plot.









### Gene expression ratio for Venn's diagram

The fold-change difference between endogenous genes in groups of patients and healthy donors for Venn's diagram was given as follows.

A1 : DRESS with autoimmune sequelae at the acute phase

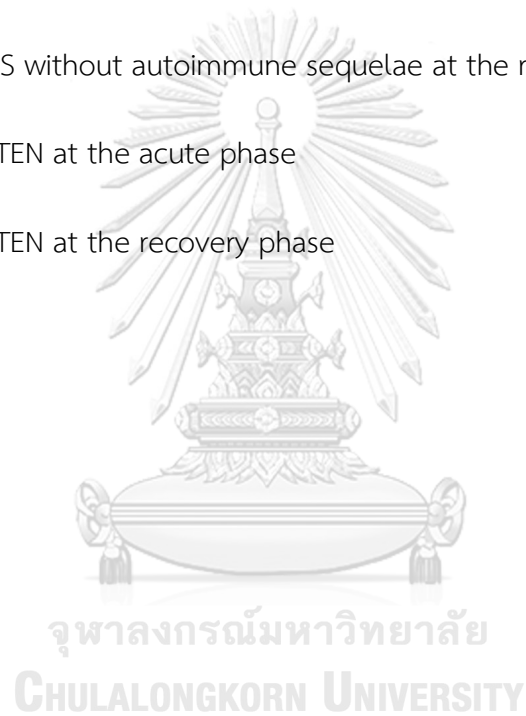
A2 : DRESS with autoimmune sequelae at the recovery phase

NA1 : DRESS without autoimmune sequelae at the acute phase

NA2 : DRESS without autoimmune sequelae at the recovery phase

SJS1 : SJS/TEN at the acute phase

SJS2 : SJS/TEN at the recovery phase



Probe Name	P value		P value		P value		P value		P value		P value		P value	
	A1 vs. HD	of: A1 vs. HD	A2 vs. HD	of: A2 vs. HD	NA1 vs. HD	of: NA1 vs. HD	NA2 vs. HD	of: NA2 vs. HD	SJ1 vs. HD	of: SJ1 vs. HD	SJ2 vs. HD	of: SJ2 vs. HD	SJ1 vs. HD	of: SJ1 vs. HD
ARHGEF1	-106.37	0.0000019	-1.57	0.086546	-1.43	0.453889	-1.14	0.423043	-19.71	0.143575	-1.63	0.197378	-19.71	0.143575
CXCR4	-86.6	0.03215079	1.14	0.645469	-7.25	0.360763	-1.37	0.281767	-36.95	0.150424	-1.47	0.660593	-36.95	0.150424
IL7R	-64.88	0.02498171	1.07	0.783685	-1.52	0.446671	1.15	0.752357	-33.64	0.100822	-2.03	0.167464	-33.64	0.100822
ADAR	-58.48	0.0000001	-1.47	0.038855	-1.02	0.950198	1.02	0.929702	-10.69	0.205991	1.1	0.795252	-10.69	0.205991
RAP1A	-55.73	0.0000001	-1.29	0.089048	-1.51	0.294175	-1.15	0.051368	-12.22	0.15189	-1.46	0.082764	-12.22	0.15189
FOXP1	-52.29	0.00000226	-1.19	0.373765	-3.13	0.461755	-1.22	0.390029	-13.37	0.111668	-1.23	0.450889	-13.37	0.111668
HLA-B	-51.81	0.04384644	-1.72	0.004115	-1.64	0.350293	-1.49	0.124684	-75.61	0.188464	-1.58	0.30193	-75.61	0.188464
SP3	-48.94	0.0000001	-1.14	0.428719	-1.06	0.885072	-1.16	0.114364	-9.29	0.215598	-1.35	0.450382	-9.29	0.215598
ERO1A	-48.24	0.00000776	-1.62	0.020506	-1.04	0.879946	-1.14	0.447692	-9.66	0.197104	-3.14	0.398387	-9.66	0.197104
OAZ1	-48.01	0.0000105	-1.35	0.368491	-1.19	0.701941	1.15	0.283053	-8.94	0.225071	-1.46	0.354783	-8.94	0.225071
HLA-E	-47.96	0.02839945	-1.53	0.029349	-1.38	0.50693	-1.15	0.466365	-32.75	0.157367	-1.82	0.177015	-32.75	0.157367
ITK	-47.08	0.02587389	-1.18	0.156573	-1.67	0.243957	-1.07	0.526665	-20.75	0.145195	-1.48	0.349013	-20.75	0.145195
VAMP2	-42.43	0.00001795	-1.53	0.059168	-2.99	0.453333	-1.27	0.254545	-10.46	0.139118	-3.68	0.343704	-10.46	0.139118
UBA52	-42.41	0.03993742	-1.12	0.617952	-1.43	0.511493	1.01	0.947255	-31.73	0.140242	-1.56	0.262451	-31.73	0.140242
IL6ST	-40.98	0.00041243	1.04	0.901017	-1.27	0.685504	-1.04	0.901365	-9.42	0.162824	-1.48	0.421991	-9.42	0.162824
LTB	-40.36	0.01527171	-1.51	0.094625	-1.47	0.601864	1.12	0.664567	-25	0.143762	-1.03	0.933138	-25	0.143762
CD46	-39.08	0.0000001	-1.13	0.589017	-3.07	0.422579	1.11	0.098589	-8.55	0.192098	-1.08	0.813242	-8.55	0.192098
SPTAN1	-38.86	0.0000001	-3.03	0.220102	-3.13	0.411129	1	0.991454	-11.49	0.09532	-1.6	0.376513	-11.49	0.09532
CD164	-38.67	0.00000053	-1.27	0.360297	1.08	0.643747	1.18	0.157607	-8.36	0.197496	-1.23	0.323746	-8.36	0.197496
ARF1	-36.91	0.00000026	-1.27	0.276417	1.2	0.425076	-1.05	0.735596	-7.04	0.256668	-1.11	0.599141	-7.04	0.256668
STAT3	-35.66	0.00001146	-2.89	0.199856	1.06	0.719652	-1.29	0.286516	-8.05	0.191357	-2.87	0.387839	-8.05	0.191357
JAK3	-34.68	0.00000805	-6.36	0.075021	1.11	0.445435	-1.14	0.400776	-8.24	0.175226	-1.31	0.215097	-8.24	0.175226

Probe Name	P value		P value		P value		P value		P value		P value		P value	
	A1 vs. HD	of: A1 vs. HD	A2 vs. HD	of: A2 vs. HD	NA1 vs. HD	of: NA1 vs. HD	NA2 vs. HD	of: NA2 vs. HD	SJ1 vs. HD	of: SJ1 vs. HD	SJ2 vs. HD	of: SJ2 vs. HD	SJ1 vs. HD	of: SJ1 vs. HD
CTNNB1	-33.27	0.00000008	1.08	0.56412	1.03	0.847235	-1.01	0.917822	-7.36	0.210522	-1.24	0.385104	-7.36	0.210522
MSN	-33.17	0.02422436	-1.17	0.436231	1.32	0.211466	-1.03	0.917406	-11.72	0.228312	-1.29	0.525715	-11.72	0.228312
SQSTM1	-32.74	0.00000011	-2.15	0.40947	-2.77	0.4462	-1.07	0.442085	-6.2	0.281356	1.81	0.006175	-6.2	0.281356
HLA-DPB1	-32.72	0.00010482	-1.18	0.686349	1.39	0.154048	-1.08	0.788171	-4.78	0.408421	1.18	0.524249	-4.78	0.408421
CD4	-30.95	0.00004421	-2.03	0.435211	1.08	0.727174	1.03	0.941402	-7.64	0.174242	-2.32	0.49121	-7.64	0.174242
ENO1	-30.14	0.0035363	-1.72	0.28683	-1.3	0.554655	-1.58	0.318569	-9.34	0.221127	-4.07	0.331668	-9.34	0.221127
CTLA4	-29.96	0.03793207	-1.31	0.40246	-1.01	0.968508	-1.35	0.416222	-13.26	0.193186	-5.41	0.296168	-13.26	0.193186
HIF1A	-29.34	0.00000003	1.13	0.633116	1.17	0.734986	-1.34	0.072036	-6.17	0.252997	1.13	0.670118	-6.17	0.252997
NFKB2	-29.25	0.00017256	-2.97	0.190993	-4.32	0.207036	-1.65	0.14428	-8.15	0.132753	-6.08	0.240461	-8.15	0.132753
JUN	-27.93	0.02017283	1.32	0.732569	-4.06	0.398598	1.14	0.873771	-13.69	0.122673	1.23	0.8325	-13.69	0.122673
ITGAL	-27.86	0.02718072	-1.35	0.173958	-1.15	0.601529	1.14	0.510049	-11.97	0.180616	-1.32	0.377399	-11.97	0.180616
YY1	-27.66	0.00000125	-1.02	0.884915	1.01	0.965571	1.01	0.947059	-6.54	0.209856	-2.77	0.418068	-6.54	0.209856
HLA-F	-27.45	0.00000003	1.06	0.733515	-1.12	0.457568	-1.02	0.873682	-7.77	0.138894	-2.95	0.346534	-7.77	0.138894
IKZF1	-27.45	0.03325018	-1.19	0.106408	-1.1	0.71841	-1.04	0.846792	-11.72	0.195184	-1.65	0.234717	-11.72	0.195184
PSMB9	-27.16	0.00954624	-2.48	0.360684	1.44	0.108003	1.17	0.567474	-7.32	0.298702	-1.09	0.731221	-7.32	0.298702
CREBBP	-26.92	0.00000001	-4.78	0.117505	-1.18	0.476203	-1.07	0.466205	-8.44	0.10624	-3.47	0.282757	-8.44	0.10624
PGK1	-25.53	0.0290957	-1.74	0.184685	-1.14	0.726937	-1.46	0.349452	-15.71	0.20068	-1.76	0.228913	-15.71	0.20068
ISG20	-24.55	0.00000002	1.07	0.754768	1.09	0.600643	1.06	0.662707	-7.05	0.14662	-1.24	0.282829	-7.05	0.14662
CASP8	-24.25	0.0373422	-1.03	0.918691	-1.34	0.588439	-1.05	0.814276	-11.96	0.165461	-1.17	0.581399	-11.96	0.165461
SELL	-23.35	0.03443152	-1.54	0.071373	-1.17	0.657521	-1.16	0.662905	-18.05	0.144936	-1.4	0.258748	-18.05	0.144936
STAT5B	-23.08	0.00000001	1.11	0.606609	-2.37	0.473355	1.15	0.484494	-5.98	0.198351	-5.36	0.232343	-5.98	0.198351
DDX24	-23.07	0.00000001	-1.21	0.332852	-2.33	0.488588	-1.24	0.017103	-7.05	0.130068	-2.35	0.425313	-7.05	0.130068

Probe Name	P value		P value		P value		P value		P value		P value		P value	
	A1 vs. HD	of: A1 vs. HD	A2 vs. HD	of: A2 vs. HD	NA1 vs. HD	of: NA1 vs. HD	NA2 vs. HD	of: NA2 vs. HD	SJ1 vs. HD	of: SJ1 vs. HD	SJ2 vs. HD	of: SJ2 vs. HD	SJ1 vs. HD	of: SJ1 vs. HD
RPL4	-22.67	0.01280747	-1.02	0.951816	-1.65	0.394728	1.12	0.527006	-68.36	0.143085	-1.34	0.390644	-1.34	0.143085
TAB2	-22.31	0.00000308	1.01	0.946524	-2.63	0.401094	1.01	0.910684	-6.77	0.134975	-1.89	0.568615	-1.89	0.134975
BAX	-22.25	0.00000163	-1.23	0.113866	1.24	0.124743	-1.12	0.306722	-5.5	0.227337	-2.7	0.390409	-2.7	0.227337
ITGB2	-22.24	0.04075113	-1.08	0.854126	1.73	0.174144	-1.02	0.948342	-7.62	0.335841	1.25	0.482284	1.25	0.335841
CD28	-21.98	0.00002195	-1.77	0.483452	-1.86	0.625925	1.28	0.141831	-6.44	0.149976	-2.31	0.424221	-2.31	0.149976
PSMB10	-21.97	0.00000034	-1.11	0.420468	1.15	0.456803	1.04	0.785379	-5.23	0.247182	-1.45	0.190075	-1.45	0.247182
CDK9	-21.95	0.0000102	-3.64	0.187084	-1.26	0.0106	-1.1	0.420087	-7.86	0.083459	-2.76	0.302544	-2.76	0.083459
BIRC3	-21.92	0.02256159	-1.29	0.432665	-1.35	0.593975	1.08	0.397007	-17.23	0.116139	-1.35	0.19294	-1.35	0.116139
CAPN1	-21.35	0.00008739	-4.01	0.132704	-2.35	0.464343	1.09	0.65498	-5.88	0.179945	-5.97	0.152049	-5.97	0.179945
GATA3	-21.32	0.00937868	-2.06	0.454451	1.49	0.080311	1.47	0.091458	-7.31	0.236377	1.05	0.858366	1.05	0.236377
ERAP2	-21.28	0.01286089	-2.08	0.478294	-1.02	0.958937	1.02	0.966192	-15.04	0.03751	-1.22	0.54529	-1.22	0.03751
MAP4K2	-21.23	0.00000001	-3.93	0.141475	-2.65	0.386769	-1.27	0.296186	-14.18	0.006417	-4.78	0.26476	-4.78	0.006417
GRB2	-20.87	0.01467694	-2.67	0.295076	1.02	0.943614	-1.03	0.906262	-7.09	0.267398	-1.51	0.202768	-1.51	0.267398
PLCG1	-20.77	0.01815263	-1.07	0.662476	-1.09	0.592679	1.14	0.508461	-10.96	0.108348	-1.27	0.511152	-1.27	0.108348
CREB1	-20.64	0.00000251	-3.83	0.146891	-1.02	0.919261	-1.07	0.384535	-5.87	0.173663	-1.82	0.579388	-1.82	0.173663
ZAP70	-20.62	0.03700981	-1.41	0.226958	-1.54	0.444949	-1.01	0.955428	-18.29	0.113783	-1.77	0.11488	-1.77	0.113783
CYLD	-20.49	0.00975129	-1.13	0.653262	-2.47	0.521874	1.08	0.642176	-8.55	0.162991	-1.44	0.392142	-1.44	0.162991
XBP1	-20.43	0.000314	-2.59	0.182514	-1.03	0.909656	-1.48	0.396909	-6	0.155301	-2.03	0.496802	-2.03	0.155301
CD45R0	-20.41	0.02814842	1.07	0.857224	-1.49	0.365036	1.13	0.369453	-14.69	0.160936	-1.85	0.041829	-1.85	0.160936
DYNLL2	-20.21	0.01199894	1.06	0.818781	-2.46	0.538298	1.11	0.650857	-2.49	0.437924	1.39	0.211926	1.39	0.437924
ATM	-20.13	0.01724667	-1.06	0.854703	-3.4	0.376127	1.14	0.505611	-11.86	0.089499	-1.59	0.178618	-1.59	0.089499
ETS1	-20.06	0.03795737	-1.37	0.081481	-1.44	0.501003	1.04	0.887007	-31.07	0.12602	-1.56	0.195232	-1.56	0.12602

Probe Name	P value		P value		P value		P value		P value		P value		P value	
	A1 vs. HD	of: A1 vs. HD	A2 vs. HD	of: A2 vs. HD	NA1 vs. HD	of: NA1 vs. HD	NA2 vs. HD	of: NA2 vs. HD	SJ1 vs. HD	of: SJ1 vs. HD	SJ2 vs. HD	of: SJ2 vs. HD		
SKP1	-19.91	0.04765227	-1.2	0.387691	-1.08	0.858778	1.06	0.67714	-15.53	0.177207	-1.3	0.419022		
TAX1BP1	-19.37	0.02529785	-1.31	0.482577	-1.03	0.929658	1.11	0.177691	-9.62	0.147711	-1.78	0.140839		
STAT5A	-19.24	0.00000231	-1.94	0.37873	-2.11	0.516131	1.08	0.386609	-12.85	0.00845	-1.86	0.546998		
ROCK1	-19.08	0.0176424	-2.43	0.335265	-1.05	0.864459	1.16	0.343829	-7.65	0.206394	-1.25	0.588048		
MALT1	-18.54	0.00000011	-1.16	0.567096	-2.15	0.495842	1.01	0.91984	-6.52	0.101333	-2.81	0.259545		
KLRB1	-18.13	0.02759655	-1.05	0.876599	-3.24	0.38027	-1.18	0.628783	-9.05	0.151683	-3.72	0.25608		
PRKCQ	-17.8	0.00000002	-3.89	0.110951	-2.36	0.420737	1.09	0.155486	-11.89	0.007714	-5.89	0.108041		
KLC1	-17.73	0.00000002	-1.79	0.440387	-2.49	0.384798	-1.03	0.655393	-5.29	0.174654	-4.3	0.263114		
FCRL3	-17.34	0.00021753	-3.17	0.202667	-3.08	0.288427	-1.24	0.5125	-11.58	0.001243	-2.2	0.465001		
OClAD2	-17.05	0.01478433	-1.2	0.559171	1.1	0.810329	1.08	0.578515	-8.69	0.133218	-2.06	0.169468		
TGFB1	-16.66	0.00000101	-3.69	0.112174	-3.01	0.256572	-1.16	0.175118	-5.59	0.129957	-2.09	0.422608		
STAT1	-16.56	0.03459803	-1.73	0.009238	1.33	0.409979	1.23	0.477005	-7.39	0.217061	-1.18	0.576184		
PKM	-16.49	0.03766559	-1.88	0.055363	-1.19	0.545071	-1.28	0.410661	-11.69	0.210686	-2.07	0.110794		
PSIP1	-16.15	0.04496546	-1.23	0.230584	-1.71	0.270132	-1.12	0.319634	-15.42	0.123498	-1.76	0.234487		
SLAMF6	-16.1	0.00237414	-1.46	0.635302	-2	0.537815	1.44	0.32619	-5.77	0.09058	-5	0.133761		
MX1	-15.99	0.01897035	-2.9	0.192472	-1	0.990318	-1.2	0.266545	-5.89	0.272817	-2.08	0.56971		
RORA	-15.82	0.01757964	-1.97	0.405231	-2.66	0.44291	-1.11	0.60448	-7.63	0.149951	1.05	0.817385		
IL10RA	-15.63	0.04282513	-1.69	0.163921	-1.28	0.612128	1.03	0.756233	-14.39	0.116005	-1.84	0.147718		
GUSB	-15.42	0.00000002	-1.76	0.416876	-2.2	0.439544	-1.04	0.7724	-4.52	0.208134	-1.05	0.646241		
TANK	-15.14	0.01680348	1.03	0.921701	-2.29	0.516145	1.3	0.238734	-6.98	0.165675	-1.22	0.491976		
CD6	-15.12	0.06697684	-1.34	0.384329	-3.03	0.425776	-1.4	0.381974	-25.61	0.003096	-7.82	0.207102		
CCR7	-15.06	0.0197935	-1.66	0.016625	-3.77	0.248811	-1.54	0.316267	-9.54	0.071246	-3.41	0.238013		

Probe Name	P value		P value		P value		P value		P value		P value		P value	
	A1 vs. HD	of: A1 vs. HD	A2 vs. HD	of: A2 vs. HD	NA1 vs. HD	of: NA1 vs. HD	NA2 vs. HD	of: NA2 vs. HD	SJ1 vs. HD	of: SJ1 vs. HD	SJ2 vs. HD	of: SJ2 vs. HD		
SOCS3	-15.06	0.07028641	-8.68	0.028209	1.09	0.864471	-2.03	0.06253	-6.41	0.316646	-7.26	0.244743		
SMN1	-15	0.03744862	-1.24	0.288711	1.11	0.4814	-1	0.996306	-9.01	0.117532	-2.75	0.385199		
TGFBR2	-14.9	0.0357777	-1.5	0.022137	-3.35	0.34758	-1.42	0.304677	-3.21	0.253607	-7.87	0.161302		
PRDX2	-14.67	0.00006124	-1.74	0.416191	-1.79	0.585342	-1.02	0.957585	-4.34	0.211565	-4.16	0.210241		
XRCC6	-14.64	0.01573222	-1.09	0.579409	-1.05	0.87613	1.09	0.57728	-6.88	0.160365	-1.26	0.482383		
ICOS	-14.59	0.00033475	-3.15	0.157705	-1.78	0.597819	1.09	0.782897	-3.78	0.292164	-4.22	0.197963		
IKBKE	-14.48	0.00005417	-3.24	0.134043	-2.3	0.406045	1	0.984319	-4.5	0.186853	-3.74	0.272149		
PTGER4	-14.45	0.02871528	-2.32	0.322677	1.18	0.736856	-1.18	0.333037	-5.68	0.28211	-5.35	0.295672		
RNF126	-14.2	0.00000358	-2.09	0.244267	1.14	0.382043	-1.06	0.552841	-5.1	0.123346	-4.99	0.108221		
ZDHHC2	-14.17	0.00013006	-1.44	0.623337	-2.18	0.425783	1.06	0.79367	-4.64	0.16142	-4.02	0.217563		
TRIM25	-14.05	0.00000184	-3.66	0.079969	-2.2	0.416248	-1	0.987196	-3.75	0.284687	-3.99	0.221376		
IKZF3	-14	0.01645864	-1.12	0.590191	-3.24	0.307839	-1.07	0.638235	-7.55	0.11329	-2.44	0.404184		
CCL5	-13.99	0.01132185	-6.06	0.038053	-3.49	0.295106	-2.42	0.156278	-6.06	0.194159	-6.63	0.129256		
TRIM14	-13.94	0.0179471	-1.23	0.030961	1.07	0.849272	1.26	0.043616	-7.46	0.118878	-1.13	0.322685		
ITGA5	-13.86	0.00000257	-3.18	0.137465	-2.47	0.330915	-1.07	0.710029	-4.53	0.17142	-4.45	0.155247		
CD81	-13.5	0.01781389	1.27	0.377901	1.4	0.158453	1.09	0.758754	-5.38	0.258255	-2.19	0.476079		
GBP2	-13.49	0.03743285	-1.21	0.275821	1.11	0.74573	1.09	0.637326	-9.64	0.203433	-1.72	0.127876		
PRF1	-13.41	0.0146752	-2.2	0.409928	1.46	0.602179	-1.4	0.508477	-4.22	0.389403	1.86	0.301065		
LPIN1	-13.38	0.00021425	-3.15	0.125927	-2.2	0.405072	-1.08	0.697789	-5.21	0.087765	-4.22	0.164353		
PTPN22	-13.21	0.00000003	-2.39	0.306966	-2	0.471661	1.19	0.604618	-4.51	0.156543	-3.83	0.22259		
GSDMD	-13.08	0.00000877	-1.28	0.736994	-2.04	0.46342	1.21	0.158279	-4.94	0.108291	-2.51	0.221316		
CD52	-13.02	0.04240187	1.52	0.342343	1.52	0.356177	1.8	0.065908	-15.58	0.224428	-1.03	0.917039		

Probe Name	P value		A2 vs. HD	P value		NA1 vs. HD	P value		NA2 vs. HD	P value		SJS1 vs. HD	P value		SJS2 vs. HD	P value	
	A1 vs. HD	of: A1 vs. HD		of: A2 vs. HD	of: NA1 vs. HD		of: NA2 vs. HD	of: SJS1 vs. HD		of: SJS2 vs. HD							
TAPBP	-12.83	0.04816975	2.26	0.482575	4.76	0.146367	1.89	0.49591	-2.16	0.655907	-1.98	0.69778					
TNFRSF1B	-12.65	0.04415543	-3.7	0.196136	-3.96	0.337976	-1.83	0.095295	-8.68	0.234087	-2.96	0.424665					
CD3D	-12.58	0.04724775	-1.03	0.897244	1	0.996997	1.19	0.408156	-7.01	0.212308	-1.39	0.255589					
DDIT4	-12.58	0.04676126	3.36	0.297939	-1.62	0.710492	1.52	0.626519	-1.85	0.740126	-1.56	0.82087					
CARD11	-12.54	0.01992825	-2.07	0.305315	-1.03	0.736676	-1.01	0.904152	-6.8	0.124941	1.1	0.631988					
POU2F2	-12.51	0.00009262	-2.95	0.142835	-2.52	0.287237	-1.14	0.553915	-8.36	0.003228	-4.42	0.114852					
SP100	-12.38	0.02313417	-1.91	0.419518	1.15	0.190489	1.08	0.65608	-6.35	0.156621	-2.41	0.399919					
RASSF5	-12.31	0.02076673	-3	0.134497	-2.22	0.499271	-1.34	0.440542	-14.09	0.007455	-6.31	0.129657					
EP300	-12.25	0.02051239	1.06	0.699928	-2.34	0.467741	1.04	0.835126	-5.97	0.170879	-4.75	0.264082					
SIPA1	-12.16	0.00000004	-3.25	0.091919	-2.52	0.280419	-1.2	0.021395	-5.15	0.076045	-4.42	0.111434					
ITGB7	-12.02	0.01950494	-3.81	0.171379	1.18	0.670256	1.38	0.331125	-5.92	0.190475	-5.13	0.244281					
IL4R	-11.88	0.02603498	-5.02	0.062123	1.13	0.455665	-1.05	0.778399	-6.52	0.140337	-2.42	0.383363					
SH2D1A	-11.79	0.00000091	-2.43	0.251615	-2.07	0.43213	1.16	0.188044	-7.88	0.007984	-3.48	0.23753					
GRK6	-11.7	0.04758935	-1.42	0.066977	-1.32	0.553647	-1.01	0.962697	-10.81	0.142086	-1.33	0.309349					
MBP	-11.69	0.02693995	-5.43	0.047985	-2.54	0.426483	-1.06	0.78244	-6.21	0.167236	-2.3	0.426328					
DNMT1	-11.48	0.00022078	-2.62	0.192385	-2.48	0.27454	1.13	0.534912	-4.07	0.154791	-1.53	0.612502					
MAF	-11.48	0.02536593	-2.43	0.236165	-3.13	0.305899	-1.04	0.826691	-6	0.175392	-2.58	0.33878					
HMGCB2	-11.46	0.02170222	-1.03	0.742767	1.35	0.094438	1.18	0.301464	-5.1	0.22512	-5.55	0.162233					
MRP57	-11.23	0.00000005	-2.7	0.168553	-1.74	0.548403	1.1	0.38424	-3.91	0.175119	-2.02	0.336872					
ITGA4	-11.18	0.02548044	-1.24	0.508559	-1.09	0.661344	1.34	0.405275	-8.24	0.04767	-2.94	0.241114					
POLR2A	-11.1	0.06484775	-6.55	0.037212	-2.96	0.371639	-1.32	0.139662	-17.95	0.00261	-2.24	0.489306					
UBE2L6	-10.99	0.03057809	-1.09	0.34831	1.93	0.001148	1.37	0.100602	-4.51	0.298119	1.03	0.896808					

Probe Name	P value		P value		P value		P value		P value		P value		P value	
	A1 vs. HD	of: A1 vs. HD	A2 vs. HD	of: A2 vs. HD	NA1 vs. HD	of: NA1 vs. HD	NA2 vs. HD	of: NA2 vs. HD	SJ1 vs. HD	of: SJ1 vs. HD	SJ2 vs. HD	of: SJ2 vs. HD	SJ1 vs. HD	of: SJ1 vs. HD
PSMB8	-10.95	0.03405857	-1.08	0.621235	1.12	0.640953	1.29	0.042463	-5.4	0.222362	-2.93	0.271606	-5.4	0.222362
PLCB2	-10.88	0.00019332	1.11	0.704636	-2.01	0.419891	1.22	0.458835	-4.2	0.118611	-4.21	0.084868	-4.2	0.118611
SLC3A2	-10.82	0.03479354	-4.64	0.072683	-1.02	0.923514	-1.29	0.01562	-1.61	0.631047	-5.82	0.151326	-1.61	0.631047
PIK3CA	-10.76	0.00000005	-1.56	0.454245	-1.52	0.667045	-1.03	0.792392	-7.19	0.011712	-3.47	0.201742	-7.19	0.011712
BIRC2	-10.56	0.0230965	1.07	0.639266	-2.51	0.38505	1.09	0.694373	-6	0.124577	1.03	0.846646	-6	0.124577
CAMK2G	-10.54	0.00000008	-2.47	0.211951	-2.17	0.351765	1.01	0.886987	-7.04	0.011446	-3.93	0.116807	-7.04	0.011446
PLEKHB2	-10.51	0.00000008	-2.61	0.167662	-1.67	0.57292	1.18	0.09553	-3.51	0.215311	-3.22	0.242131	-3.51	0.215311
LAT	-10.45	0.0412757	-1.88	0.408932	1.05	0.900651	1.24	0.298507	-7.19	0.087384	-6.25	0.11727	-7.19	0.087384
CD59	-10.44	0.04320109	-1.05	0.473015	1.44	0.244826	-1.02	0.740908	-5.19	0.229248	-2.27	0.412285	-5.19	0.229248
IKKB	-10.39	0.00020403	-2.36	0.230507	-2.13	0.38224	1.12	0.508011	-6.94	0.003726	-3.81	0.1202	-6.94	0.003726
SMAD4	-10.32	0.00000051	-2.52	0.180731	1.11	0.784548	-1.03	0.866373	-2.34	0.446092	-3.61	0.159001	-2.34	0.446092
IFI44	-10.11	0.00011532	-2.07	0.335735	-1.61	0.61855	1.22	0.471679	-4.02	0.115417	-3.15	0.237663	-4.02	0.115417
MTMR14	-9.99	0.00000008	-2.42	0.205617	-1.65	0.570895	-1.08	0.295282	-3.4	0.21434	-3.32	0.19747	-3.4	0.21434
GBP5	-9.89	0.03039755	-1.74	0.447254	1.5	0.492841	1.65	0.000744	-6.7	0.079363	-6.87	0.052924	-6.7	0.079363
MTR	-9.73	0.00001631	-1.79	0.470085	-2.15	0.342741	1.24	0.45525	-6.5	0.00751	-3.15	0.223121	-6.5	0.00751
SMAD2	-9.73	0.03752545	1.5	0.030463	1.17	0.381246	1.29	0.140334	-4.1	0.32187	1.85	0.056187	-4.1	0.32187
BCLAF1	-9.66	0.03453068	-1.06	0.728676	-1.08	0.810971	1.08	0.727182	-5.11	0.188727	-2.47	0.337452	-5.11	0.188727
KMT2A	-9.63	0.04660111	-1.76	0.41892	-2.62	0.368981	-1	0.990157	-2.16	0.394179	-5.07	0.193841	-2.16	0.394179
NFE2L1	-9.58	0.00000209	-3.09	0.052129	-1.9	0.432452	-1.25	0.264367	-6.4	0.009894	-3.25	0.192028	-6.4	0.009894
AKT2	-9.4	0.04510645	-1.88	0.526898	-1.16	0.899141	1.67	0.507189	-1.91	0.663922	-1.84	0.678375	-1.91	0.663922
ISG15	-9.33	0.00000062	-1.55	0.416782	1.42	0.169308	1.15	0.574261	-1.19	0.805875	-2.82	0.29025	-1.19	0.805875
NFKB1	-9.29	0.00002944	-1.42	0.536747	-1.81	0.47414	1.15	0.413185	-6.21	0.007393	-2.77	0.302607	-6.21	0.007393



Probe Name	P value		A2 vs. HD	P value		NA1 vs. HD	P value		NA2 vs. HD	P value		SJS1 vs. HD	P value		SJS2 vs. HD	P value	
	A1 vs. HD	of: A1 vs. HD		of: A2 vs. HD	of: NA1 vs. HD		of: NA2 vs. HD	of: SJS1 vs. HD		of: SJS2 vs. HD	of: SJS1 vs. HD		of: SJS2 vs. HD				
ACTR1B	-9.23	0.05380875	-2.54	0.185492	-1.36	0.383175	-1.23	0.278631	-8.26	0.032816	-3.58	0.128699					
HLA-DRB3/4	-9.17	0.04156178	1.27	0.799574	-1.94	0.574035	-1.62	0.300431	-2.36	0.652033	-1.46	0.770359					
ATP6V1H	-9.07	0.00000414	-1.3	0.654861	-1.41	0.700551	1.39	0.012688	-2.89	0.290077	-1.54	0.543258					
OTULIN	-8.94	0.04585854	-1.93	0.494084	1.02	0.985713	1.93	0.400926	-2.6	0.419564	-2.38	0.466222					
VAV1	-8.57	0.03438823	-1.42	0.632981	-2.38	0.379267	1.2	0.190629	-4.47	0.207653	-1.67	0.593557					
RAC1	-8.5	0.03545675	-1.71	0.436278	-1	0.982771	-1.04	0.688412	-4.04	0.263883	-1.02	0.843506					
NFATC1	-8.38	0.00000856	-2.62	0.086868	-2.46	0.189389	-1.14	0.387129	-5.6	0.010566	-3.32	0.114969					
TROVE2	-8.38	0.03108288	-2.7	0.242613	-1.7	0.62034	1.1	0.363101	-4.47	0.188724	-3.89	0.245615					
PARP1	-8.33	0.03530878	-2.98	0.209311	-1.06	0.86223	1.16	0.53607	-5.53	0.109627	-2.34	0.320379					
MAPK3	-8.32	0.03808264	-1.53	0.565079	-2.08	0.484972	1.14	0.396918	-4.12	0.266557	-3.67	0.316434					
ATG5	-8.29	0.00000159	-1.22	0.730526	-1.53	0.605765	1.49	0.048617	-3.06	0.206795	-2.65	0.285041					
TXN	-8.26	0.04160582	1.18	0.531681	1.88	0.02815	1.52	0.013747	-3.4	0.374897	-2.26	0.335926					
DTX3L	-8.23	0.05154969	-1.67	0.426889	1.26	0.044542	1.24	0.118476	-4.18	0.261201	1.02	0.898522					
SDHA	-7.97	0.07265836	-1.14	0.417519	-2.09	0.493972	1.05	0.778227	-3.06	0.167622	-1.59	0.008721					
CASP1	-7.96	0.03981702	-1.33	0.668282	1.03	0.86487	1.14	0.247777	-1.85	0.412383	1.03	0.836275					
RB1	-7.95	0.00033354	-2.05	0.247405	-1.82	0.414619	1.04	0.852962	-2.71	0.278924	-2.88	0.188174					
MTMR3	-7.79	0.03484271	-2.72	0.212471	-1.94	0.498909	1.08	0.619728	-4.79	0.131487	-3.81	0.229781					
CHUK	-7.76	0.00000012	-2.09	0.221694	-1.39	0.69108	1.24	0.218299	-3.06	0.177643	-2.74	0.219715					
NPRL2	-7.59	0.00017851	-1.92	0.297668	-2.09	0.272059	1.04	0.848922	-5.07	0.007758	-1.26	0.739123					
CD7	-7.56	0.04607873	-2.3	0.308273	1.06	0.959904	1.87	0.407698	-2.23	0.475768	-2.41	0.382232					
STAT4	-7.46	0.00003983	-1.81	0.353292	-1.85	0.3777	1.03	0.846705	-4.99	0.010643	-2.07	0.172152					
ANXA1	-7.45	0.00246066	1.49	0.242101	1.26	0.42634	1.36	0.296856	-14.48	0.30734	-1.03	0.952102					

Probe Name	P value		A2 vs. HD	P value		NA1 vs. HD	P value		NA2 vs. HD	P value		SJS1 vs. HD	P value		SJS2 vs. HD	P value	
	A1 vs. HD	of: A1 vs. HD		of: A2 vs. HD	of: NA1 vs. HD		of: NA2 vs. HD	of: SJS1 vs. HD		of: SJS2 vs. HD							
CD45RA	-7.39	0.03877944	-2.03	0.399861	-1.16	0.881965	-1.36	0.510324	-9.29	0.001971	1.02	0.986888					
TP53	-7.35	0.0323994	-3.02	0.133419	1.03	0.908112	1.42	0.154339	-1.64	0.511884	-4.22	0.138076					
TRAF1	-7.34	0.08478144	-2.22	0.348915	-3.18	0.331092	-1.34	0.233716	-10.88	0.034911	-3.72	0.245431					
IL2RB	-7.27	0.08596673	-2.69	0.250746	-3	0.375873	-1.86	0.010112	-6.72	0.204878	-2.39	0.454403					
PLD3	-7.13	0.04510086	-1.7	0.533483	-1.16	0.887347	1.75	0.41521	-1.6	0.729747	1.86	0.626408					
TRAF5	-7.13	0.05106594	-2.8	0.187586	-2.51	0.311775	-1.2	0.065264	-8.68	0.009692	-3.49	0.276562					
GBP3	-7.04	0.00000204	-1.12	0.837784	1.08	0.715029	1.28	0.389089	-2.67	0.232926	-1.59	0.405952					
AP2A1	-6.94	0.04258628	-2.02	0.367906	-1.25	0.816404	1.58	0.485123	-1.97	0.550947	-2.02	0.503566					
E2F4	-6.7	0.0000096	-2.07	0.164271	-1.57	0.517402	1.23	0.051337	-4.48	0.018457	-2.86	0.109407					
IMPDH2	-6.7	0.04409433	-2.02	0.361267	-1.16	0.883299	1.72	0.441253	-4.48	0.073333	-1.96	0.516182					
HSP90B1	-6.57	0.04213423	-1.72	0.493984	-1.22	0.831061	1.28	0.688058	-4.39	0.070577	-1.27	0.867557					
XIAP	-6.56	0.00006772	-1.9	0.242277	1.39	0.05384	1.24	0.283249	-4.38	0.012814	-2.6	0.166725					
NFKBIE	-6.37	0.0010315	-3.02	0.026289	-1.58	0.586661	-1.59	0.175768	-2.38	0.282123	-1.22	0.751574					
IL10RB	-6.34	0.07687437	-1.3	0.672729	1.14	0.506953	1.35	0.002078	-3.66	0.254013	-1.49	0.70048					
TBP	-6.3	0.04211631	-1.54	0.588763	-1.33	0.745899	1.55	0.477164	-1.85	0.567908	-1.8	0.571979					
TRIM35	-6.23	0.00001477	-1.7	0.343159	-1.83	0.364253	1.12	0.541004	-4.16	0.017065	-2.47	0.181513					
TRAF3	-6.18	0.04728999	-1.38	0.563219	-1.67	0.574808	1.13	0.143096	-3.61	0.200103	-3.25	0.239963					
PRKDC	-6.17	0.04529048	-1.27	0.706802	-1.49	0.678809	1.22	0.324098	-3.56	0.206685	-3.07	0.280557					
TRAT1	-6.04	0.09018733	1.21	0.465166	-1.02	0.943801	1.58	0.024947	-10.58	0.158363	1.11	0.752656					
NKIRAS2	-5.73	0.00002562	-1.74	0.291921	-1.5	0.517939	1.25	0.026188	-3.83	0.030083	-2.66	0.084938					
BTLA	-5.7	0.00003097	-1.36	0.615811	-1.48	0.542101	1.54	0.013541	-3.81	0.018997	-2.17	0.260385					
TRAF6	-5.64	0.04125997	-1.4	0.662183	-1.06	0.952679	1.62	0.414828	-3.77	0.074342	-1.65	0.615694					

Probe Name	P value		P value		P value		P value		P value		P value		P value	
	A1 vs. HD	of: A1 vs. HD	A2 vs. HD	of: A2 vs. HD	NA1 vs. HD	of: NA1 vs. HD	NA2 vs. HD	of: NA2 vs. HD	SJ1 vs. HD	of: SJ1 vs. HD	SJ2 vs. HD	of: SJ2 vs. HD	SJ1 vs. HD	of: SJ1 vs. HD
UBE2L3	-5.53	0.0000053	-1.17	0.815189	-1.21	0.781139	1.44	0.002281	-1.8	0.502715	-2.07	0.294899	-1.8	0.502715
CBL	-5.3	0.04148122	-1.25	0.772824	-1.06	0.94411	2.19	0.206736	-1.15	0.901342	1.28	0.80633	-1.15	0.901342
SAR1B	-5.28	0.05880856	1.34	0.035444	1.33	0.008426	1.15	0.143176	-3.33	0.187369	-2.74	0.299998	-3.33	0.187369
MAPK7	-5.13	0.06961362	-2.53	0.131373	-2.53	0.193012	-1.46	0.014871	-6.07	0.010136	-3.82	0.072816	-6.07	0.010136
TRIM21	-5.12	0.04318518	-1.47	0.578779	1.09	0.929476	1.91	0.278578	-3.42	0.082239	-3.6	0.074072	-3.42	0.082239
AGER	-5.1	0.00305291	-2.24	0.12639	-2.31	0.05337	-1.06	0.86482	-3.41	0.014687	-3.58	0.004107	-3.41	0.014687
IMPDH1	-5.04	0.04319404	-1.67	0.424993	2.73	0.224958	1.13	0.820471	-1.22	0.872732	-1.5	0.669885	-1.22	0.872732
DIABLO	-4.96	0.03993035	-1.79	0.343421	-1.25	0.768262	1.35	0.566081	-3.31	0.078031	-1.78	0.464616	-3.31	0.078031
BCL2L1	-4.95	0.04209389	-2.58	0.13825	-1.19	0.824978	1.36	0.55906	-3.3	0.082161	-1.74	0.49678	-3.3	0.082161
STK26	-4.94	0.00000438	-1.43	0.480349	-1.45	0.504601	1.07	0.715677	-3.3	0.029388	-3.48	0.004279	-3.3	0.029388
CYC1	-4.93	0.04018118	1.53	0.619927	-1.12	0.884214	1.43	0.500711	-1.3	0.816966	-3.47	0.070034	-1.3	0.816966
TNFSF10	-4.93	0.14080551	1.2	0.572783	1.53	0.462861	1.56	0.026586	-4.37	0.277706	1	0.97069	-4.37	0.277706
ATG9A	-4.86	0.04273273	-2.18	0.24026	-1.04	0.958097	1.81	0.300883	2.84	0.380613	-1.51	0.650184	2.84	0.380613
HERC6	-4.82	0.04376639	-1.29	0.716672	-1.07	0.938497	1.9	0.278746	-3.22	0.086726	1.99	0.520288	-3.22	0.086726
CAMK2D	-4.68	0.07813258	-1.2	0.725368	-1.85	0.41264	1.21	0.225492	-5.54	0.007396	-3.15	0.141326	-5.54	0.007396
JAK2	-4.68	0.04517156	-1.07	0.925832	1.22	0.830894	2.14	0.202174	-1.18	0.885725	2.09	0.497266	-1.18	0.885725
NFKBIZ	-4.67	0.20557946	-1.59	0.015039	-1.64	0.462602	-1.59	0.241528	-10.62	0.221616	-3.08	0.462943	-10.62	0.221616
TRADD	-4.58	0.03952649	-1.41	0.592571	-1.49	0.574313	1.59	0.369697	-3.06	0.082217	-3.22	0.071287	-3.06	0.082217
SKIL	-4.41	0.07411327	-3.87	0.019554	-2.27	0.314633	-1.94	0.145106	-5.04	0.011756	-5.31	0.010606	-5.04	0.011756
CTSW	-4.27	0.10460928	-2.59	0.129581	-1.62	0.556544	1.3	0.562853	-5.2	0.015873	-1.79	0.628238	-5.2	0.015873
MEF2A	-4.19	0.04338612	-1.21	0.767785	1.16	0.861366	2.35	0.140006	-1.23	0.838307	-1.52	0.574662	-1.23	0.838307
TSC2	-4.17	0.03776206	-1.2	0.772858	-1.11	0.884019	1.56	0.393688	-1.31	0.769881	-1.18	0.865196	-1.31	0.769881

Probe Name	P value		A2 vs. HD	P value		NA1 vs. HD	P value		NA2 vs. HD	P value		SJS1 vs. HD	P value		SJS2 vs. HD	P value	
	A1 vs. HD	of: A1 vs. HD		of: A2 vs. HD	of: NA1 vs. HD		of: NA2 vs. HD	of: SJS1 vs. HD		of: SJS2 vs. HD	of: SJS1 vs. HD		of: SJS2 vs. HD				
MLLT3	-4.14	0.04123675	-1.29	0.676385	-1.17	0.822487	1.19	0.724077	-2.76	0.093611	-2.91	0.078425					
ADAM17	-4.12	0.13496721	-2.12	0.226119	-1.75	0.464063	1	0.980063	-5.39	0.018723	-3.14	0.13784					
CD84	-4.1	0.14807871	1.49	0.192864	1.26	0.561365	1.6	0.035947	-4.24	0.190014	-3.48	0.286716					
NRBF2	-4.05	0.08831017	-1.07	0.906883	-1.36	0.690201	1.41	0.048598	-2.72	0.209975	-3.13	0.072535					
CSF1	-4.03	0.04366433	-1.44	0.515711	-1.43	0.611678	1.19	0.729159	-2.69	0.100844	-2.83	0.08416					
MAP2K1	-4.03	0.20684035	-3.87	0.099733	-2.57	0.365954	-1.03	0.859515	-4.48	0.250728	2.03	0.008256					
USP21	-3.98	0.03767316	-1.44	0.49452	-1.21	0.764069	1.69	0.283535	-2.66	0.090602	-1.77	0.32168					
MTOR	-3.77	0.03960368	-1.28	0.659299	-1.05	0.937421	2.11	0.150925	-2.52	0.10042	-1.4	0.628164					
TRIM8	-3.76	0.21190605	-1.95	0.375262	1.24	0.487051	-1.1	0.391505	-4.04	0.30488	1.73	0.029327					
HMGBl	-3.74	0.04330638	1.13	0.864468	-1.18	0.789419	2	0.228149	-2.5	0.108601	-2.63	0.087604					
NF1	-3.62	0.03555991	1.56	0.481585	-1.09	0.888663	1.44	0.396832	1.11	0.91718	-2.55	0.074425					
ACP5	-3.6	0.03578802	-1.12	0.834266	1.26	0.760391	1.51	0.364337	-1.42	0.621761	-1.57	0.420448					
TBK1	-3.52	0.03909532	-1.01	0.983579	-1.01	0.982063	1.77	0.214361	-2.35	0.108711	1.16	0.89532					
PIK3R2	-3.49	0.03681561	-1.82	0.205477	-1.32	0.589588	1.29	0.532338	-2.33	0.105594	1.18	0.881223					
BST2	-3.43	0.13746564	-1.98	0.191553	1.45	0.040279	1.31	0.185425	-2.27	0.334651	-2.82	0.098574					
TIGIT	-3.37	0.21777771	-1.23	0.413515	-3.7	0.304947	-1.25	0.37913	-20.61	0.000391	-1.12	0.629814					
ATG101	-3.36	0.03376471	-1.98	0.129664	-1.19	0.752442	1.2	0.633832	-2.24	0.106109	-2.36	0.075883					
RELB	-3.33	0.03555818	-1.77	0.201643	1.09	0.908587	-1.4	0.541028	1.12	0.91269	-2.34	0.080299					
CD3E	-3.2	0.01609154	-1.09	0.736545	1.12	0.749407	-1.03	0.941319	-4.03	0.267179	1.02	0.952646					
TCIRG1	-3.18	0.18740875	-1.61	0.022428	-1.02	0.889504	-1.13	0.472941	-7.25	0.135636	-3.08	0.266002					
LRR1	-3.14	0.03428875	-1.01	0.977379	-1.22	0.685095	1.21	0.592261	-2.1	0.120426	-1.07	0.927406					
TRAF2	-3.12	0.03694483	-1.03	0.95331	-1.1	0.860097	1.53	0.279436	-2.08	0.127873	-2.19	0.089035					

Probe Name	P value		P value		P value		P value		P value		P value		P value	
	A1 vs. HD	of: A1 vs. HD	A2 vs. HD	of: A2 vs. HD	NA1 vs. HD	of: NA1 vs. HD	NA2 vs. HD	of: NA2 vs. HD	SJ1 vs. HD	of: SJ1 vs. HD	SJ2 vs. HD	of: SJ2 vs. HD		
TRIM26	-3.08	0.04704307	-1.64	0.273905	1.22	0.763469	-1.05	0.934668	-2.06	0.151059	1.13	0.907919		
IL12RB1	-3.04	0.04104529	-1.3	0.551812	1.26	0.731895	2.15	0.101421	-2.03	0.142311	-2.14	0.100471		
TELO2	-3.03	0.04382255	-1.16	0.754227	-1.45	0.399347	1.17	0.719084	-2.02	0.14879	-2.13	0.106756		
UNC93B1	-2.98	0.03729715	-1.48	0.374978	-1.15	0.766081	-1.31	0.604613	-1.99	0.13989	-2.1	0.094603		
PANX1	-2.93	0.03122203	1.07	0.887398	-1.46	0.447411	1.47	0.270911	-1.96	0.132082	-2.06	0.08285		
CD274	-2.88	0.03444972	1.08	0.87406	1.15	0.810952	1.88	0.118162	1.49	0.745548	1.41	0.754426		
TATDN1	-2.87	0.00004422	-1.06	0.850029	-1.44	0.206158	1.19	0.616286	-1.92	0.111258	-1.72	0.019563		
IRF9	-2.81	0.00613644	-1.36	0.054659	-1.05	0.8408	1.04	0.698794	-9.71	0.173081	-1.35	0.273725		
ORAI1	-2.79	0.16488992	-1.72	0.197031	-1.13	0.855207	1.89	0.037187	-2.05	0.263304	-1.85	0.333148		
NFKB1B	-2.76	0.03171115	-1.58	0.200404	1.08	0.895515	1.3	0.424188	-1.84	0.153879	-1.94	0.092359		
ELK1	-2.71	0.02973309	-1.15	0.694345	1.02	0.964989	1.5	0.244442	-1.81	0.156386	-1.91	0.090241		
G6PD	-2.7	0.21431696	-2.01	0.087977	-1.42	0.556902	-1.11	0.737569	-3.3	0.018849	-2.12	0.18213		
TNFRSF10A	-2.59	0.03464128	-1.2	0.685967	-1.28	0.491537	1.29	0.449348	-1.73	0.187107	-1.82	0.110897		
POLR3H	-2.57	0.02907865	-1.34	0.401975	-1.45	0.307753	-1.19	0.696654	-1.72	0.179134	-1.81	0.098421		
LAG3	-2.53	0.02739424	-1.19	0.682257	-1.03	0.944209	1.08	0.838874	-1.69	0.183416	-1.78	0.097269		
IL18RAP	-2.49	0.03460839	-1.23	0.586444	-1.82	0.097127	-1.13	0.768105	-1.66	0.206646	-1.75	0.119417		
PPIA	-2.4	0.33702135	-2.59	0.141013	-2.19	0.320419	-1.2	0.507518	-6.51	0.013446	-3.6	0.135007		
ATP6V0A1	-2.32	0.02861687	1.16	0.698174	-1.37	0.261803	1.11	0.813101	-1.55	0.241856	-1.63	0.124926		
GHDC	-2.23	0.02631578	1.03	0.922148	-1.07	0.842596	1.59	0.110536	-1.49	0.268699	-1.57	0.133192		
S1PR1	-2.23	0.34564942	-2.47	0.104199	-1.85	0.398103	-1.03	0.879355	-5.14	0.019074	-1.99	0.345098		
CREB3	-2.22	0.02963821	-1.23	0.448982	-1.31	0.310439	-1.01	0.986184	-1.48	0.279916	-1.56	0.144962		
CSK	-2.2	0.00913901	-1.14	0.396562	1.01	0.958034	1.08	0.619256	-7.98	0.204039	-1.01	0.983495		

Probe Name	P value		A2 vs. HD	P value		NA1 vs. HD	P value		NA2 vs. HD	P value		SJS1 vs. HD	P value		SJS2 vs. HD	P value	
	A1 vs. HD	of: A1 vs. HD		of: A2 vs. HD	of: NA1 vs. HD		of: NA2 vs. HD	of: SJS1 vs. HD		of: SJS2 vs. HD	of: SJS1 vs. HD		of: SJS2 vs. HD				
H2AFY2	-2.13	0.00022839	-1.22	0.221546	-1.4	0.025441	-1.06	0.878898	-1.42	0.274129	-1.34	0.039641					
ATG4B	-2.07	0.36014435	-2	0.23811	-1.71	0.450057	1.13	0.49587	-2.84	0.192129	-5.08	0.000563					
GCLC	-2.03	0.3222799	-1.07	0.892882	1.02	0.969162	1.54	0.053034	-2.41	0.043753	-2.53	0.006226					
EZH2	-2.01	0.02802499	-1.44	0.161495	1.82	0.356854	1.8	0.045137	1.54	0.618106	-1.41	0.199394					
TIRAP	-1.95	0.03094317	1.17	0.604303	-1.18	0.485442	-1.33	0.297456	-1.31	0.425727	-1.37	0.22949					
RSAD2	-1.94	0.02243296	1.01	0.985192	1.11	0.729457	-1.08	0.810848	-1.3	0.423297	-1.37	0.211301					
RNASEH2A	-1.9	0.02458822	1.23	0.510745	1.02	0.949273	1.1	0.805602	-1.27	0.458962	-1.34	0.239058					
ELAVL1	-1.83	0.0316134	1.37	0.351299	-1.27	0.250137	1.78	0.180052	-1.22	0.529148	1.06	0.829787					
HRAS	-1.79	0.04712967	1.5	0.291315	1.01	0.974956	1.9	0.146416	-1.2	0.581209	1.05	0.848839					
FLT4	-1.68	0.01402003	1.33	0.320328	-1.23	0.178664	1.45	0.361689	-1.12	0.699476	-1.18	0.417204					
IL15	-1.61	0.01514429	1.02	0.897664	-1.18	0.238346	-1.23	0.196544	-1.08	0.795033	-1.13	0.519996					
CLU	-1.56	0.04753165	1.46	0.248782	1.26	0.503062	1.67	0.26517	1.63	0.472595	1.45	0.410949					
RORC	-1.55	0.00591128	1.06	0.590229	-1.13	0.255347	-1.12	0.468586	-1.03	0.909113	-1.09	0.643601					
CTSO	-1.39	0.69179767	-1.45	0.478911	-1.35	0.630818	1.43	0.252632	-3.28	0.018926	-1.87	0.339039					
PYCARD	-1.1	0.87868541	1.28	0.4584	1.18	0.609877	1.95	0.031204	-1.26	0.479202	-1.33	0.265186					
HLA-DQB2	-1.01	0.98721719	-1.51	0.39877	4.36	0.031867	3.27	0.019672	-1.42	0.680706	-2.49	0.046216					
MDM2	1.01	0.99359804	-1.6	0.257408	-1.55	0.257316	-1.11	0.447609	-2.34	0.070271	-2.47	0.022855					
HIST1H3G	1.07	0.92532223	1.34	0.385772	4.69	0.030745	1.89	0.06376	1.5	0.533659	-1.2	0.517038					
ATP6V0C	1.13	0.57432312	-1.06	0.873002	1.52	0.325284	-1.06	0.710503	1.9	0.022794	1.12	0.5952					
RPS6KA5	1.4	0.65400159	-1.44	0.516967	1	0.981251	1.25	0.350404	-3.73	0.029448	-1.25	0.687874					
CDK8	1.43	0.61120588	-1.32	0.496885	-1.49	0.367271	1.3	0.010181	-1.97	0.198512	-2.8	0.015743					
SIRT1	1.53	0.01092101	1.09	0.580187	-1.1	0.491095	-1.07	0.71107	-2.19	0.37779	-1.2	0.355682					

Probe Name	P value		P value		P value		P value		P value		P value		P value	
	A1 vs. HD	of: A1 vs. HD	A2 vs. HD	of: A2 vs. HD	NA1 vs. HD	of: NA1 vs. HD	NA2 vs. HD	of: NA2 vs. HD	SJ1 vs. HD	of: SJ1 vs. HD	SJ2 vs. HD	of: SJ2 vs. HD	SJ1 vs. HD	of: SJ1 vs. HD
C1QA	2.38	0.32804987	2.65	0.025515	1	0.975648	2	0.276194	1.08	0.786241	1.02	0.886837	1.02	0.886837
AP2A2	2.56	0.01912193	1.45	0.018424	-1.18	0.082971	1.43	0.307789	1.33	0.561726	-1.05	0.517381	-1.05	0.517381
KIT	2.71	0.23951596	1.42	0.030697	1.14	0.216112	1.1	0.463808	1.26	0.446811	1.19	0.352708	1.19	0.352708
TPSAB1/B2	2.91	0.28616402	2.41	0.040153	-1.04	0.713623	2.07	0.21235	2.64	0.306152	1.88	0.267995	1.88	0.267995
LBP	2.92	0.23404059	1.49	0.039412	1.16	0.164513	1.11	0.395365	1.27	0.422665	1.21	0.319072	1.21	0.319072
PADI2	3.05	0.25909662	1.25	0.041168	1.04	0.590926	1.51	0.337866	1.14	0.641661	1.08	0.63759	1.08	0.63759
NOTCH3	3.19	0.20300326	1.28	0.461716	-1.54	0.006485	1.54	0.399789	-1.37	0.317603	-1.48	0.106284	-1.48	0.106284
IL21	3.29	0.2571142	2.2	0.024646	1.03	0.705652	1.6	0.359623	1.13	0.66931	1.07	0.684341	1.07	0.684341
HLA-DOB	3.32	0.19160751	1.12	0.755251	-1.6	0.09599	1.26	0.593455	1.2	0.760262	-1.74	0.037221	-1.74	0.037221
NOTCH1	4.31	0.04057587	1.65	0.504954	-1.23	0.773033	1.55	0.413947	-3.09	0.080097	-1.46	0.670063	-1.46	0.670063
IFNA1	5.19	0.00200792	1.4	0.366929	1.11	0.825697	1.51	0.358089	-1.25	0.47952	-1.08	0.66958	-1.08	0.66958
ID1	7.62	0.0073395	2.27	0.248055	1.59	0.612735	1.34	0.606475	7.6	0.027387	2.54	0.340659	2.54	0.340659
TLR4	8.75	0.00335525	2.17	0.199324	1.7	0.557804	1.37	0.481209	1.42	0.694656	-1.54	0.283296	-1.54	0.283296
ZNF385A	13.66	0.00027259	3.25	0.085431	-1.01	0.985964	2.26	0.290011	1.71	0.531948	3.32	0.233921	3.32	0.233921

## VITA

**NAME** Suparada Khanaruksombat

**DATE OF BIRTH** 20 February 1988

**PLACE OF BIRTH** Ratchaburi, Thailand

**INSTITUTIONS ATTENDED** B.Sc. (second honor) in Biological Science, Kasetsart University, Bangkok, Thailand  
M.Sc. in Bioioproduct Science, Kasetsart University, Bangkok, Thailand

**HOME ADDRESS** 65/44-45 Khatha Thorn Rd., Na Muang, Mueang Ratchaburi, Ratchaburi 70000

**PUBLICATION** Khanaruksombat S., Srisomsap C., Punyarit P., Chokchaichamnankit D. and Phiriyangkul P. Identification of a novel allergen from muscle and various organs in banana shrimp (*Fenneropenaeus merguensis*). *Annals of Allergy, Asthma & Immunology*. 2014; 113 (3), pp301-306. doi:10.1016/j.anai.2014.06.002

**AWARD RECEIVED** AAIAT Awards, 7th FIMSA Congress (FIMSA 2018); November 10-13, 2018 at the Mandarin Hotel, Bangkok, Thailand.